Climate4you update November 2018
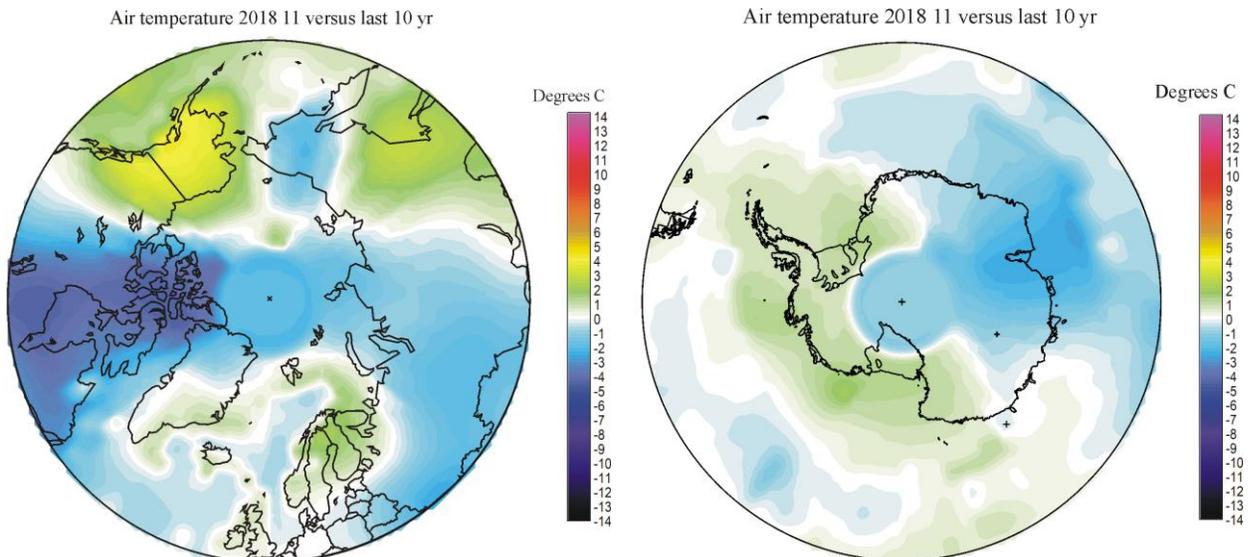
Climate4you.com

Contents:

November 2018 global surface air temperature overview

Surface air temperature anomaly 2018 11 vs last 10yr

Air temperature 2018 11 versus last 10 yr

Air temperature 2018 11 versus last 10 yr

November 2018 surface air temperature compared to the average of the last 10 years. Green-yellow-red colours indicate areas with higher temperature than the 10-year average, while blue colours indicate lower than average temperatures. Data source: Goddard Institute for Space Studies (GISS) using Hadl_Reyn_v2 ocean surface temperatures.

Comments to the November 2018 global surface air temperature overview

General: This newsletter contains graphs showing a selection of key meteorological variables for the past month. *All temperatures are given in degrees Celsius*.

In the above maps showing the geographical pattern of surface air temperatures, *the last previous 10 years are used as reference period*.

The rationale for comparing with this recent period instead of the official WMO 'normal' period 1961-1990, is that the latter period is affected by the cold period 1945-1980. Most comparisons with this time period will automatically appear as warm, and it will be difficult to decide if modern surface air temperatures are increasing or decreasing. Comparing instead with the last previous 10 years overcomes this problem and displays the modern dynamics of ongoing change. This decadal approach also corresponds well to the typical memory horizon for many people.

In addition, the GISS temperature data used for preparing the above diagrams display distinct temporal instability for data before the turn of the century (see p. 7). Any comparison with the WMO 'normal' period 1961-1990 is therefore influenced by ongoing monthly mainly administrative changes. An unstable value is clearly not suited as reference value. Simply comparing with the last previous 10 years makes more sense and is more useful. See also the additional reflections on page 46.

The different air temperature records have been divided into three quality classes, QC1, QC2 and QC3, respectively, as described on page 7.

In many diagrams shown in this newsletter the thin line represents the monthly global average value, and the thick line indicate a simple running average, in most cases a simple moving 37-month average, nearly corresponding to a three-year average. The 37-month average is calculated from values covering a range from 18 months before to 18 months after, with equal weight given to all individual months.

The year 1979 has been chosen as starting point in many diagrams, as this roughly corresponds to both the beginning of satellite observations and the onset of the late 20th century warming period. However, several of the data series have a much longer record length, which may be inspected in greater detail on www.climate4you.com.

**November 2018 global surface air temperatures**

General: For November 2018 GISS supplied 15955 interpolated surface air data points; all values are used to produce the diagrams shown on page 2. According to the GISS data, the average global November temperature anomaly was lower than in the previous month. By this, the overall decrease of global surface air temperatures since the 2016-17 El Niño global temperature peak persists, as illustrated by the diagrams on p. 4-6.

The Northern Hemisphere anomality pattern was characterised by large regional contrasts. Most of Russia and North America were cold compared to the previous 10 years, with only Alaska being relatively warm. Europe had temperatures close to the average, although northern Scandinavia was relatively warm. Also, western Siberia was relatively warm. The peak Northern Hemisphere cold anomaly was located in eastern North America. The Canadian and West Siberia sector of the Arctic was cold, while the Alaska sector was warm. The GISS surface air temperatures north of 80° N still appears to have an issue with interpolation, resulting in an unrealistic circular anomaly pattern.

Near the Equator temperatures were mainly near the 10-year average. In the Pacific, however, temperatures were somewhat above average.

The Southern Hemisphere temperatures were near or below the average for the previous 10 years. Most of Australia and South America was relatively cold. Also, South America was mainly below the 10-yr average. In the Antarctica, much of East Antarctica was relatively cold, while West Antarctica was relatively warm. South of 80°S the GISS anomaly pattern is influenced by an interpolation artefact.

3
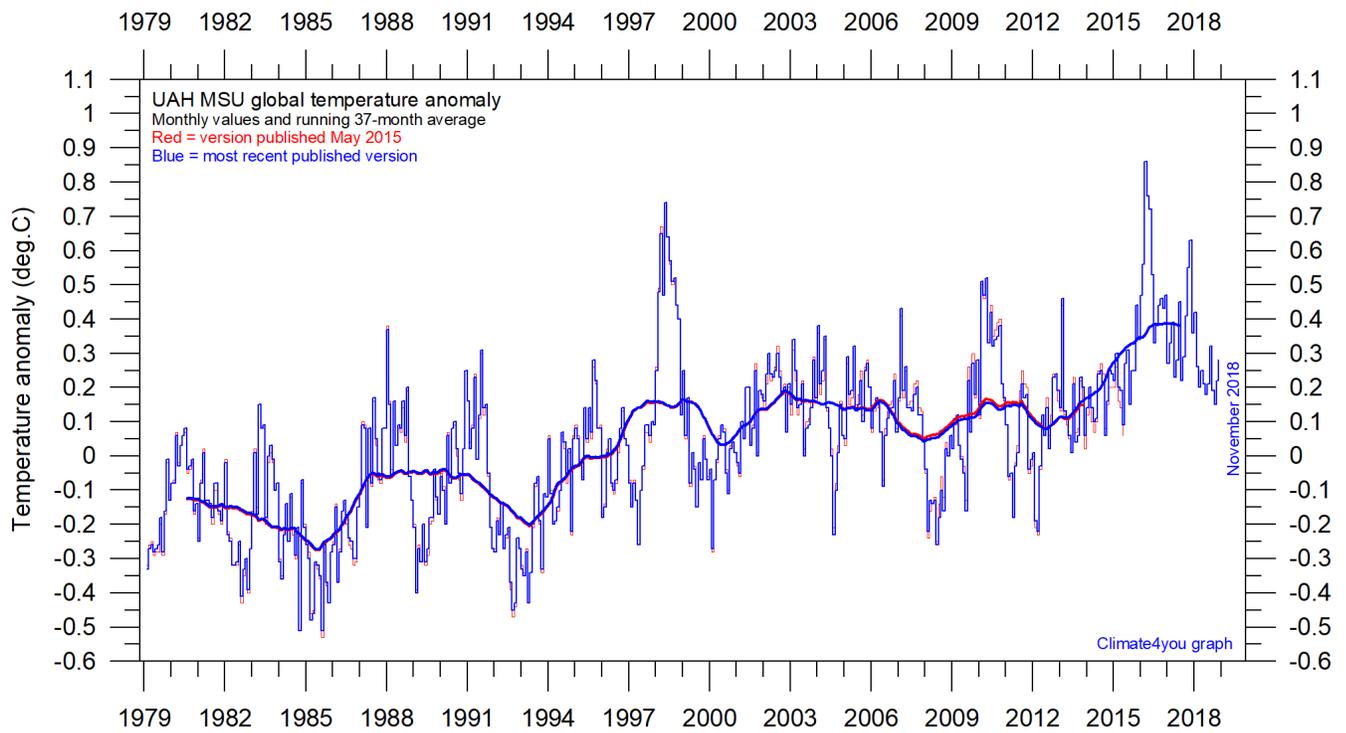
Global monthly average lower troposphere temperature (thin line) since 1979 according to *University of Alabama* at Huntsville, USA. The thick line is the simple running 37-month average.
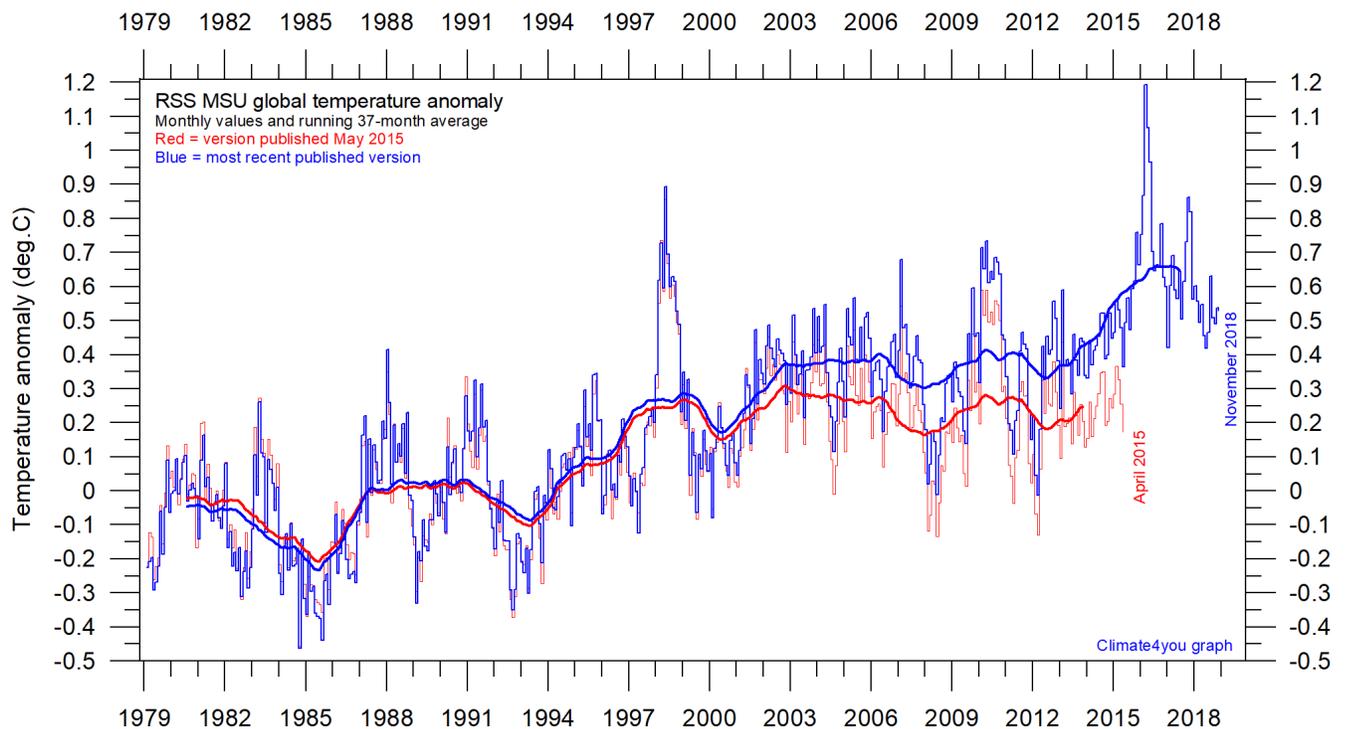
Global monthly average lower troposphere temperature (thin line) since 1979 according to according to *Remote Sensing Systems* (RSS), USA. The thick line is the simple running 37-month average.

Temperature quality class 2: HadCRUT global surface air temperature, updated to October 2018

HadCRUT4 global temperature anomaly
Monthly values and running 37-month average
Red = version published May 2015
Blue = most recent published version

Global monthly average surface air temperature (thin line) since 1979 according to according to the Hadley Centre for Climate Prediction and Research and the University of East Anglia's Climatic Research Unit (CRU), UK. The thick line is the simple running 37-month average.

Temperature quality class 3: GISS and NCDC global surface air temperature, updated to November 2018
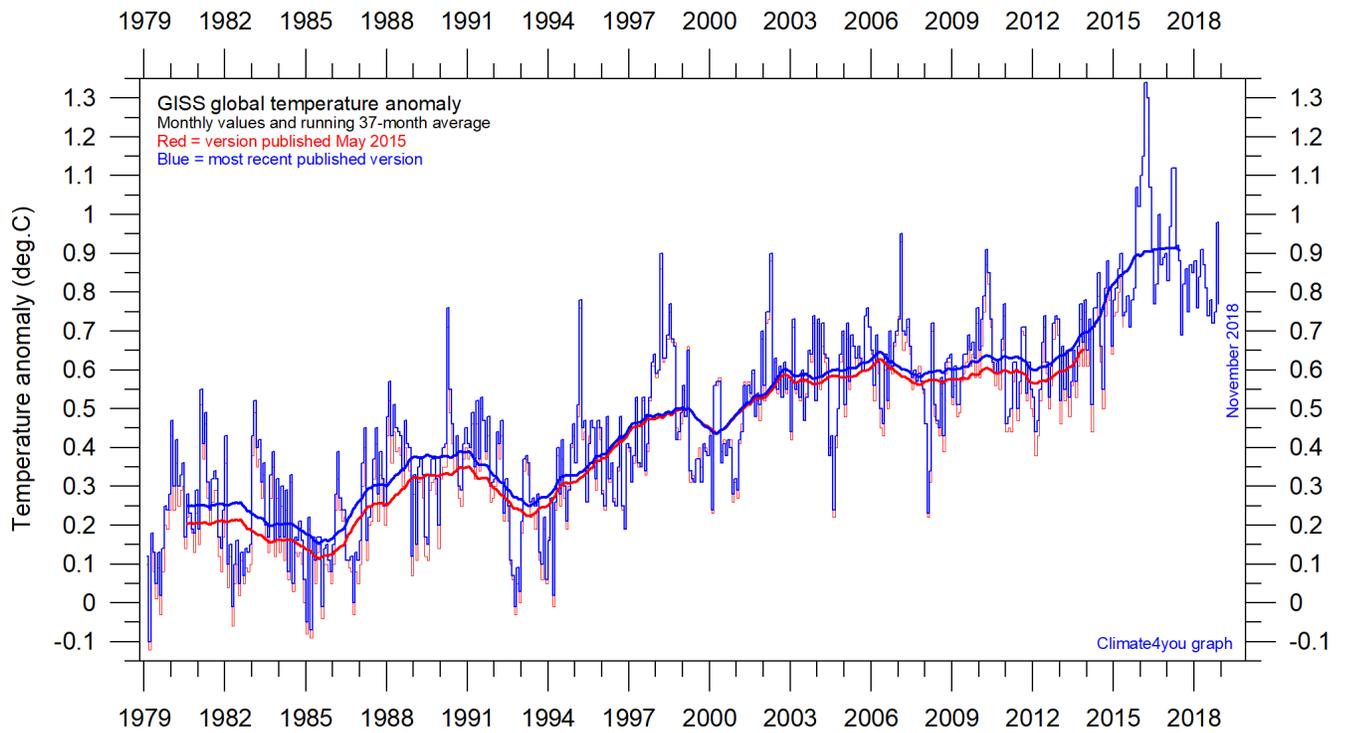
Global monthly average surface air temperature (thin line) since 1979 according to according to the _Goddard Institute for Space Studies_ (GISS), at Columbia University, New York City, USA, using ERSST_v4 ocean surface temperatures. The thick line is the simple running 37-month average.
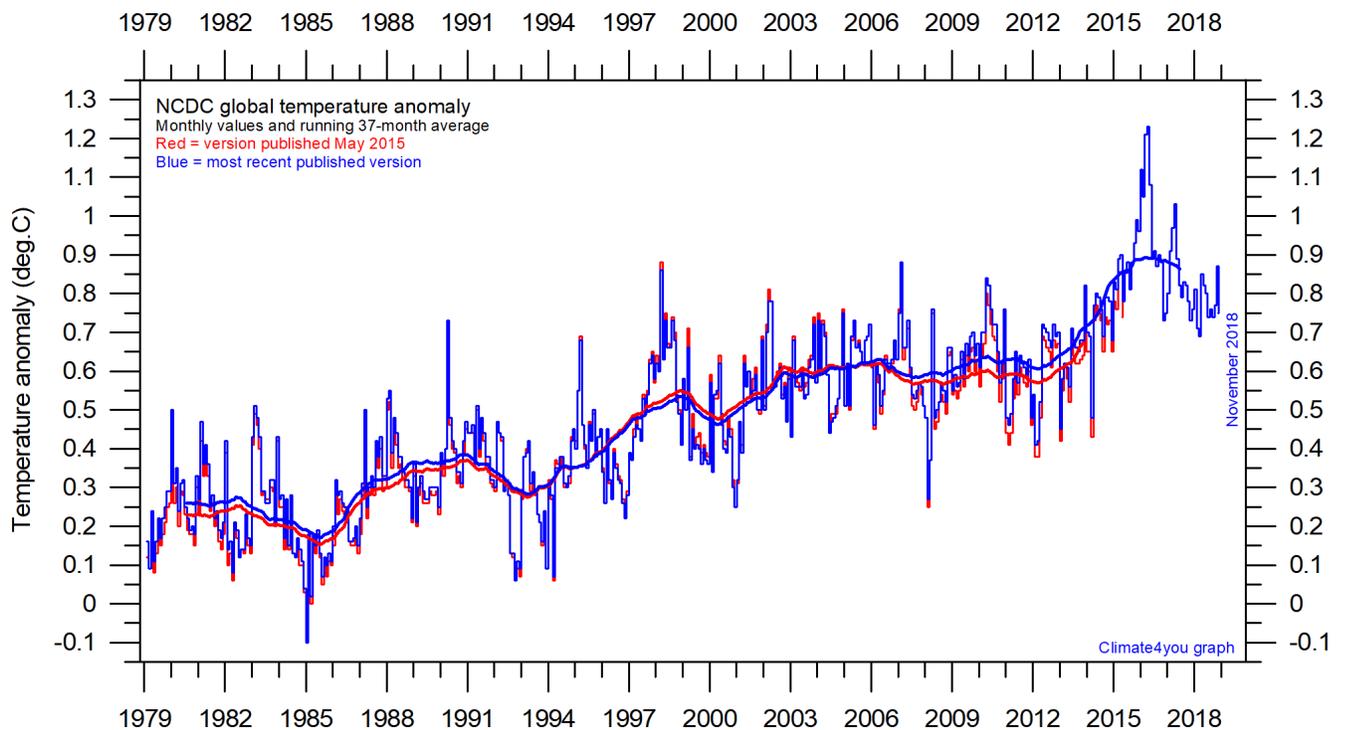
Global monthly average surface air temperature since 1979 according to according to the _National Climatic Data Center_ (NCDC), USA. The thick line is the simple running 37-month average.

A note on data record stability and -quality:

The temperature diagrams shown above all have 1979 as starting year. This roughly marks the beginning of the recent episode of global warming, after termination of the previous episode of global cooling from about 1940. In addition, the year 1979 also represents the starting date for the satellite-based global temperature estimates (UAH and RSS). For the three surface air temperature records (HadCRUT, NCDC and GISS), they begin much earlier (in 1850 and 1880, respectively), as can be inspected on www.climate4you.com.

For all three surface air temperature records, but especially NCDC and GISS, administrative changes to anomaly values are quite often introduced, even for observations many years back in time. Some changes may be due to the delayed addition of new station data or change of station location, while others probably have their origin in changes of the technique adopted to calculate average values. It is clearly impossible to evaluate the validity of such administrative changes for the outside user of these records; it is only possible to note that such changes appear very often (se example diagram next page).

In addition, the three surface records represent a blend of sea surface data collected by moving ships or by other means, plus data from land stations of partly unknown quality and unknown degree of representativeness for their region. Many of the land stations also has been moved geographically during their period of operation, their instrumentation have been changed, and they are influenced by changes in their near surroundings (vegetation, buildings, etc.).

The satellite temperature records also have their problems, but these are generally of a more technical nature and therefore correctable. In addition, the temperature sampling by satellites is more regular and complete on a global basis than that represented by the surface records. It is also important that the sensors on satellites measure temperature directly by emitted radiation, while most surface temperature measurements are indirect, using electronic resistance.

Everybody interested in climate science should gratefully acknowledge the efforts put into maintaining the different temperature databases referred to in the present newsletter. At the same time, however, it is also important to realise that all temperature records cannot be of equal scientific quality. The simple fact that they to some degree differ shows that they cannot all be correct.

On this background, and for practical reasons, Climate4you operates with three quality classes (1-3) for global temperature records, with 1 representing the highest quality level:

Quality class 1: The satellite records (UAH and RSS).

Quality class 2: The HadCRUT surface record.

Quality class 3: The NCDC and GISS surface records.

The main reason for discriminating between the three surface records is the following:

While both NCDC and GISS often experience quite large administrative changes (see example on p.8), and therefore essentially are unstable temperature records, the changes introduced to HadCRUT are fewer and smaller. For obvious reasons, as the past does not change, any record undergoing continuing changes cannot describe the past correctly all the time. Frequent and large corrections in a database also signal a fundamental doubt about what is likely to represent the correct values.

You can find more on the issue of lack of temporal stability on www.climate4you.com (go to: *Global Temperature*, followed by *Temporal Stability*).
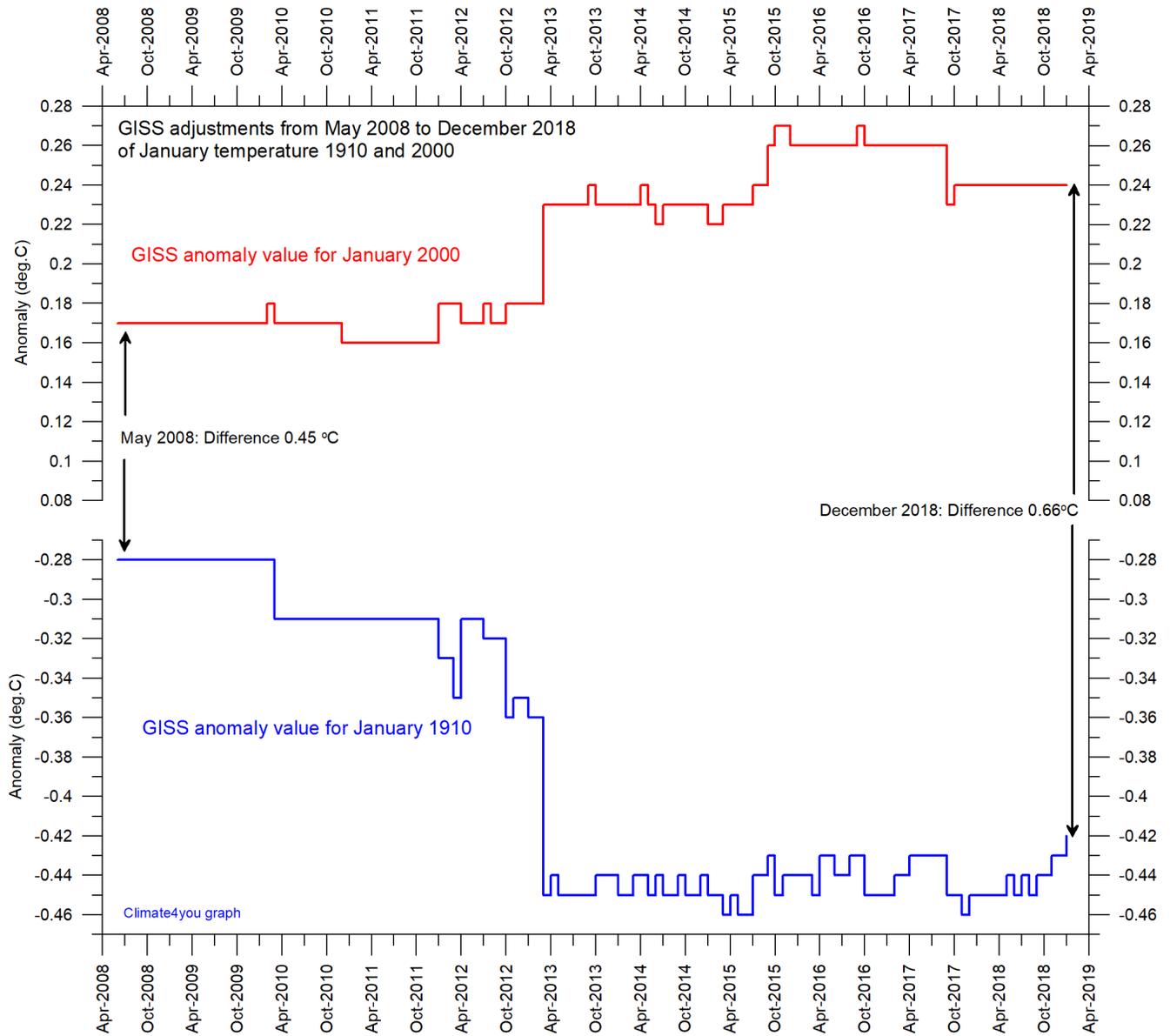
Diagram showing the adjustments made since May 2008 by the Goddard Institute for Space Studies (GISS), USA, in published anomaly values for the months January 1910 and January 2000.

Note: The administrative upsurge of the temperature increase from January 1915 to January 2000 has grown from 0.45 (reported May 2008) to 0.66°C (reported December 2018). This represents an about 47% administrative temperature increase over this period, meaning that nearly half of the apparent global temperature increase from January 1910 to January 2000 (as reported by GISS) is due to administrative changes of the original data since May 2008.
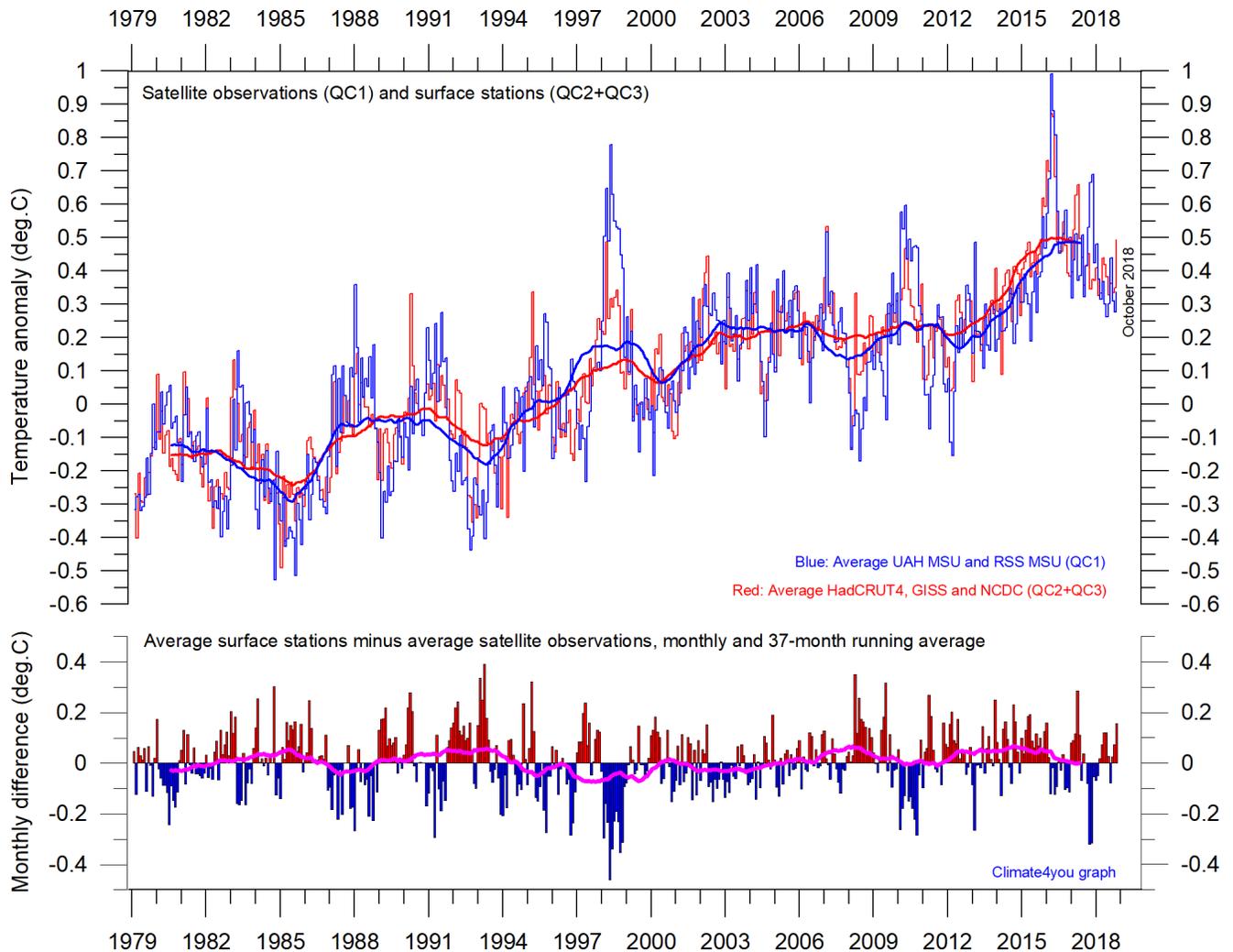
Plot showing the average of monthly global surface air temperature estimates (HadCRUT4, GISS and NCDC) and satellite-based temperature estimates (RSS MSU and UAH MSU). The thin lines indicate the monthly value, while the thick lines represent the simple running 37-month average, nearly corresponding to a running 3-yr average. The lower panel shows the monthly difference between average surface air temperature and satellite temperatures. As the base period differs for the different temperature estimates, they have all been normalised by comparing to the average value of 30 years from January 1979 to December 2008.

NOTE: Since about 2003, the average global surface air temperature has slowly been drifting away in positive direction from the average satellite temperature, meaning that the surface records show warming in relation to the troposphere records. The reason(s) for this is not entirely clear but can presumably at least partly be explained by the recurrent administrative adjustments made to the surface records (see p. 7-8).

Global air temperature linear trends updated to October 2018

Diagram showing the latest 5, 10, 20 and 30-yr linear annual global temperature trend, calculated as the slope of the linear regression line through the data points, for two satellite-based temperature estimates (UAH MSU and RSS MSU).
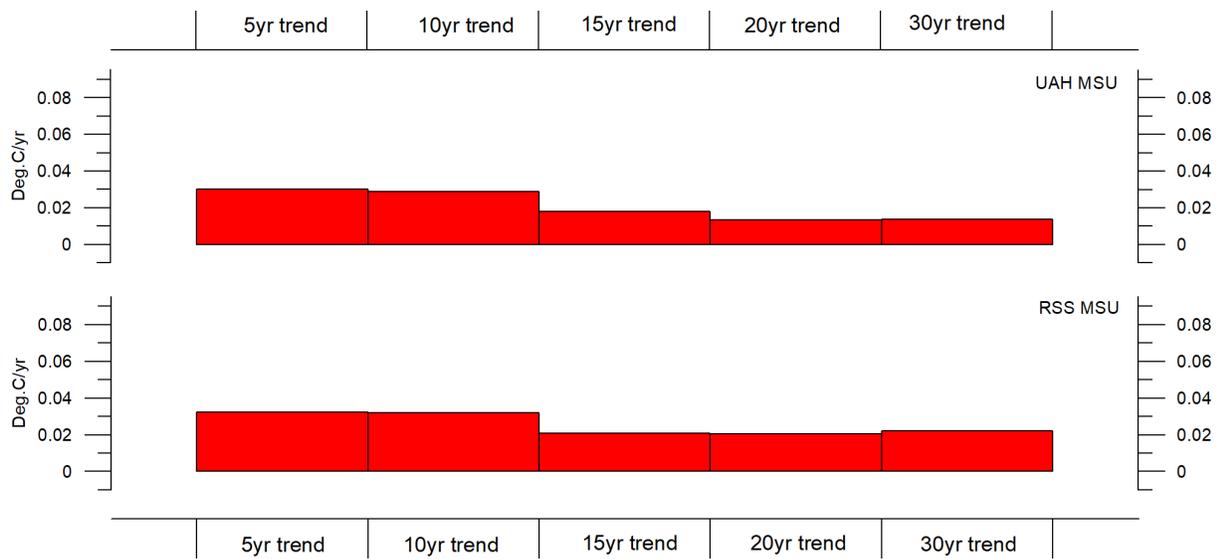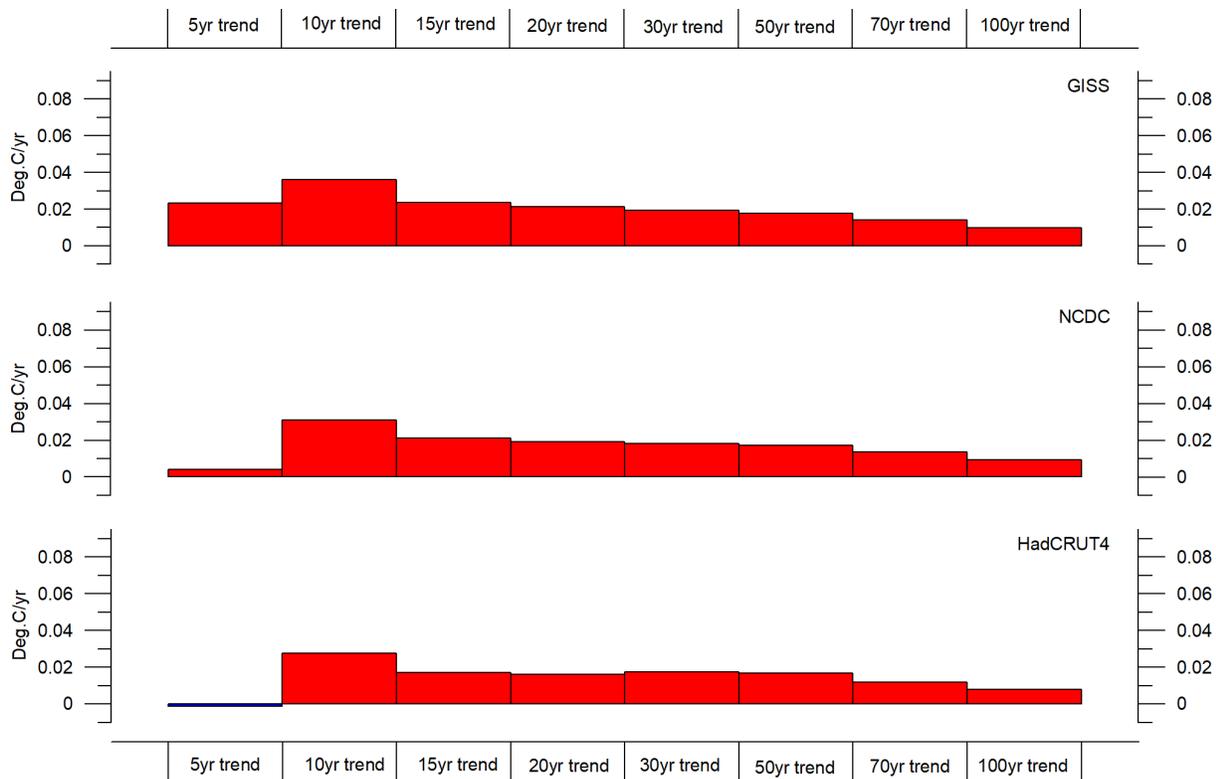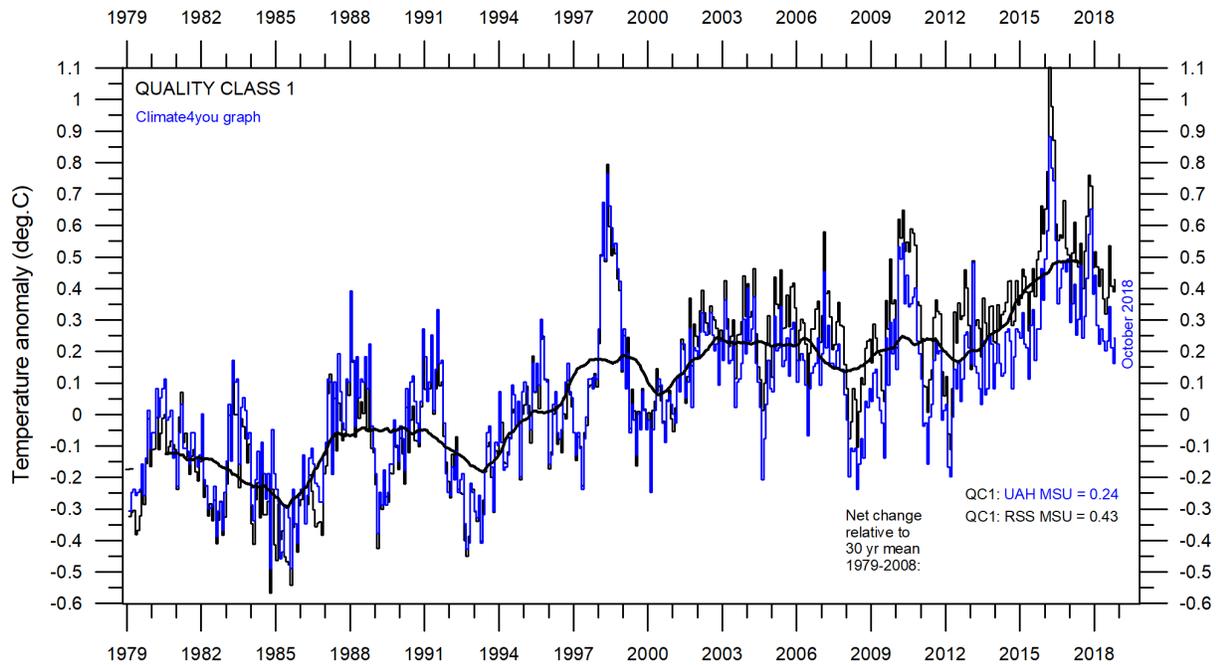
Diagram showing the latest 5, 10, 20, 30, 50, 70 and 100-year linear annual global temperature trend, calculated as the slope of the linear regression line through the data points, for three surface-based temperature estimates (GISS, NCDC and HadCRUT4).

Superimposed plot of Quality Class 1 (UAH and RSS) global monthly temperature estimates. As the base period differs for the individual temperature estimates, they have all been normalised by comparing with the average value of the initial 120 months (30 years) from January 1979 to December 2008. The heavy black line represents the simple running 37 month (c. 3 year) mean of the average of both temperature records. The numbers shown in the lower right corner represent the temperature anomaly relative to the individual 1979-2008 averages.

11
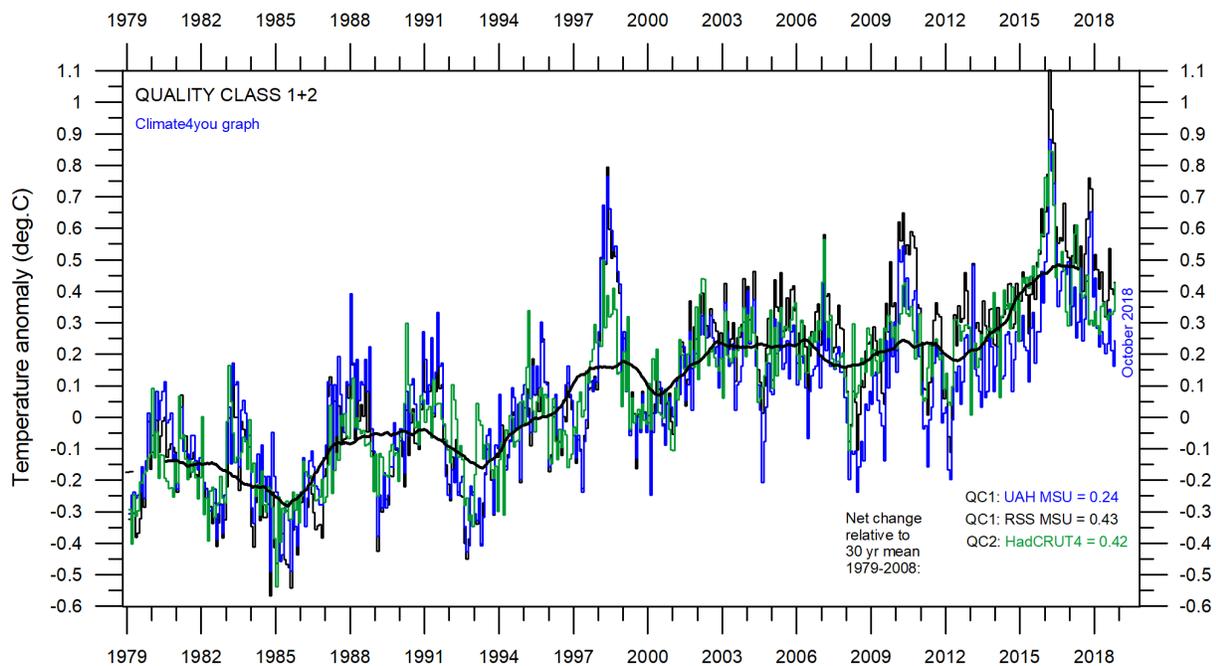
Superimposed plot of Quality Class 1 and 2 (UAH, RSS and HadCRUT4) global monthly temperature estimates. As the base period differs for the individual temperature estimates, they have all been normalised by comparing with the average value of the initial 120 months (30 years) from January 1979 to December 2008. The heavy black line represents the simple running 37 month (c. 3 year) mean of the average of all three temperature records. The numbers shown in the lower right corner represent the temperature anomaly relative to the individual 1979-2008 averages.
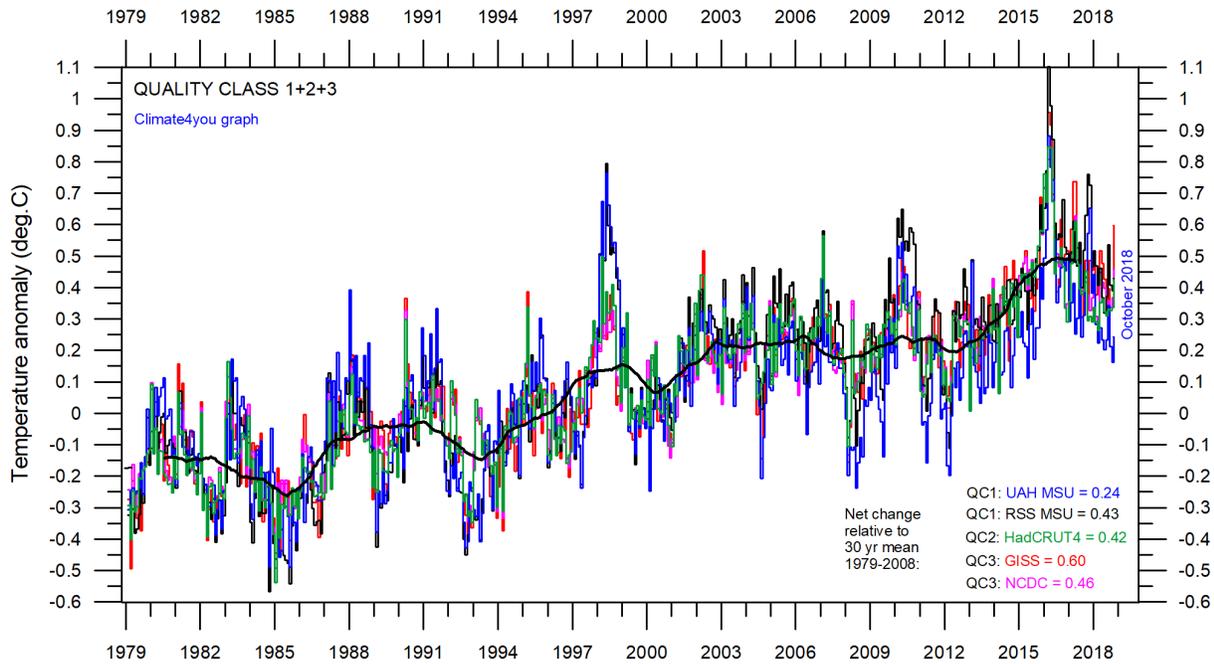
Superimposed plot of Quality Class 1, 2 and 3 global monthly temperature estimates (UAH, RSS, HadCRUT4, GISS and NCDC). As the base period differs for the individual temperature estimates, they have all been normalised by comparing with the average value of the initial 120 months (30 years) from January 1979 to December 2008. The heavy black line represents the simple running 37 month (c. 3 year) mean of the average of all five temperature records. The numbers shown in the lower right corner represent the temperature anomaly relative to the individual 1979-2008 averages.

Please see notes on page 7 relating to the above three quality classes.

It should be kept in mind that satellite- and surface-based temperature estimates are derived from different types of measurements, and that comparing them directly as done in the diagram above therefore may be somewhat problematical.

However, as both types of estimate often are discussed together, the above diagram may nevertheless be of some interest. In fact, the different types of temperature estimates appear to agree as to the overall temperature variations on a 2-3-year scale, although on a shorter time scale there are often considerable differences between the individual records. However, since about 2003 the surface records are slowly drifting towards higher temperatures than the combined satellite record (see p. 9).

The average of all five global temperature estimates presently shows an overall stagnation, at least since 2002-2003. There has been no significant increase in global air temperature since 1998, which however was affected by the oceanographic El Niño event. Also, the recent (2015-16) El Niño event may well represent a relatively short-lived spike on a longer development. The coming years will show if this is the case or not. Neither has there been a temperature decrease since about 2002-2003.

The present temperature stagnation does not exclude the possibility that global temperatures will begin to increase significantly again later. On the other hand, it also remains a possibility that Earth just now is passing an overall temperature peak, and that global temperatures will begin to decrease during the coming years. Again, time will show which of these possibilities is correct.

Global sea surface temperature, updated to November 2018
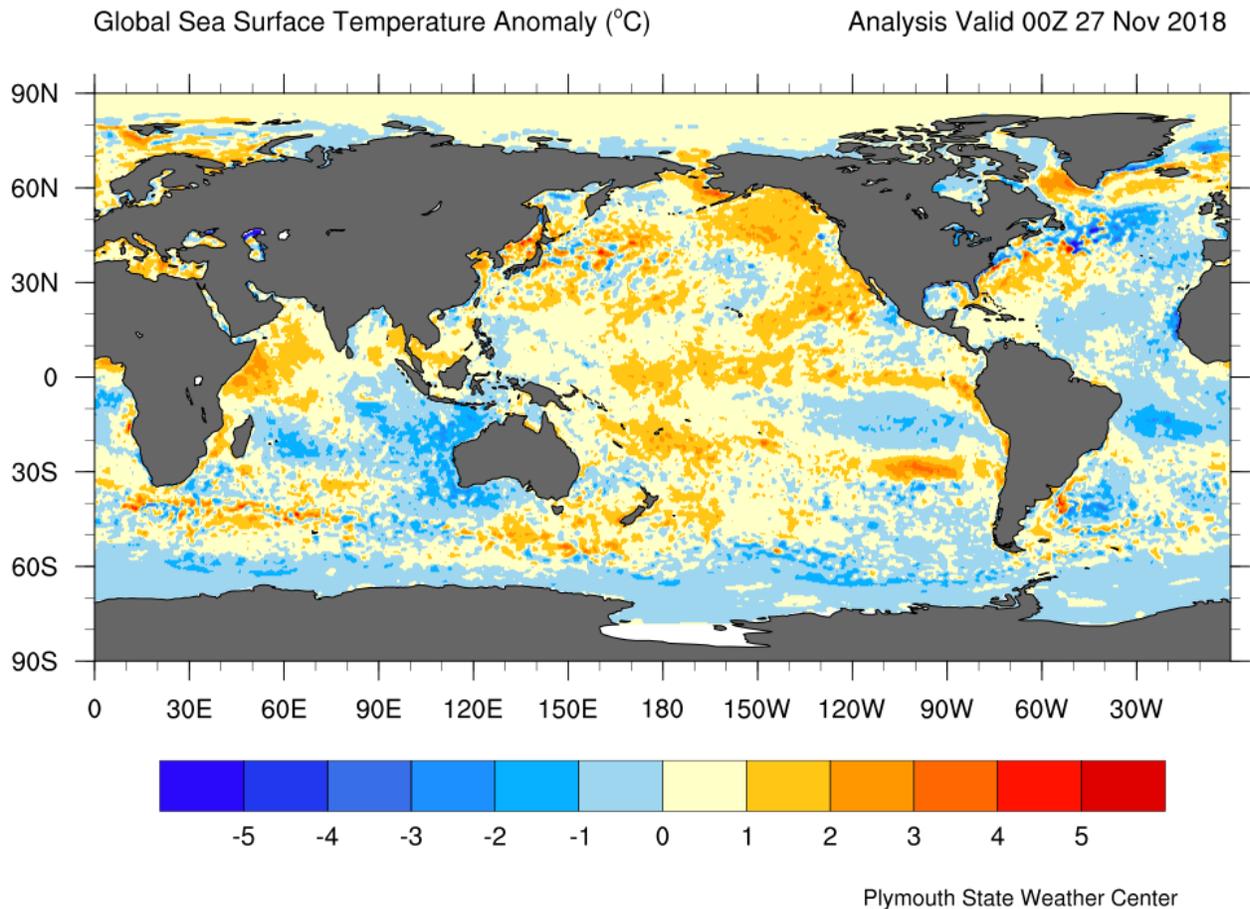
Sea surface temperature anomaly on 27 November 2018. Map source: Plymouth State Weather Center. Reference period: 1977-1991.

Because of the large surface areas near Equator, the temperature of the surface water in these regions is especially important for the global atmospheric temperature (p. 4-6). No less than 50% of planet Earth's surface area is located within 30°N and 30°S.

A mixture of relatively warm and cold water in August 2018 dominates much of the oceans near the Equator. In addition, parts of the North Atlantic are cooling. Presumably, all this will be influencing global air temperatures in the months to come.

However, the significance of any short-term cooling or warming reflected in air temperatures should not be overstated. Whenever Earth experiences cold La Niña or warm El Niño episodes (Pacific Ocean) major heat exchanges takes place between the Pacific Ocean and the atmosphere above, eventually showing up in estimates of the global air temperature.

However, this does not reflect similar changes in the total heat content of the atmosphere-ocean system. In fact, global net changes can be small and such heat exchanges may mainly reflect redistribution of energy between ocean and atmosphere. What matters is the overall temperature development when seen over several years.
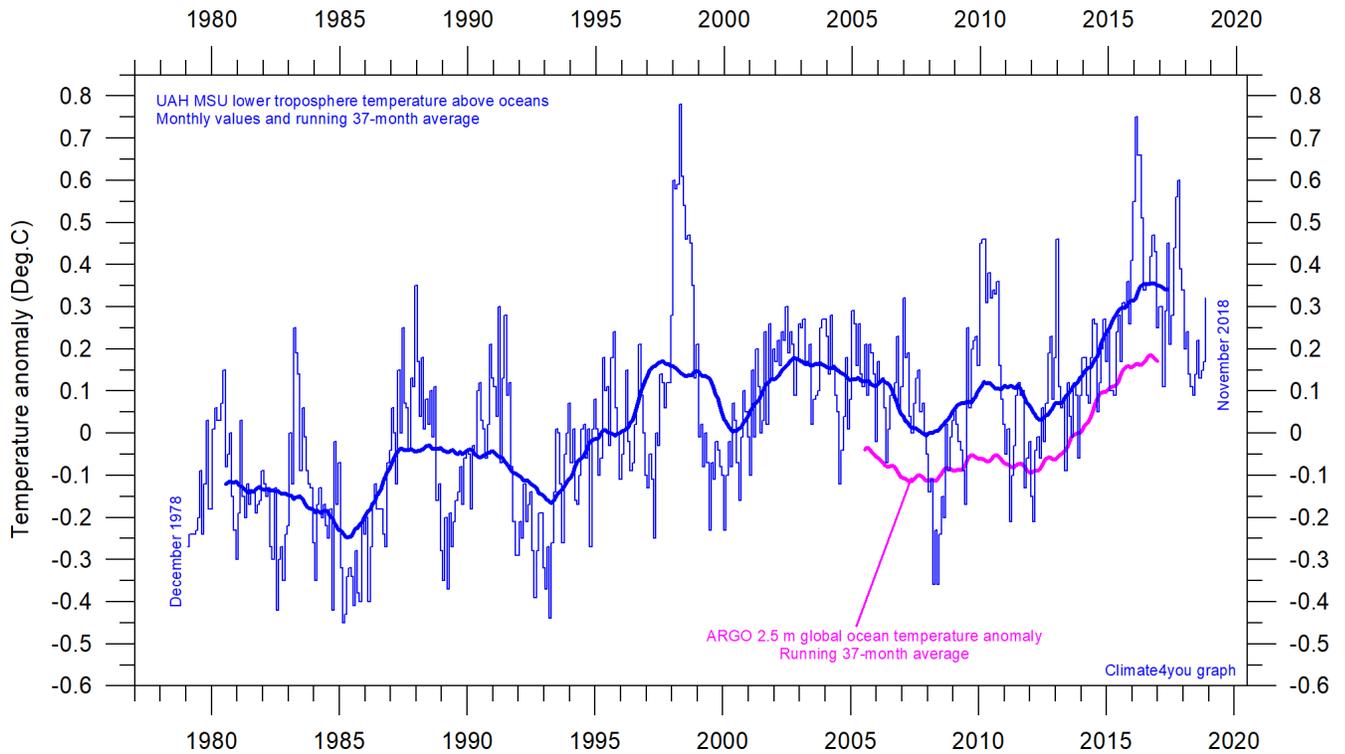
*Global monthly average lower troposphere temperature over oceans (thin line) since 1979 according to University of Alabama at Huntsville, USA. The thick line is the simple running 37-month average. Insert: Argo global ocean temperature anomaly from floats.*
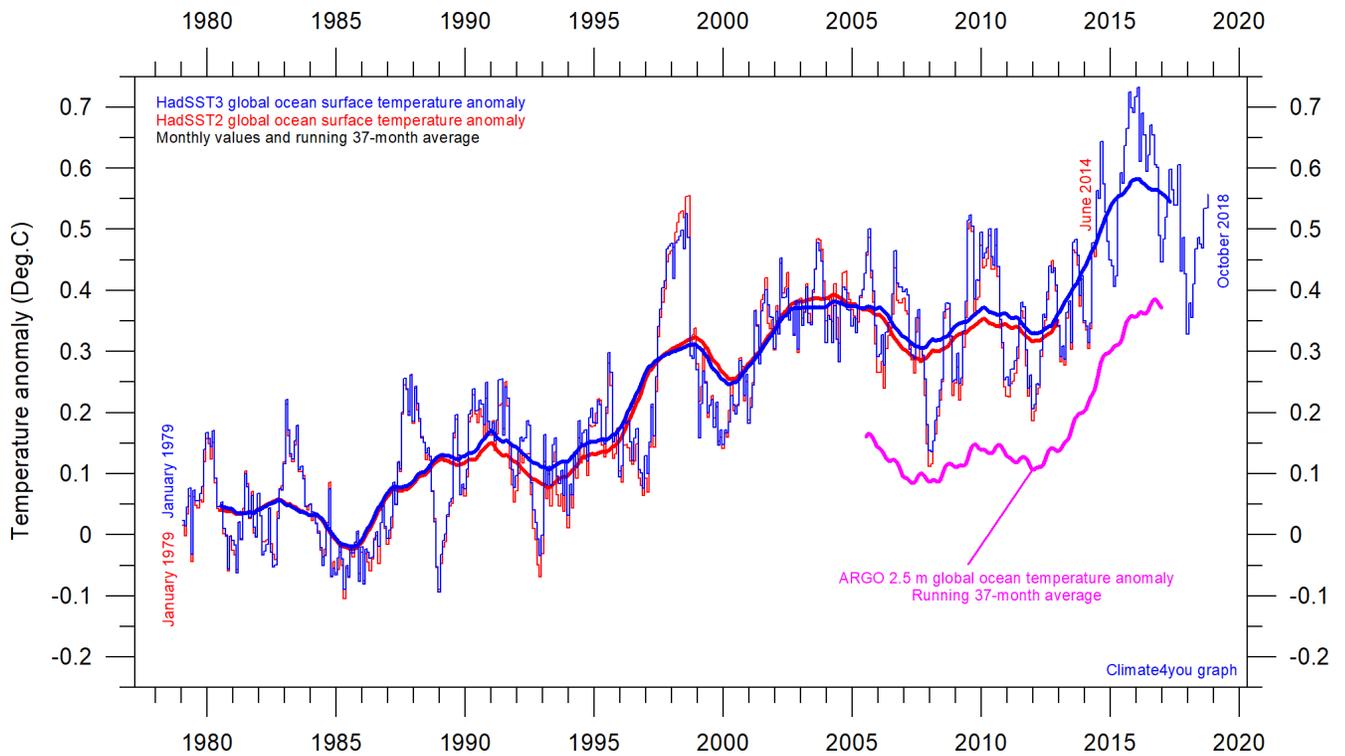
Global monthly average sea surface temperature since 1979 according to University of East Anglia's Climatic Research Unit (CRU), UK. Base period: 1961-1990. The thick line is the simple running 37-month average. Insert: Argo global ocean temperature anomaly from floats.
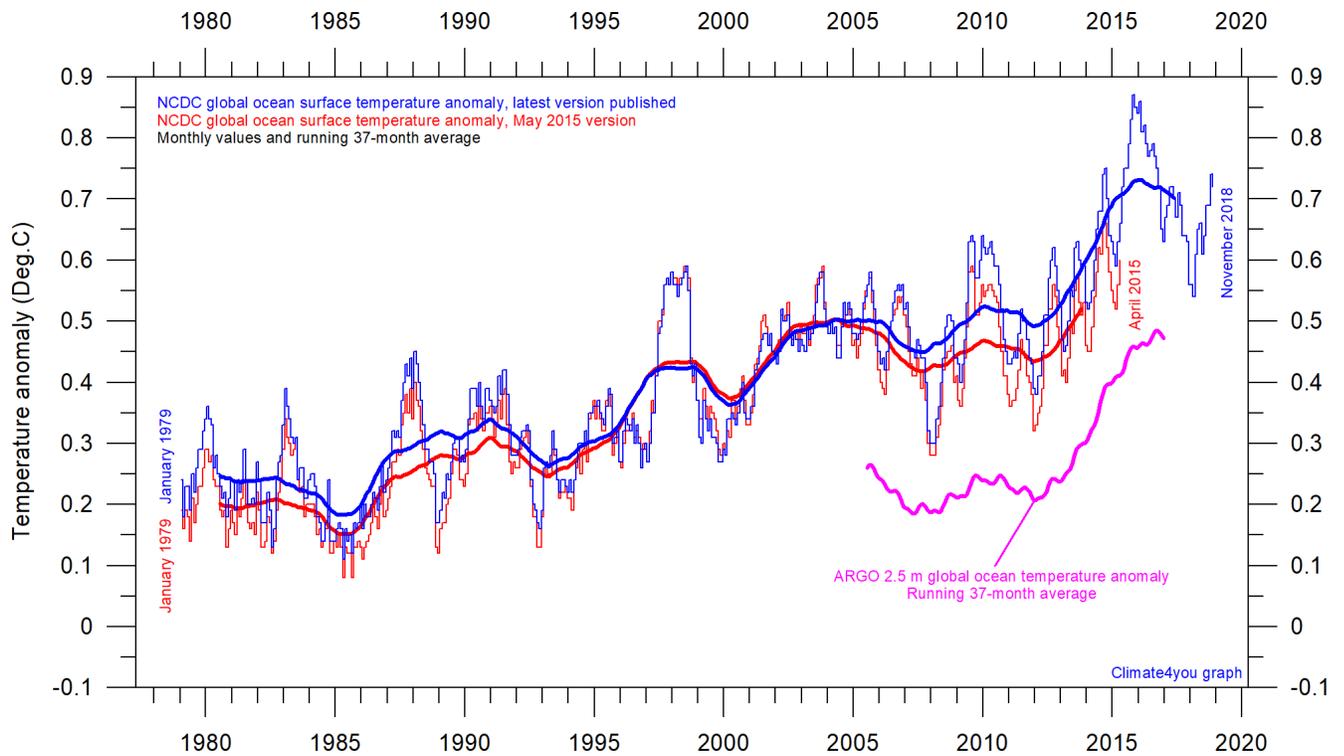
Global monthly average sea surface temperature since 1979 according to the [National Climatic Data Center](#) (NCDC), USA. Base period: 1901-2000. The thick line is the simple running 37-month average. Insert: Argo global ocean temperature anomaly from floats.

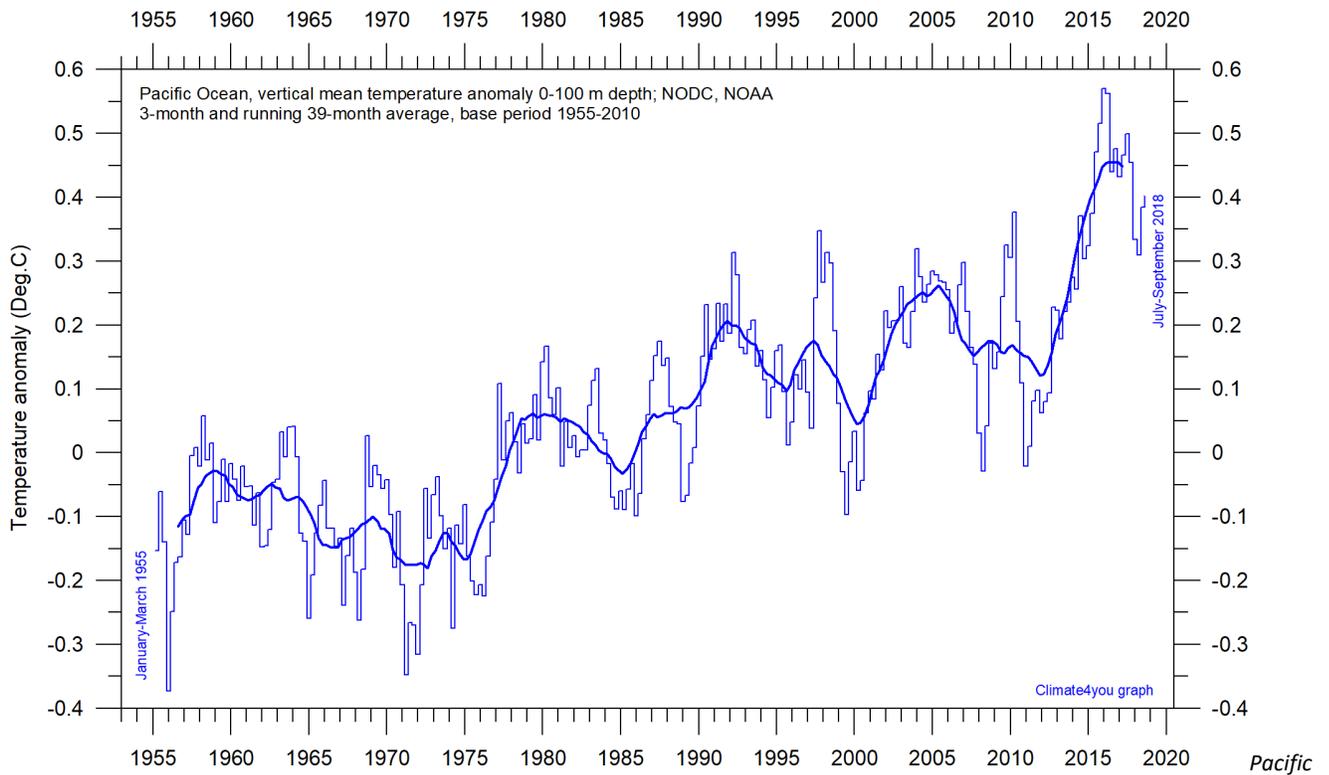**June 18, 2015:** *NCDC has introduced several rather large administrative changes to their sea surface temperature record. The overall result is to produce a record giving the impression of a continuous temperature increase, also in the 21st century. As the oceans cover about 71% of the entire surface of planet Earth, the effect of this administrative change is clearly seen in the NCDC record for global surface air temperature (p. 6).*

Ocean temperature in uppermost 100 m, updated to September 2018
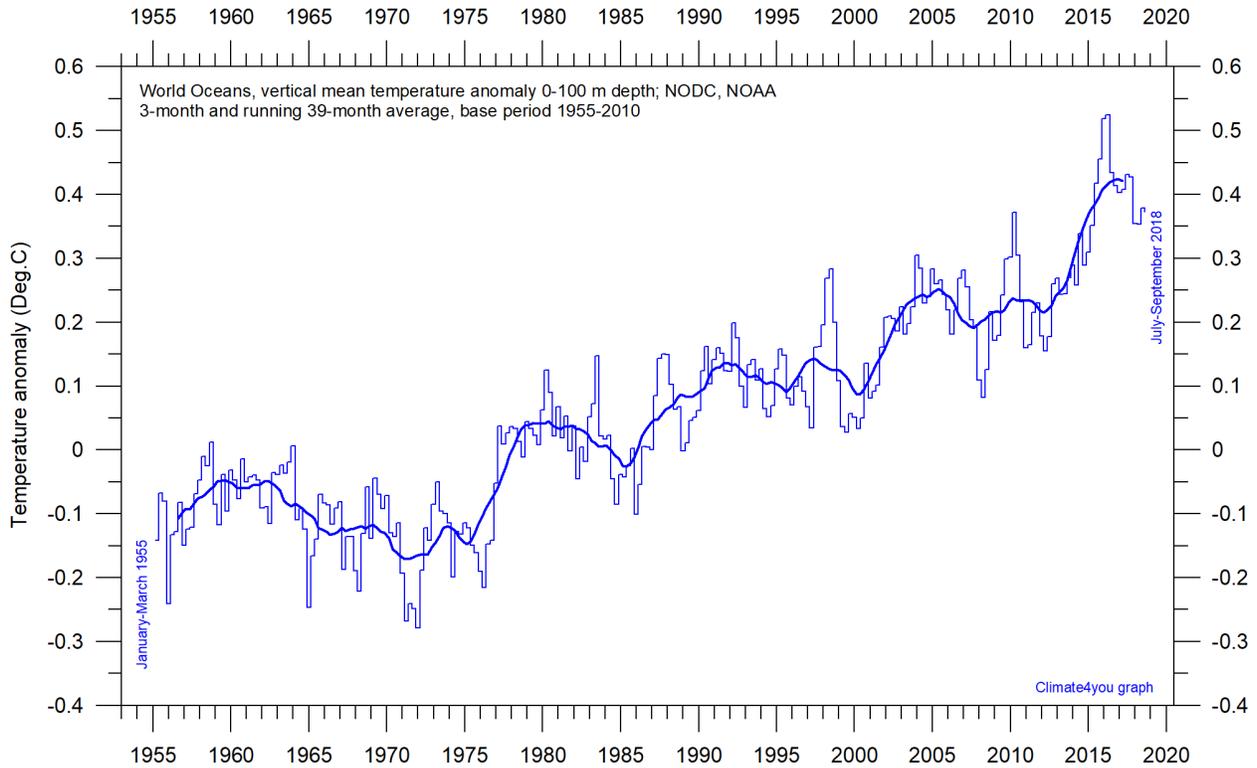
World Oceans vertical average temperature 0-100 m depth since 1955. The thin line indicates 3-month values, and the thick line represents the simple running 39-month (c. 3 year) average. Data source: NOAA National Oceanographic Data Center (NODC). Base period 1955-2010.

Ocean vertical average temperature 0-100 m depth since 1955. The thin line indicate 3-month values, and the thick line represents the simple running 39-month (c. 3 year) average. Data source: NOAA National Oceanographic Data Center (NODC). Base period 1955-2010.

Ocean vertical average temperature 0-100 m depth since 1955. The thin line indicate 3-month values, and the thick line represents the simple running 39-month (c. 3 year) average. Data source: NOAA National Oceanographic Data Center (NODC). Base period 1955-2010.
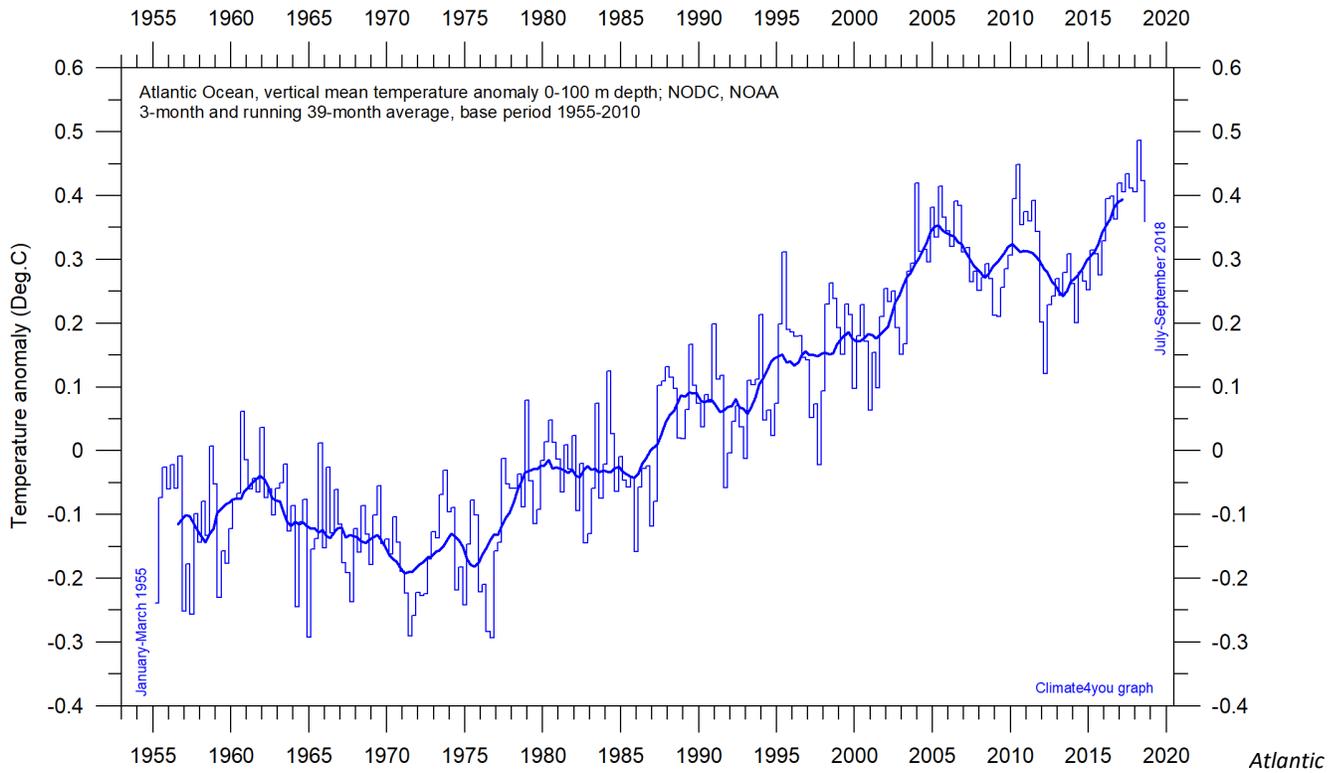
Indian Ocean vertical average temperature 0-100 m depth since 1955. The thin line indicate 3-month values, and the thick line represents the simple running 39-month (c. 3 year) average. Data source: NOAA National Oceanographic Data Center (NODC). Base period 1955-2010.
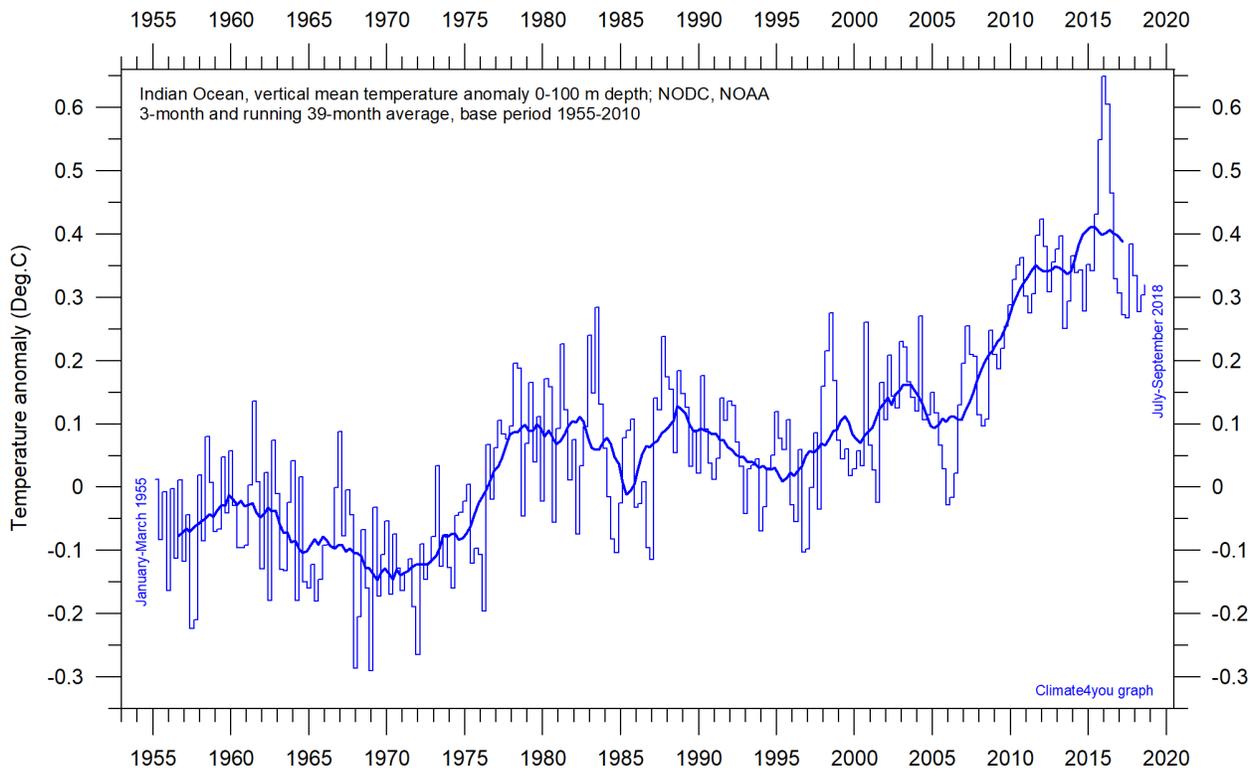
North Atlantic heat content uppermost 700 m, updated to September 2018
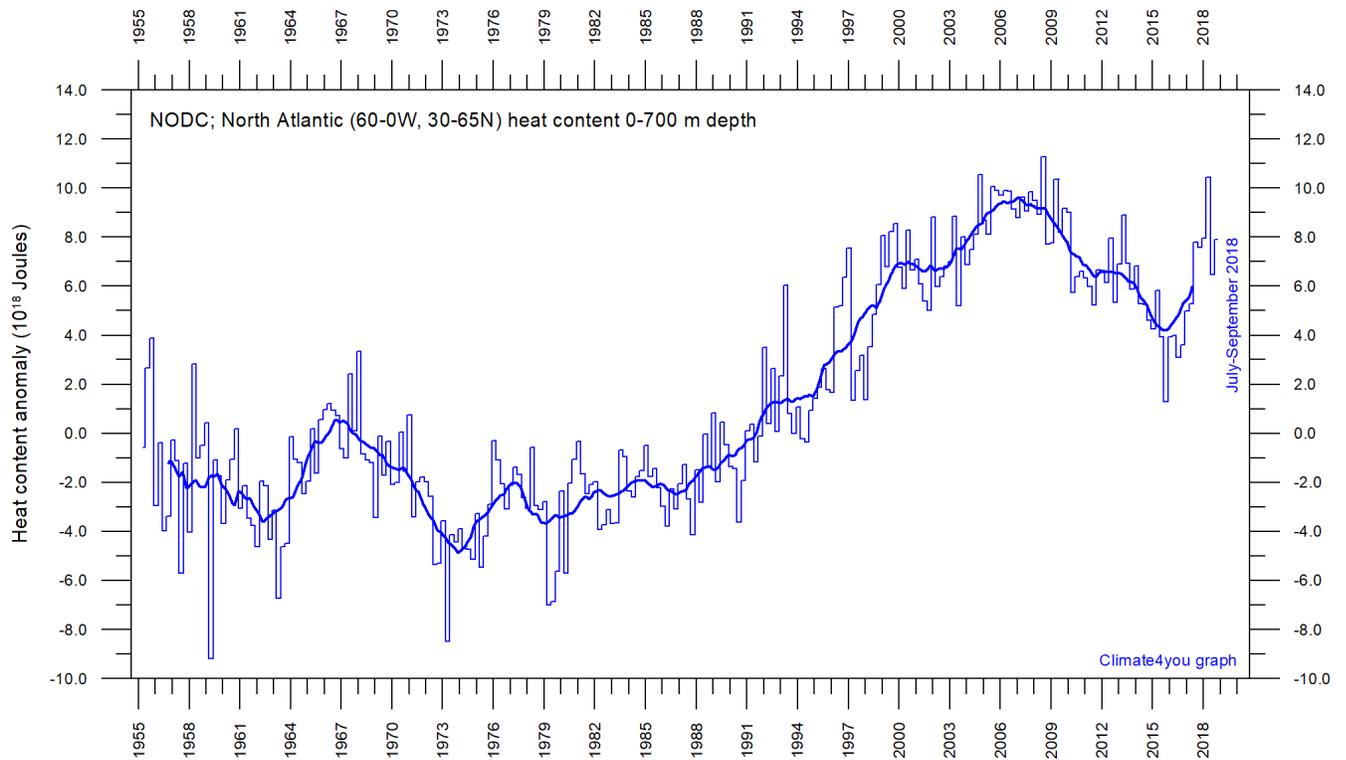
Global monthly heat content anomaly (10^{18} Joules) in the uppermost 700 m of the North Atlantic (60-0W, 30-65N; see map above) ocean since January 1955. The thin line indicates monthly values, and the thick line represents the simple running 37-month (c. 3 year) average. Data source: National Oceanographic Data Center (NODC).

North Atlantic temperatures 0-800 m depth along 59ºN, 30-0W, updated to June 2018
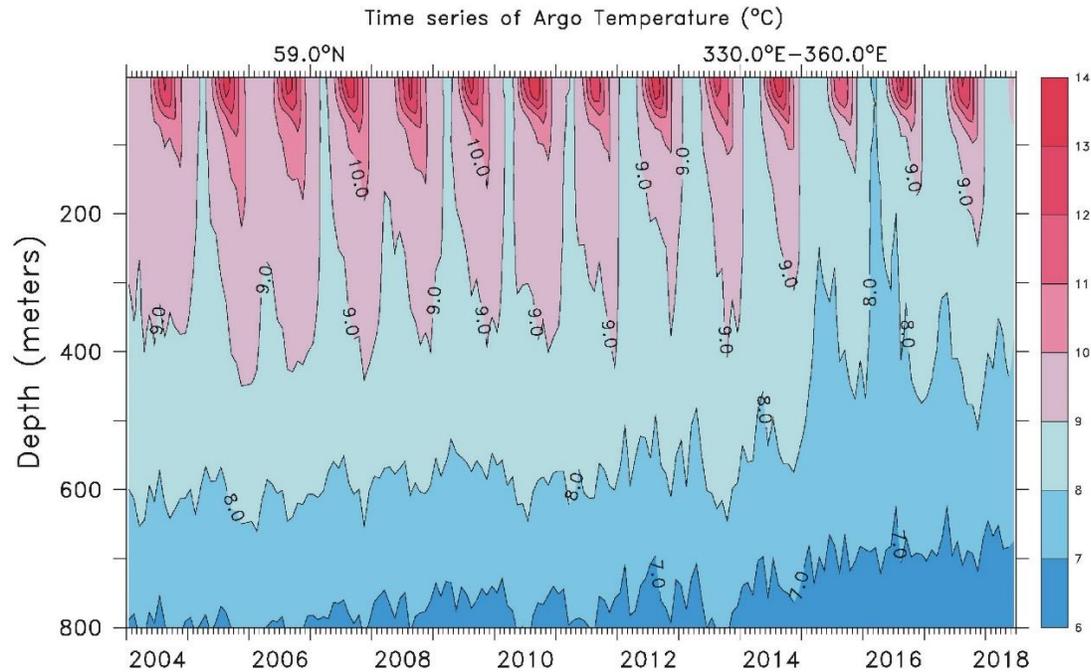
Time series depth-temperature diagram along 59 N across the North Atlantic Current from 30ºW to 0ºW, from surface to 800 m depth. Source: Global Marine Argo Atlas. See also the diagram below.
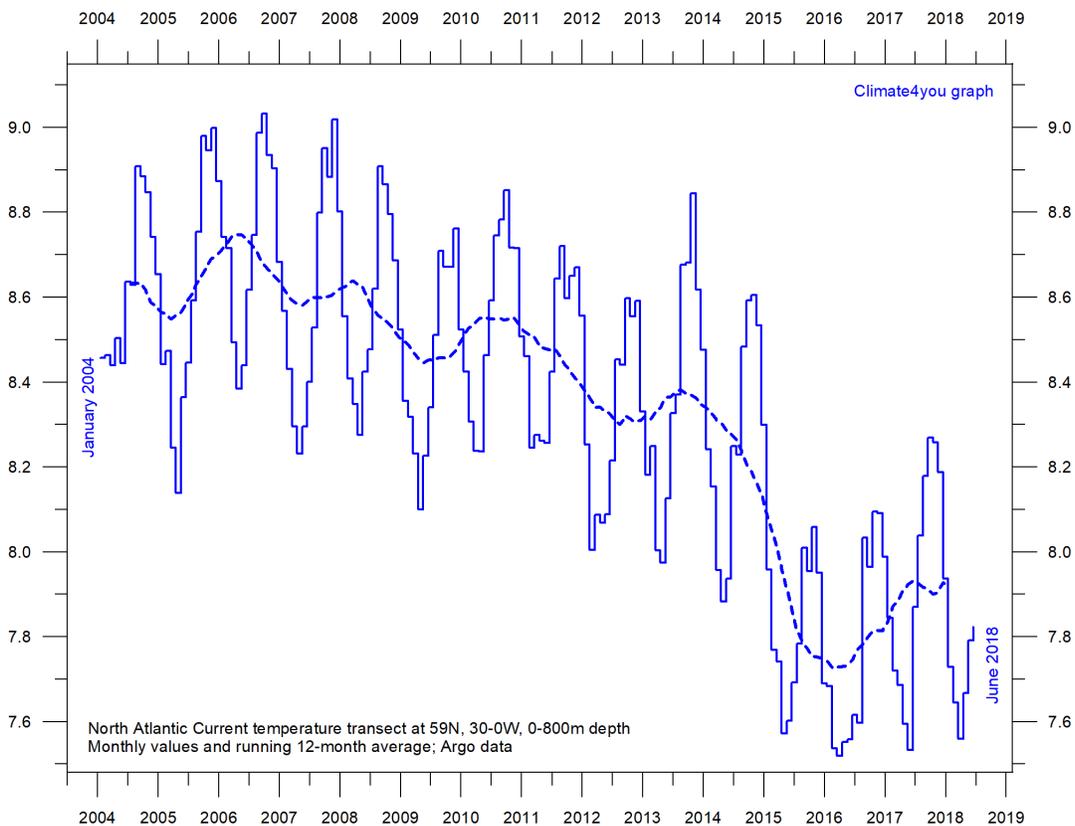
Average temperature along 59 N, 30-0W, 0-800m depth, corresponding to the main part of the North Atlantic Current, using Argo-data. Source: Global Marine Argo Atlas. Additional information can be found in: Roemmich, D. and J. Gilson, 2009. The 2004-2008 mean and annual cycle of temperature, salinity, and steric height in the global ocean from the Argo Program. Progress in Oceanography, 82, 81-100.

Global ocean temperature 0-1900 m depth summary, updated to June 2018
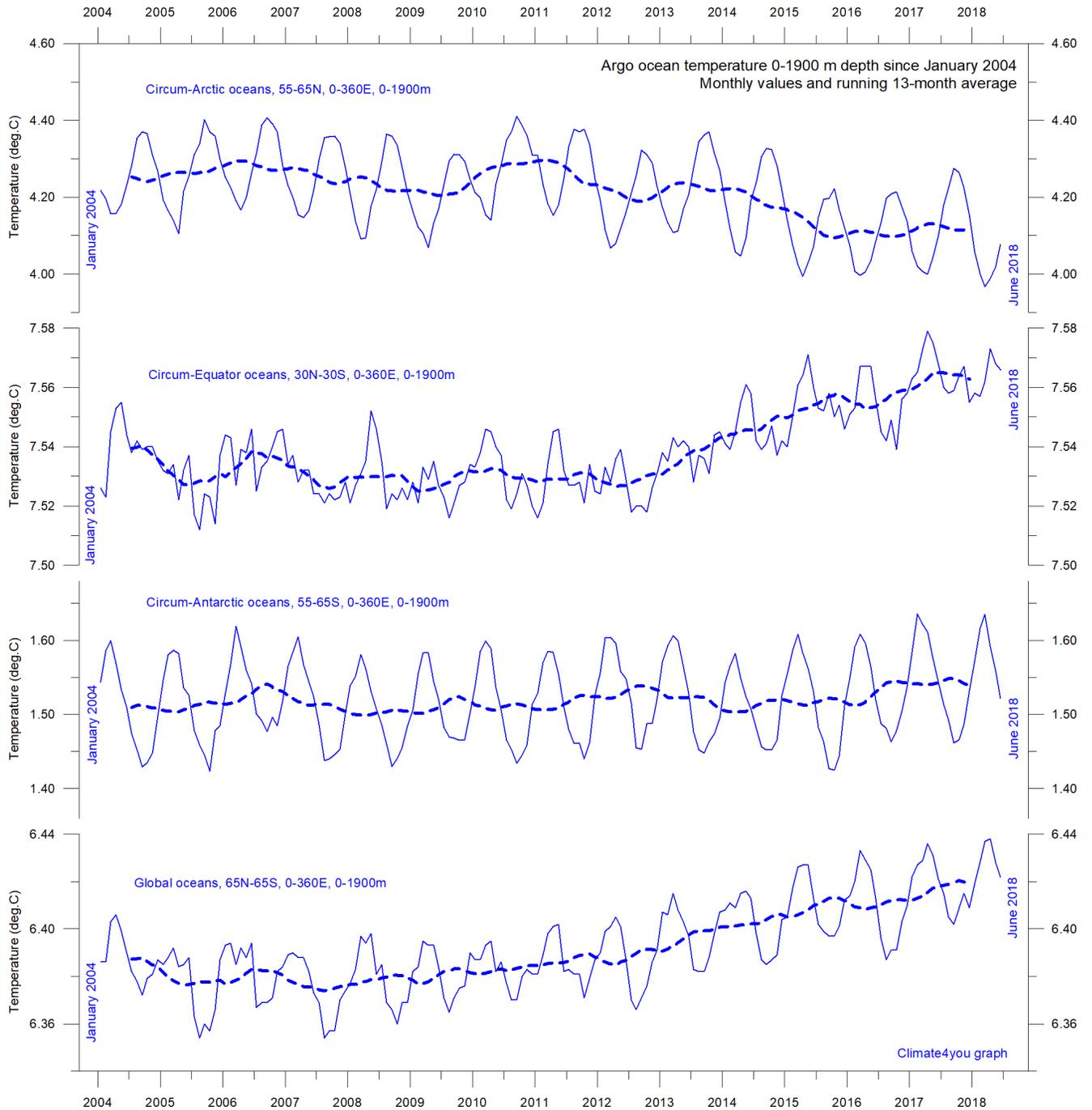
Summary of average temperature in uppermost 1900 m in different parts of the global oceans, using Argo-data. Source: Global Marine Argo Atlas. Additional information can be found in: Roemmich, D. and J. Gilson, 2009. The 2004-2008 mean and annual cycle of temperature, salinity, and steric height in the global ocean from the Argo Program. Progress in Oceanography, 82, 81-100.

Global ocean net temperature change since 2004 at different depths, updated to June 2018

Arctic oceans, 55N-65N, 0-360E, 0-1900 m depth
Argo temperature change from 2004 to 2018

Argo temperature change from
first 12 month in record (Jan-Dec 2004) to
last 12 months in record (July 2017 - June 2018)

Equatorial oceans, 30N-30S, 0-360E, 0-1900 m depth

Antarctic oceans, 55S-65S, 0-360E, 0-1900 m depth

Climate4you graph
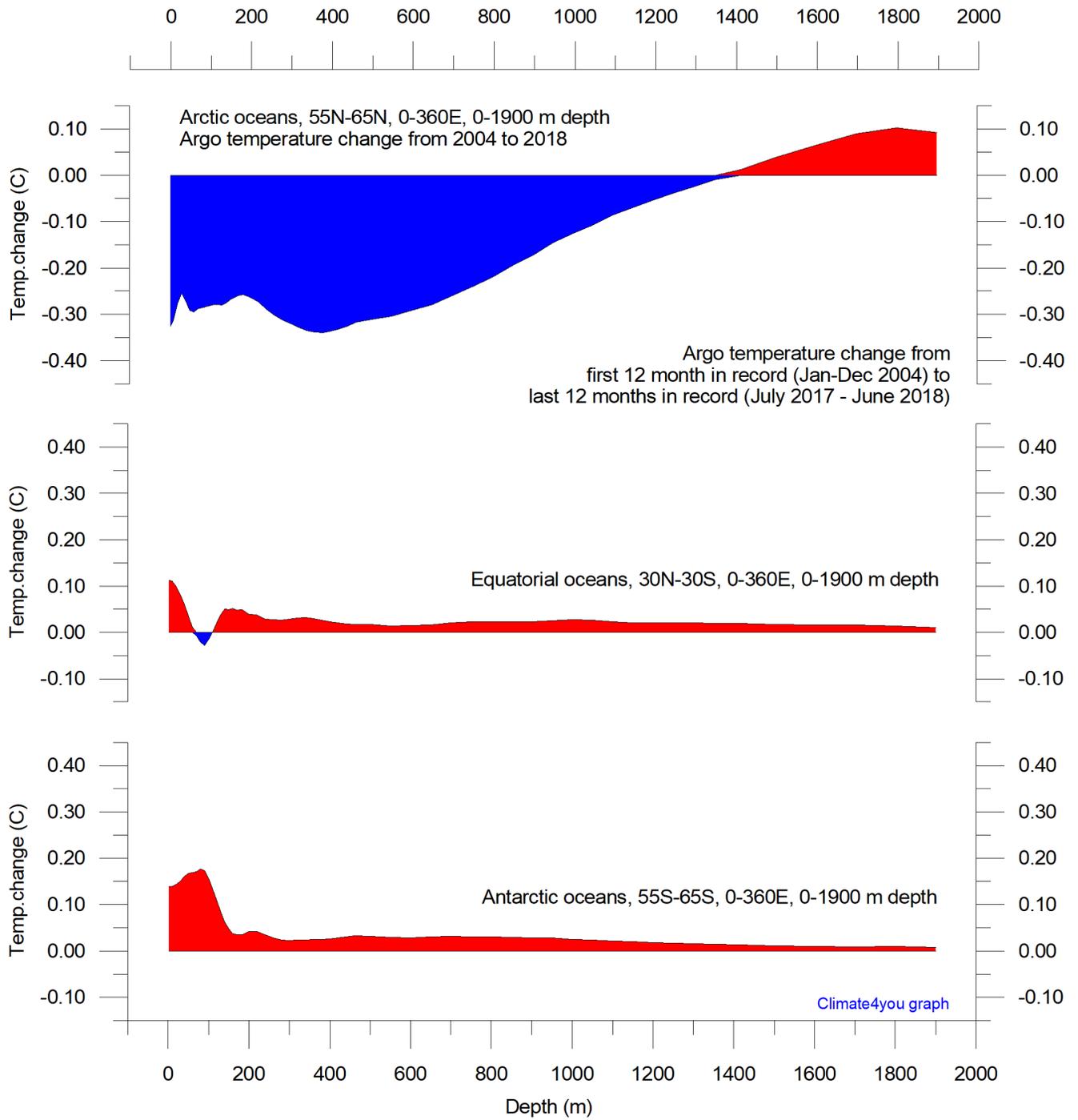
Net temperature change since 2004 from surface to 1900 m depth in different parts of the global oceans, using Argo-data. Source: Global Marine Argo Atlas. Additional information can be found in: Roemmich, D. and J. Gilson, 2009. The 2004-2008 mean and annual cycle of temperature, salinity, and steric height in the global ocean from the Argo Program. Progress in Oceanography, 82, 81-100. Please note that due to the spherical form of Earth, northern and southern latitudes represent only small ocean volumes, compared to latitudes near the Equator.

La Niña and El Niño episodes, updated to November 2018
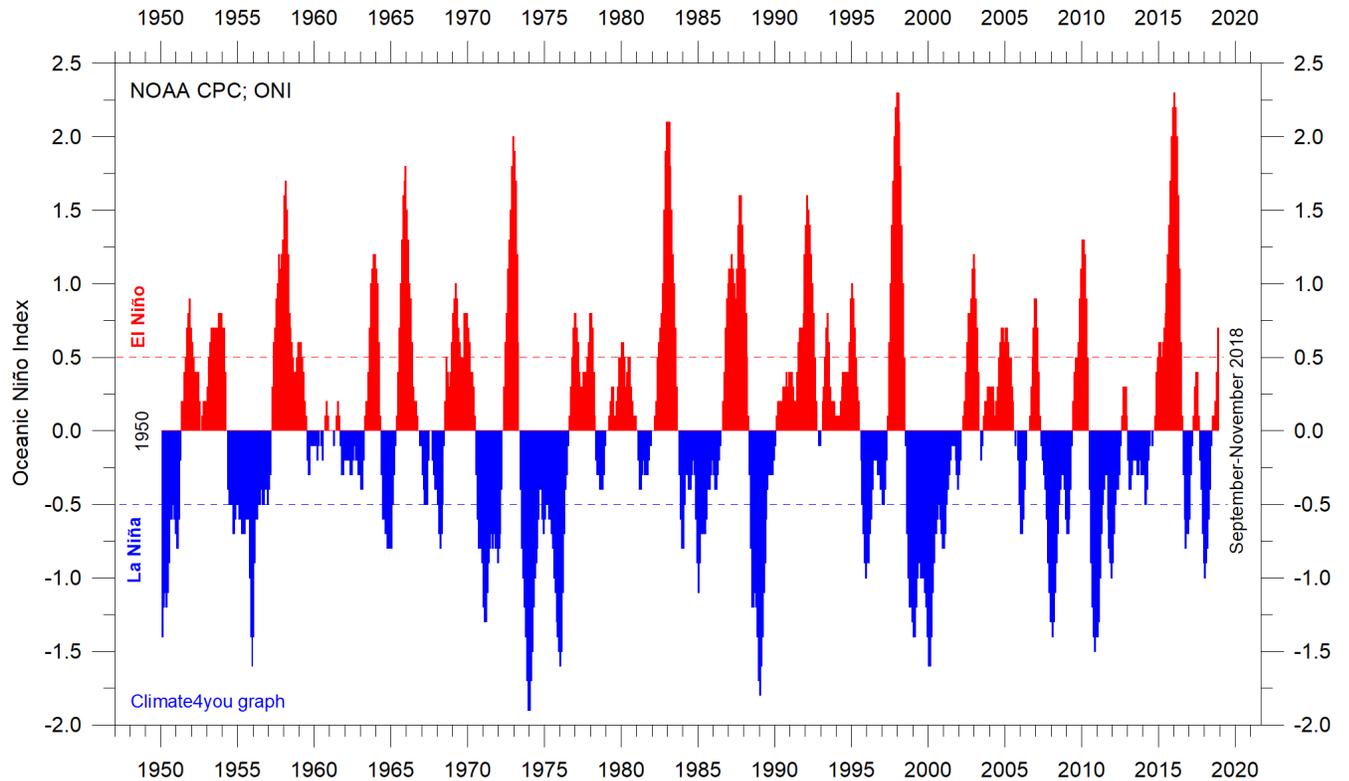
Warm (>+0.5ºC) and cold (<0.5ºC) episodes for the Oceanic Niño Index (ONI), defined as 3 month running mean of ERSSTv4 SST anomalies in the Niño 3.4 region (5ºN-5ºS, 120º-170ºW)]. For historical purposes cold and warm episodes are defined when the threshold is met for a minimum of 5 consecutive over-lapping seasons. Anomalies are centred on 30-yr base periods updated every 5 years.

Troposphere and stratosphere temperatures from satellites, updated to November 2018
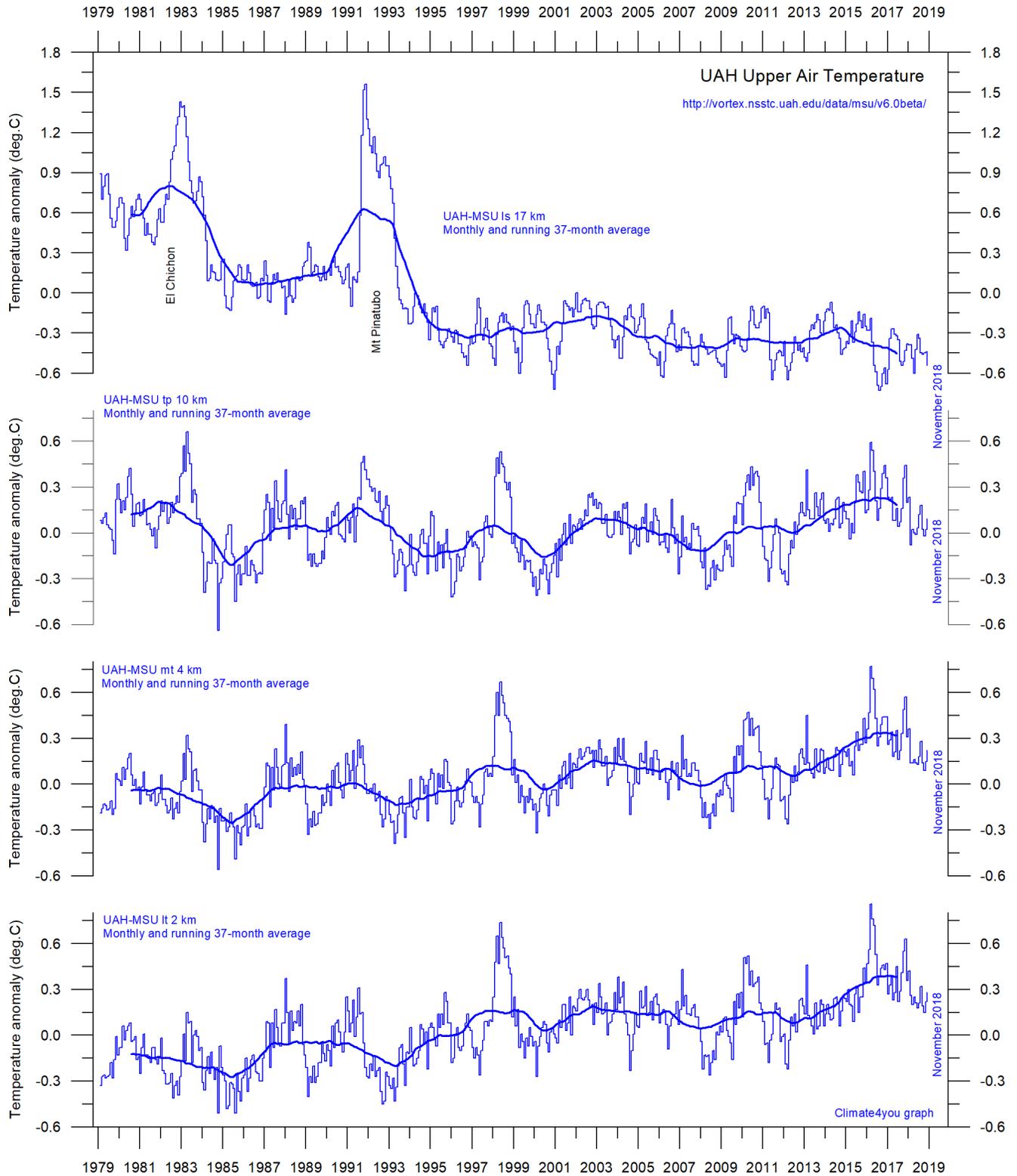
Global monthly average temperature in different according to University of Alabama at Huntsville, USA. The thin lines represent the monthly average, and the thick line the simple running 37-month average, nearly corresponding to a running 3-year average.

Zonal lower troposphere temperatures from satellites, updated to November 2018
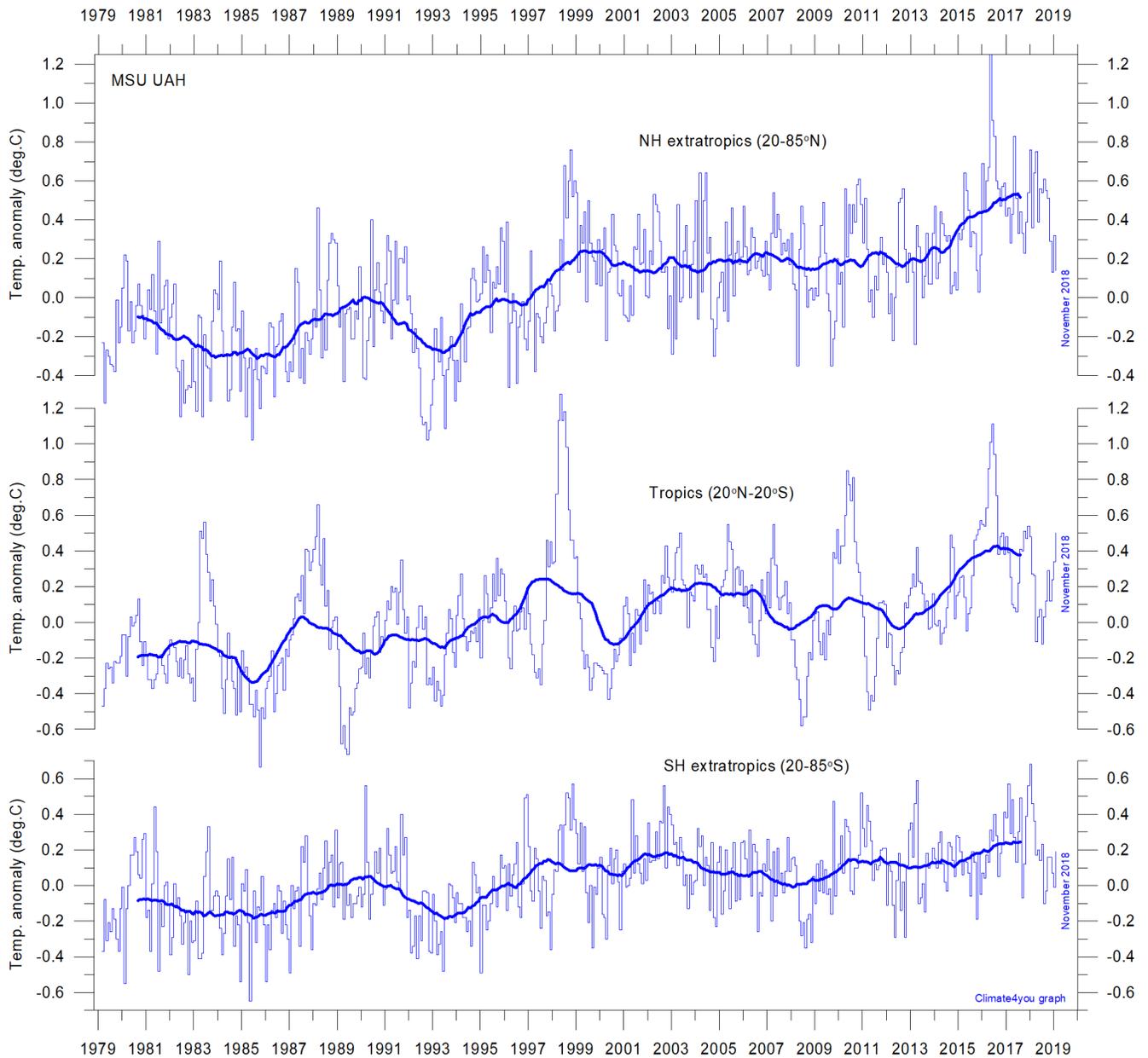
Global monthly average lower troposphere temperature since 1979 for the tropics and the northern and southern extratropics, according to University of Alabama at Huntsville, USA. Thin lines show the monthly temperature. Thick lines represent the simple running 37-month average, nearly corresponding to a running 3-year average. Reference period 1981-2010.

Arctic and Antarctic lower troposphere temperature, updated to November 2018
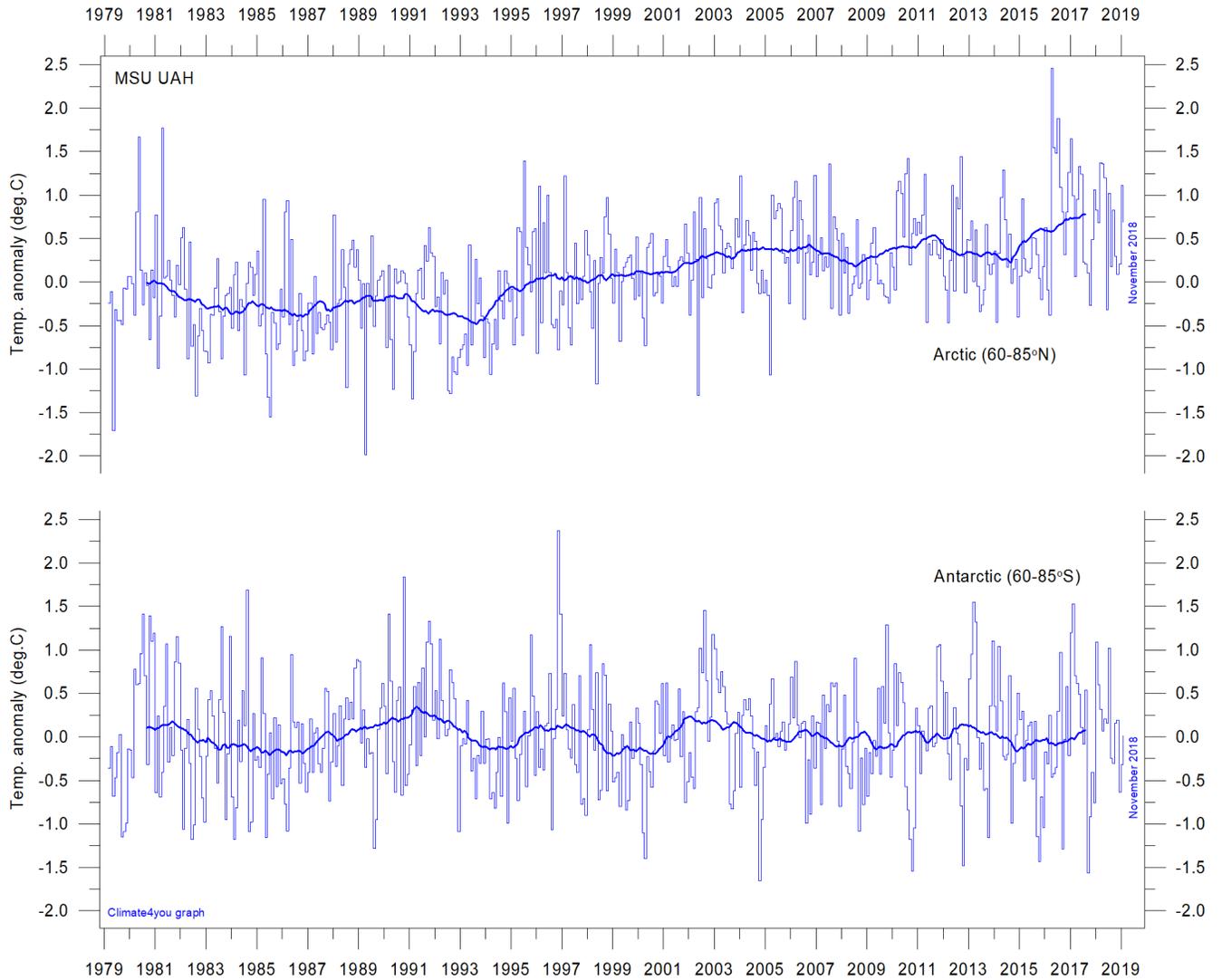
Global monthly average lower troposphere temperature since 1979 for the North Pole and South Pole regions, based on satellite observations ([University of Alabama](#) at Huntsville, USA). Thin lines show the monthly temperature. The thick line is the simple running 37-month average, nearly corresponding to a running 3-year average. Reference period 1981-2010.

Temperature over land versus over oceans, updated to November 2018
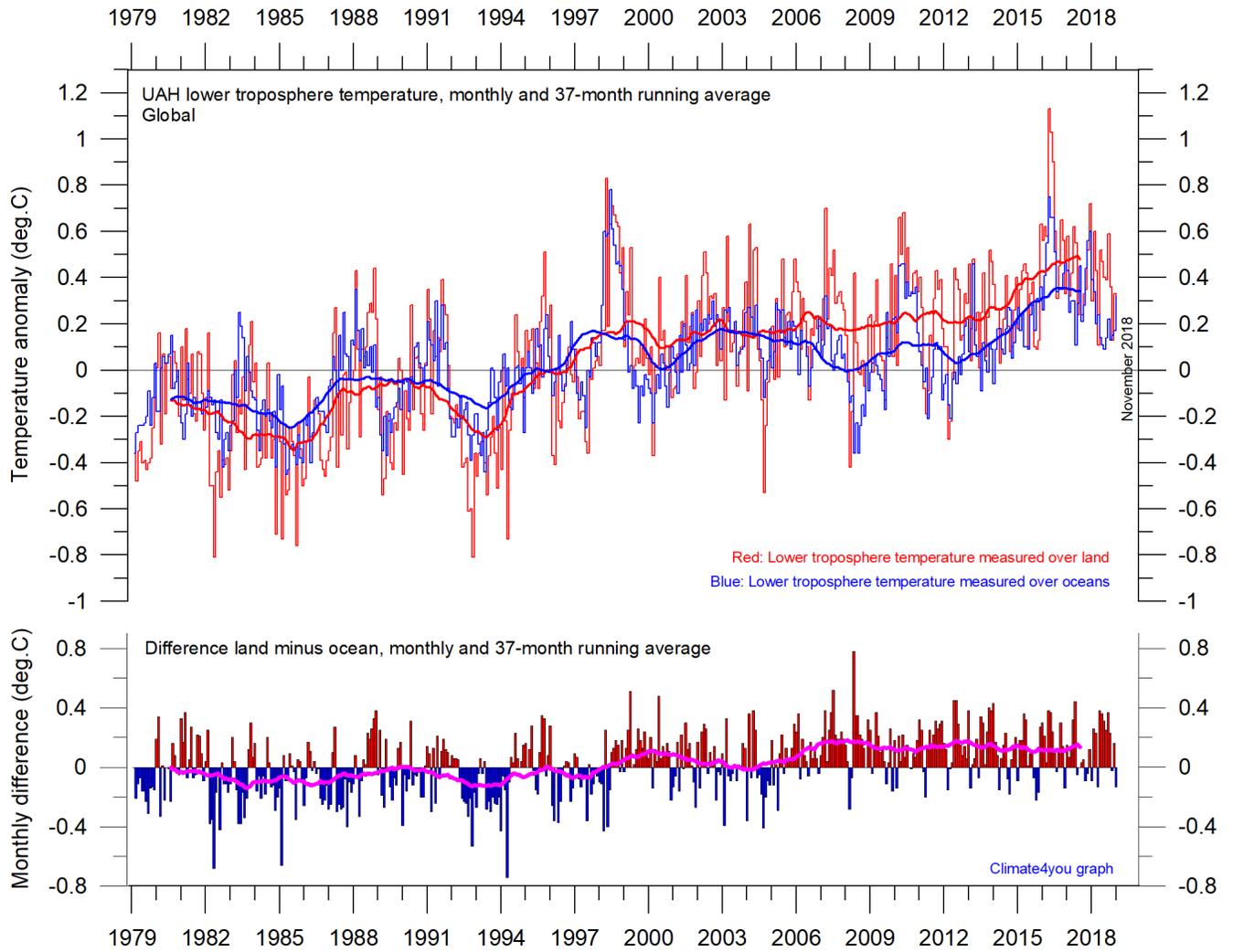
Global monthly average lower troposphere temperature since 1979 measured over land and oceans, respectively, according to *University of Alabama* at Huntsville, USA. Thick lines are the simple running 37-month average, nearly corresponding to a running 3-year average. Reference period 1981-2010.

Arctic and Antarctic surface air temperature, updated to October 2018

Diagram showing area weighted Arctic (70-90ºN) monthly surface air temperature anomalies ([HadCRUT4](#)) since January 2000, in relation to the WMO [normal period](#) 1961-1990. The thin line shows the monthly temperature anomaly, while the thicker line shows the running 37-month (c. 3 year) average.

Diagram showing area weighted Antarctic (70-90ºN) monthly surface air temperature anomalies ([HadCRUT4](#)) since January 2000, in relation to the WMO [normal period](#) 1961-1990. The thin line shows the monthly temperature anomaly, while the thicker line shows the running 37-month (c. 3 year) average.

Diagram showing area weighted Arctic (70-90ᵒN) monthly surface air temperature anomalies ([HadCRUT4](#)) since January 1957, in relation to the WMO [normal period](#) 1961-1990. The thin line shows the monthly temperature anomaly, while the thicker line shows the running 37-month (c. 3 year) average.

Diagram showing area weighted Antarctic (70-90ᵒN) monthly surface air temperature anomalies ([HadCRUT4](#)) since January 1957, in relation to the WMO [normal period](#) 1961-1990. The thin line shows the monthly temperature anomaly, while the thicker line shows the running 37-month (c. 3 year) average.
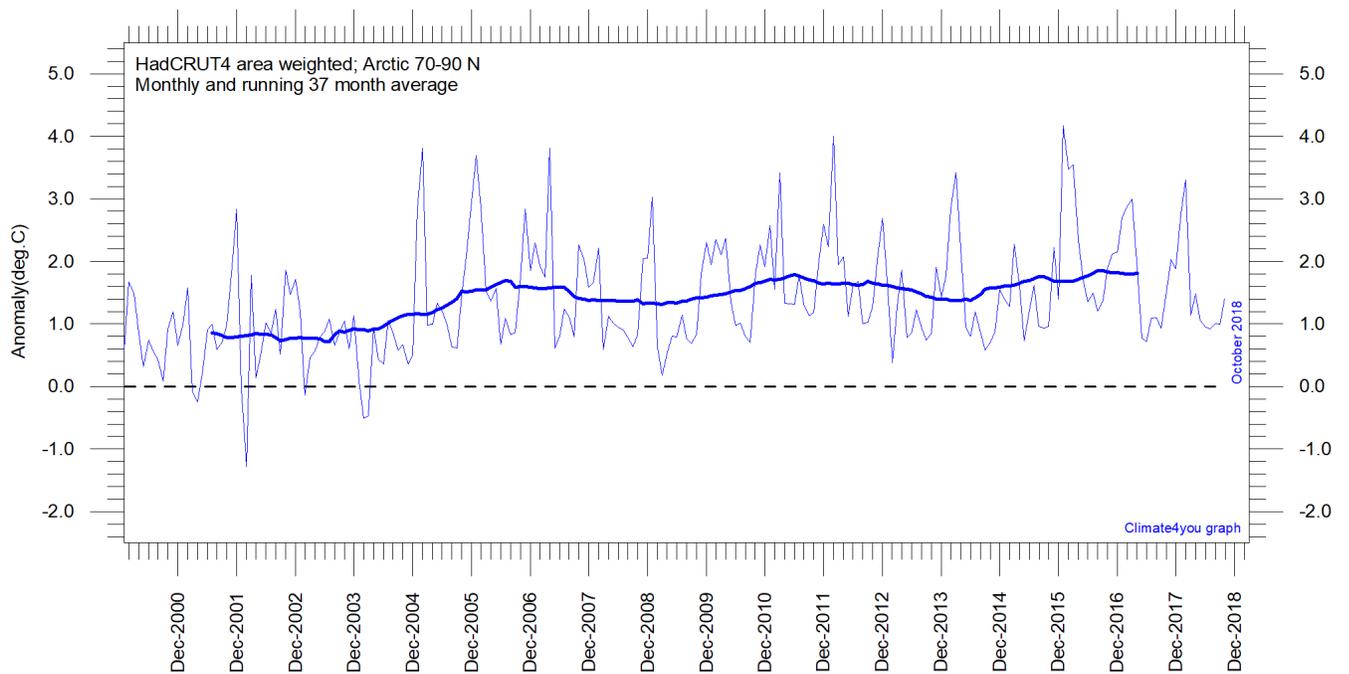
Diagram showing area-weighted Arctic (70-90ºN) monthly surface air temperature anomalies ([HadCRUT4](#)) since January 1920, in relation to the WMO [normal period](#) 1961-1990. The thin line shows the monthly temperature anomaly, while the thicker line shows the running 37-month (c. 3 year) average.
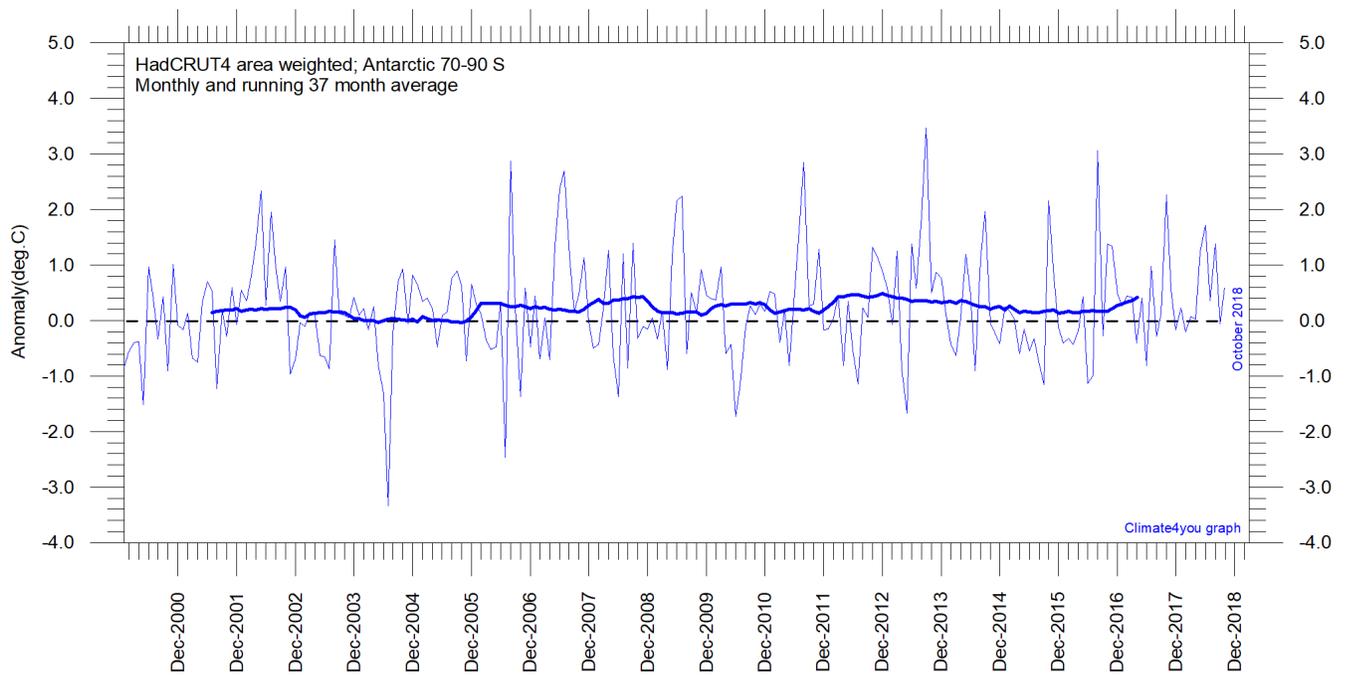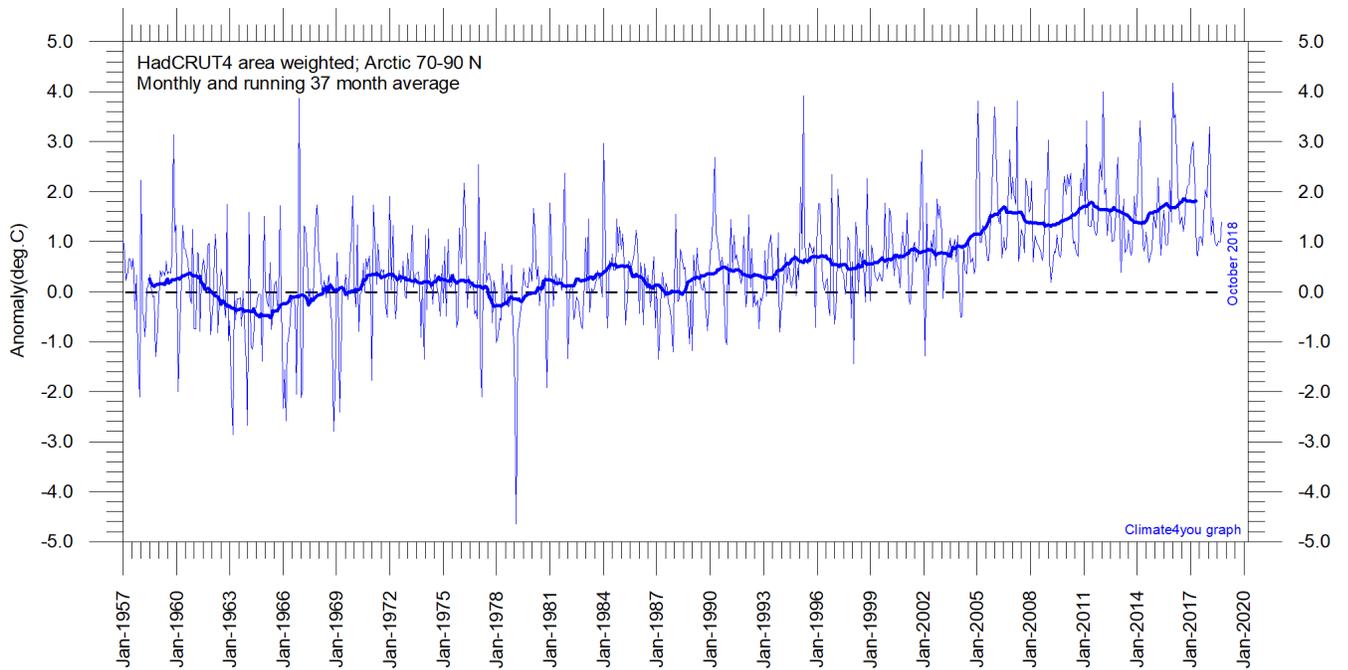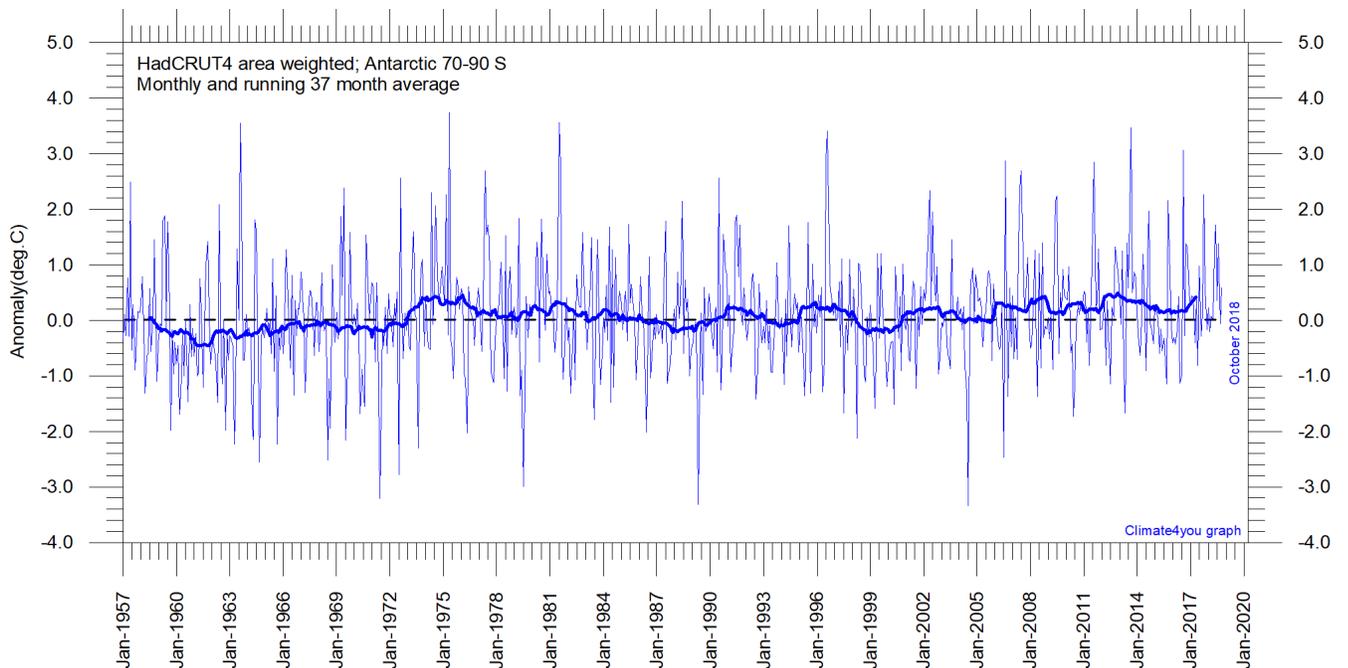
Because of the relatively small number of Arctic stations before 1930, month-to-month variations in the early part of the Arctic temperature record 1920-2018 are larger than later (diagram above).

The period from about 1930 saw the establishment of many new Arctic meteorological stations, first in Russia and Siberia, and following the 2nd World War, also in North America. The period since 2005 is warm, about as warm as the period 1930-1940.

As the HadCRUT4 data series has improved high latitude coverage data coverage (compared to the HadCRUT3 series), the individual 5ºx5º grid cells has been weighted according to their surface area. This area correction is especially important for polar regions.

This approach contrasts with that adopted by [Gillet et al. 2008](#), which calculated a simple average, with no correction for the significant surface area effect of latitude in polar regions.

Literature:

Gillett, N.P., Stone, D.A., Stott, P.A., Nozawa, T., Karpechko, A.Y.U., Hegerl, G.C., Wehner, M.F. and Jones, P.D. 2008. Attribution of polar warming to human influence. *Nature Geoscience* 1, 750-754.

Arctic and Antarctic sea ice, updated to November 2018
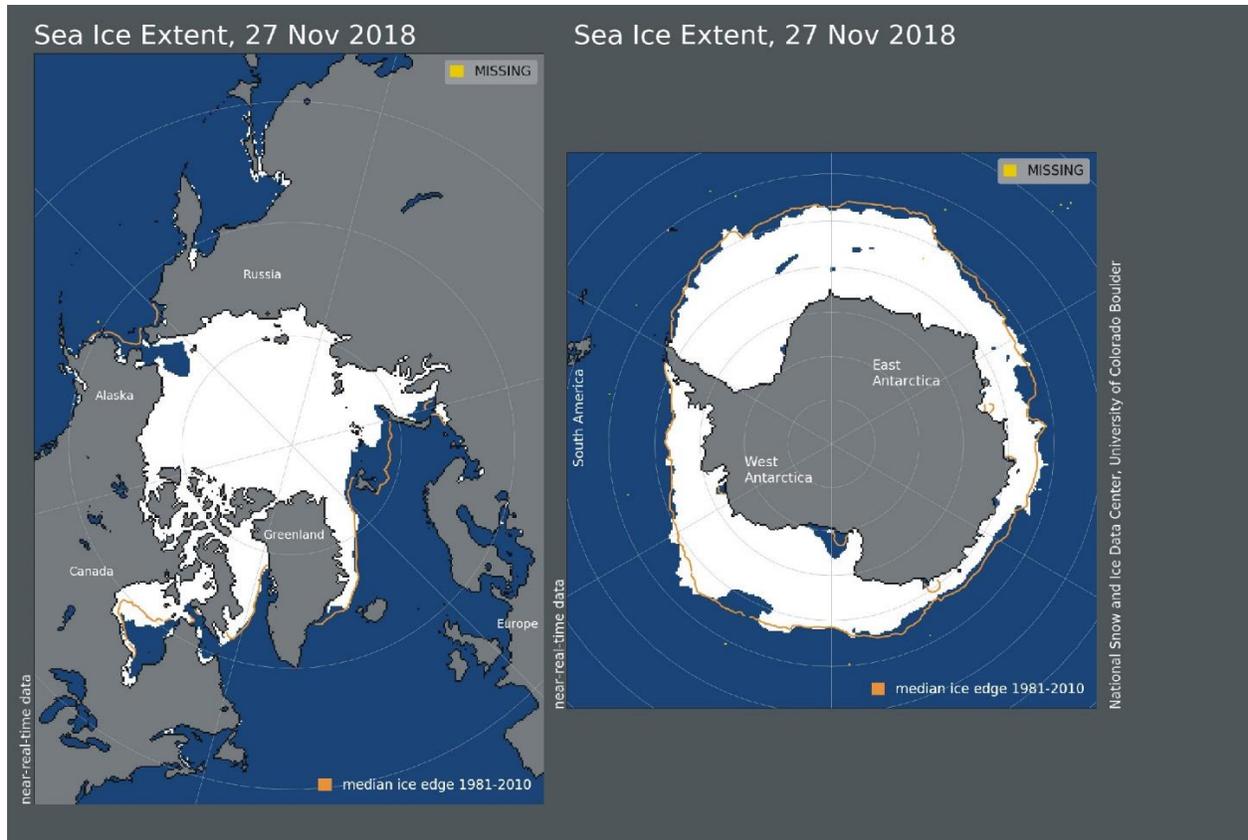
Sea ice extent 27 November 2018. The median limit of sea ice (orange line) is defined as 15% sea ice cover, according to the average of satellite observations 1981-2010 (both years included). Sea ice may therefore well be encountered outside and open water areas inside the limit shown in the diagrams above. Map source: National Snow and Ice Data Center (NSIDC).
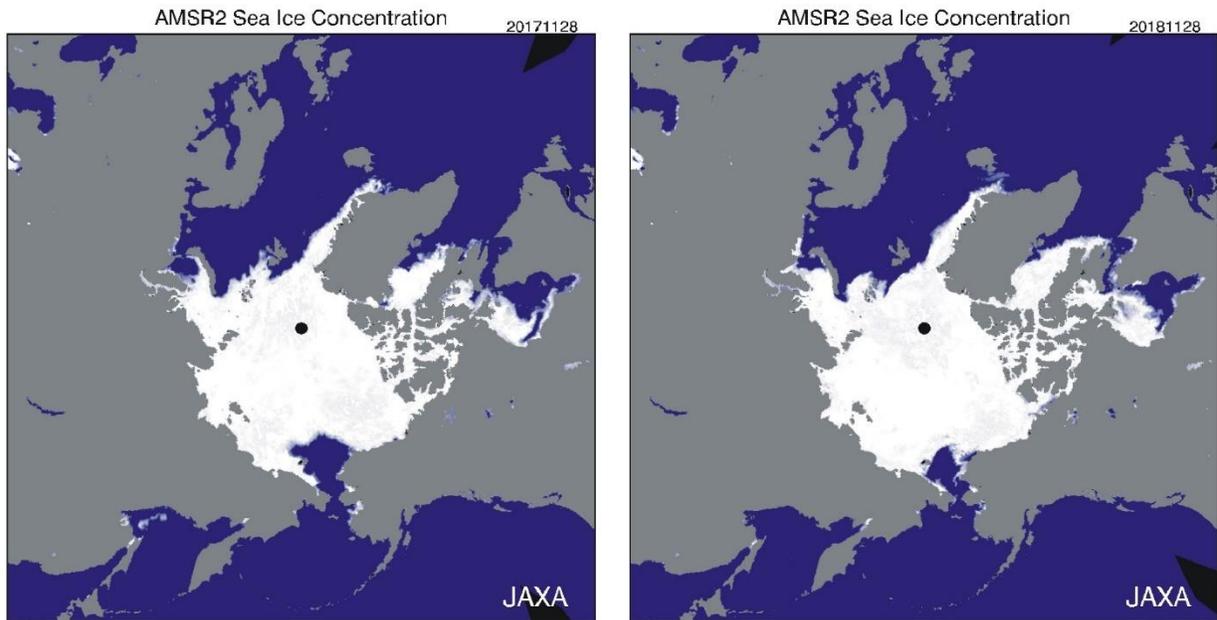
Diagrams showing Arctic sea ice extent and concentration 28 November 2017 (left) and 2018 (right), according to the Japan Aerospace Exploration Agency (JAXA).
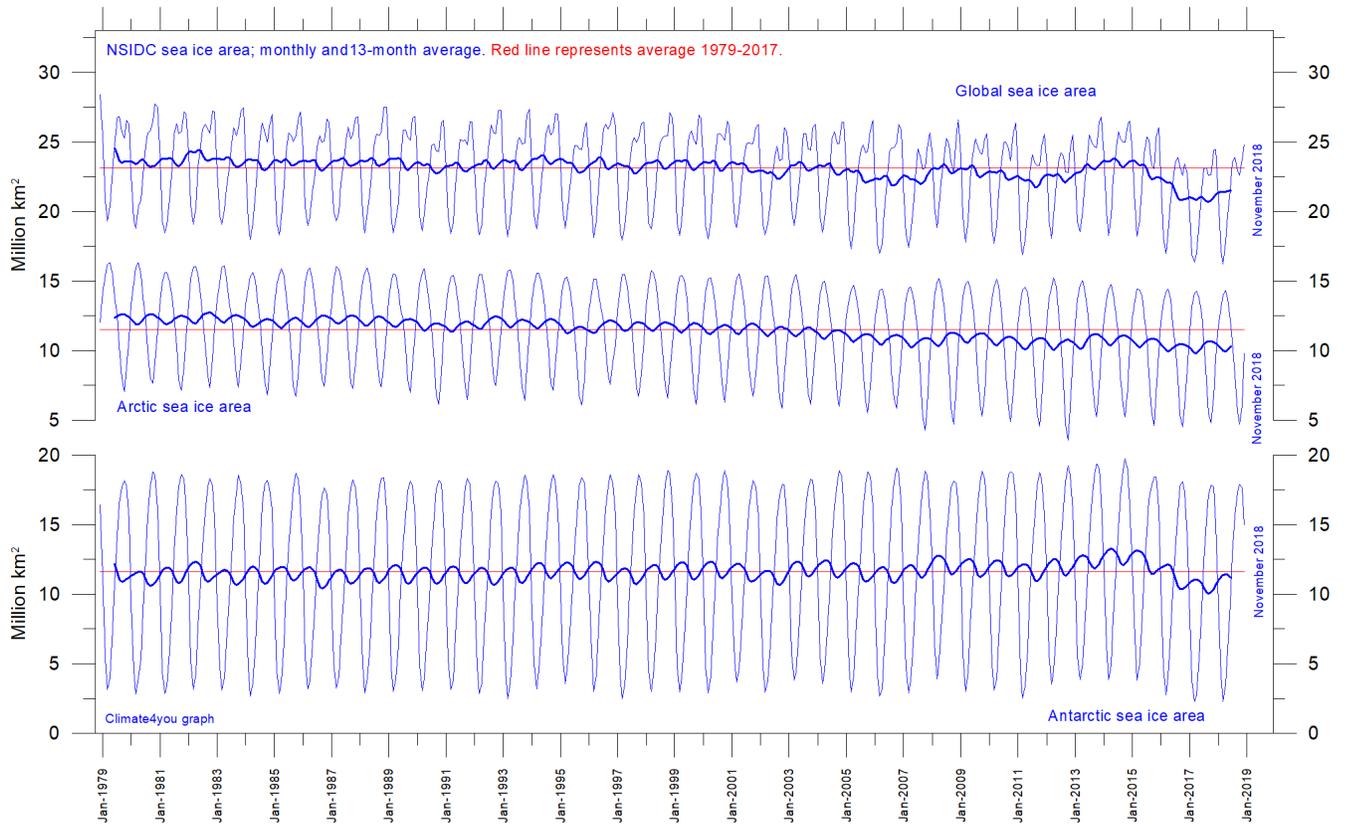
Graphs showing monthly Antarctic, Arctic and global sea ice extent since November 1978, according to the [National Snow and Ice data Center](#) (NSIDC).
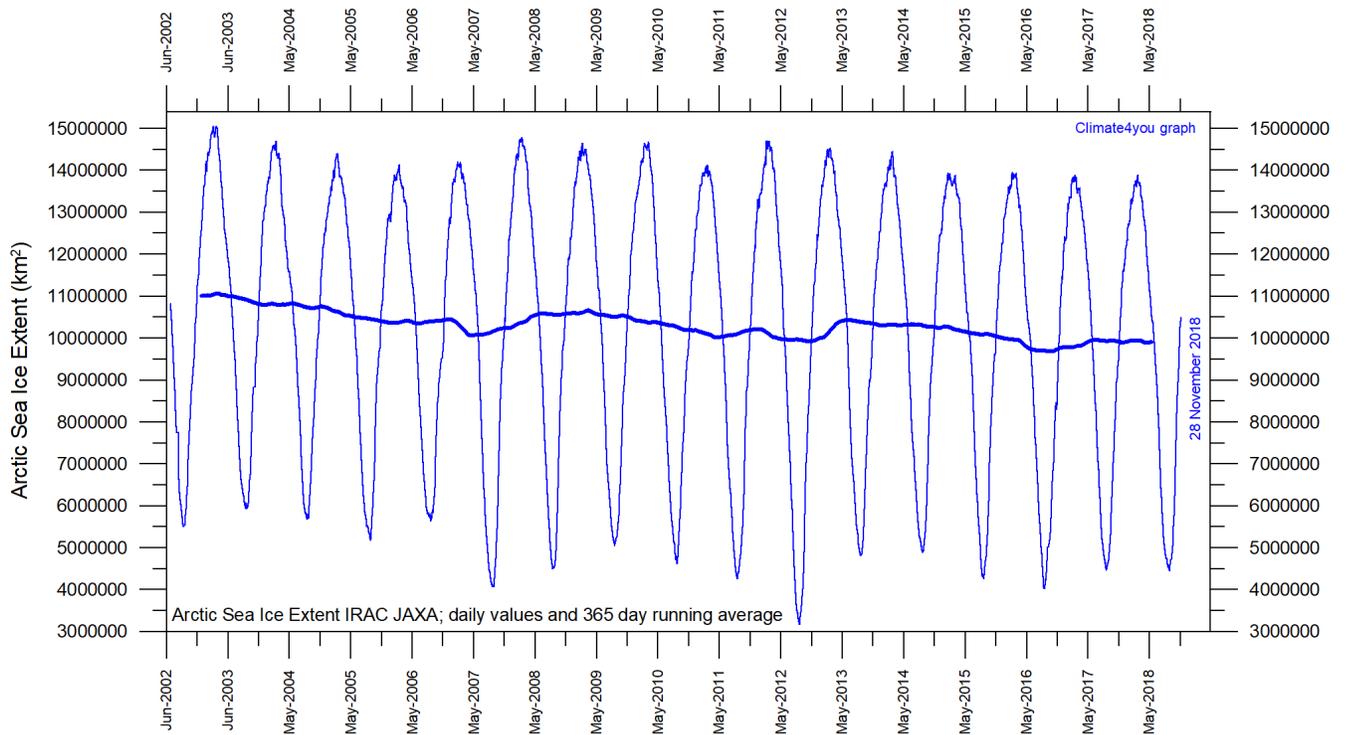
Diagram showing daily Arctic sea ice extent since June 2002, to 28 November 2018, by courtesy of [Japan Aerospace Exploration Agency](#) (JAXA).

Sea Ice Thickness, 28-Nov-2018
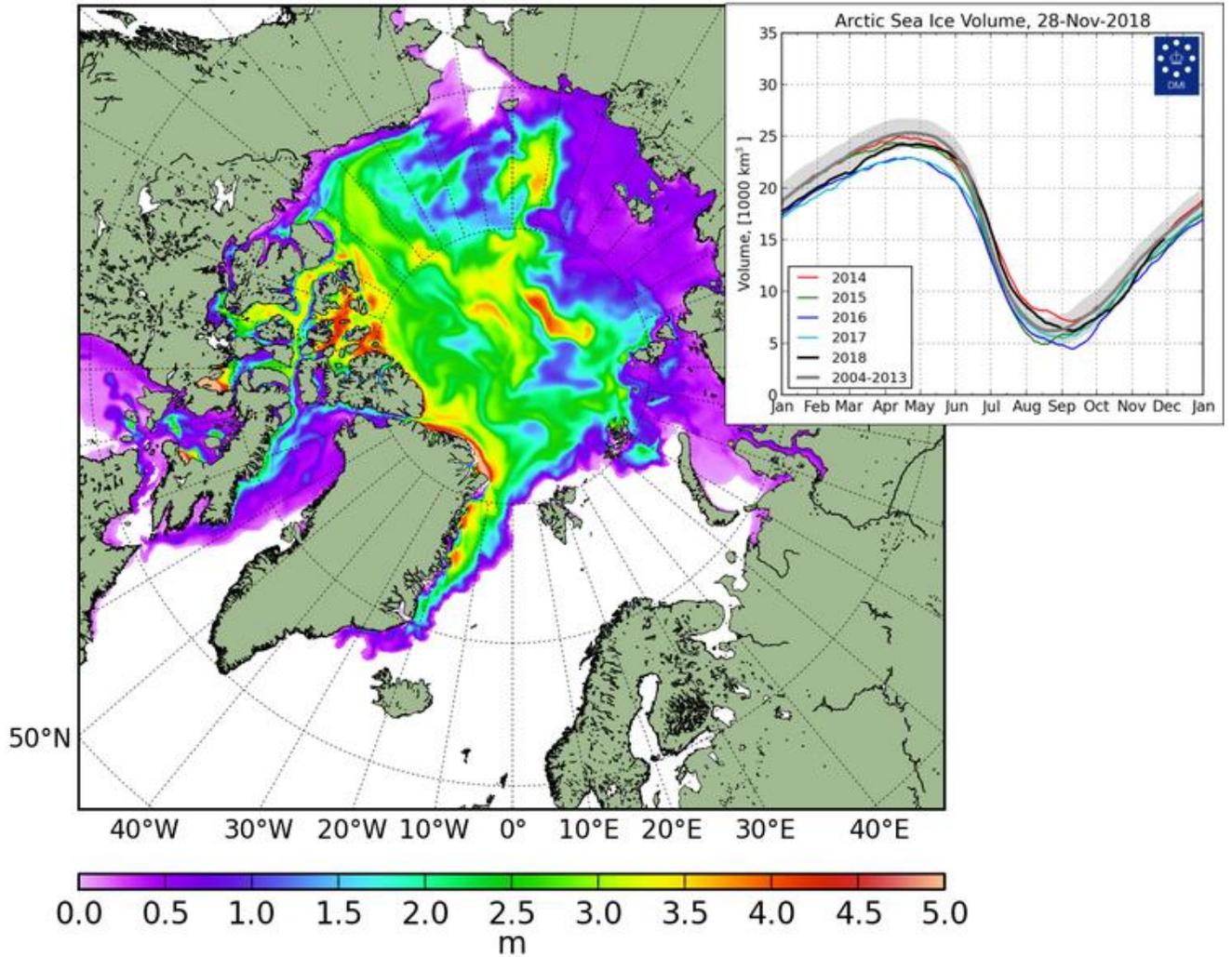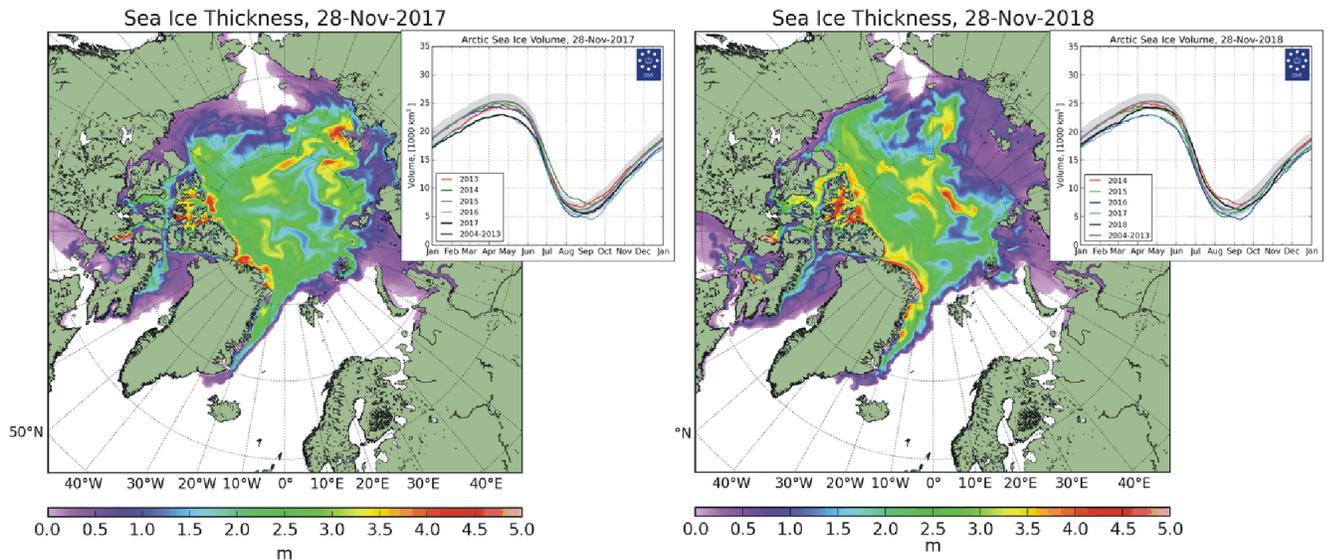
Diagrams showing Arctic sea ice extent and thickness 28 November 2017 (left) and 2018 (right and above) and the seasonal cycles of the calculated total arctic sea ice volume, according to [The Danish Meteorological Institute (DMI)](). The mean sea ice volume and standard deviation for the period 2004-2013 are shown by grey shading.

12 month average sea ice extent (Mill. km²); NSIDC

October 1979

October 1979

Southern Hemisphere

Northern Hemisphere

November 2018

November 2018

Global 12 month average sea ice extent (Mill. km²); NSIDC

October 1979

Global average 1979-2017

November 2018

Climate4you graph
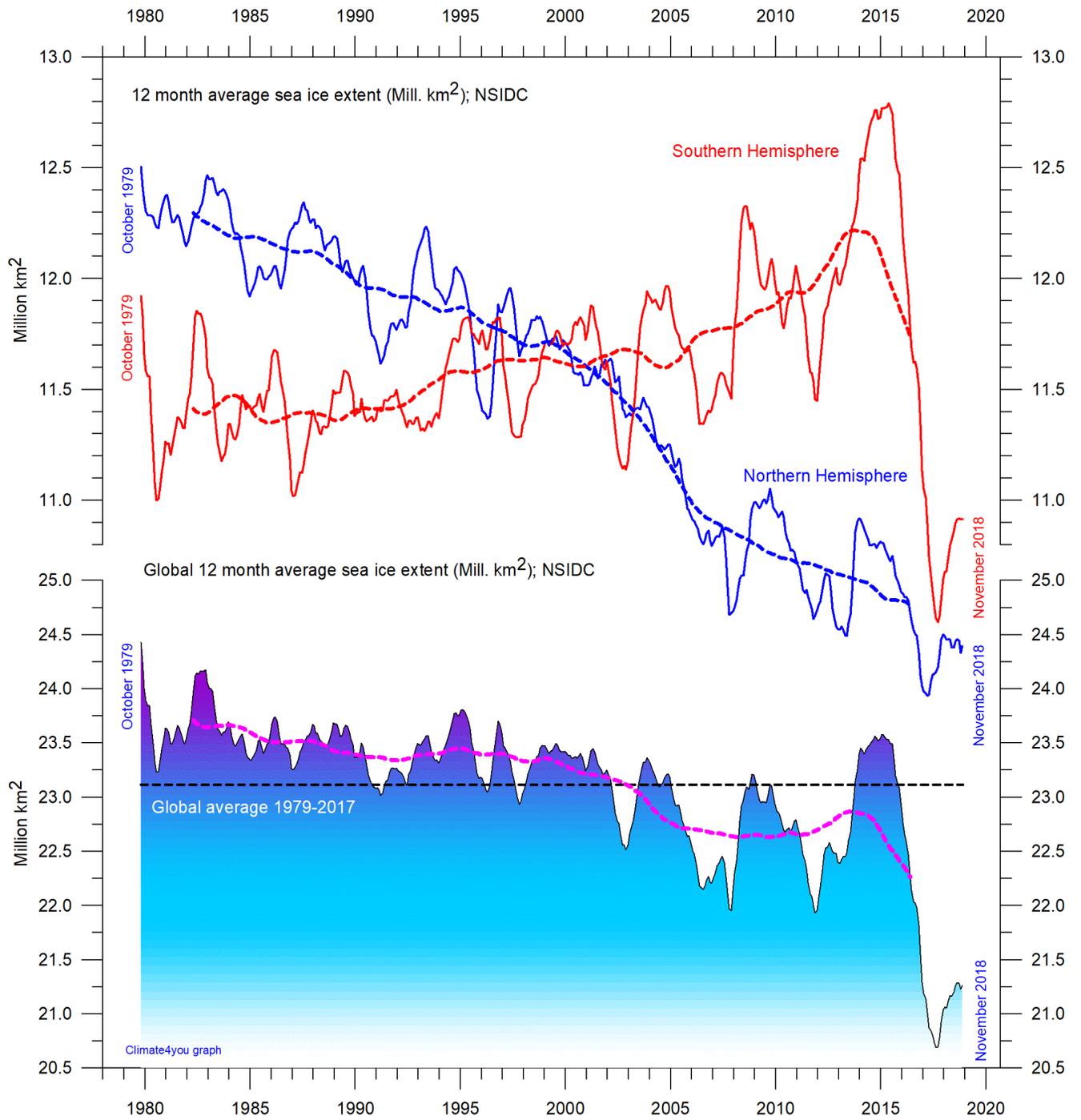
12 month running average sea ice extension, global and in both hemispheres since 1979, the satellite-era. The October 1979 value represents the monthly 12-month average of November 1978 - October 1979, the November 1979 value represents the average of December 1978 - November 1979, etc. The stippled lines represent a 61-month (ca. 5 years) average. Data source: National Snow and Ice Data Center (NSIDC).

Sea level in general

Global (or eustatic) sea-level change is measured relative to an idealised reference level, the geoid, which is a mathematical model of planet Earth's surface (Carter et al. 2014). Global sea-level is a function of the volume of the ocean basins and the volume of water they contain. Changes in global sea-level are caused by – but not limited to - four main mechanisms:

1. Changes in local and regional air pressure and wind, and tidal changes introduced by the Moon.
2. Changes in ocean basin volume by tectonic (geological) forces.
3. Changes in ocean water density caused by variations in currents, water temperature and salinity.
4. Changes in the volume of water caused by changes in the mass balance of terrestrial glaciers.

In addition to these there are other mechanisms influencing sea-level; such as storage of ground water, storage in lakes and rivers, evaporation, etc.

Mechanism 1 is controlling sea-level at many sites on a time scale from months to several years. As an example, many coastal stations show a pronounced annual variation reflecting seasonal changes in air pressures and wind speed. Longer-term climatic changes playing out over decades or centuries will also affect measurements of sea-level changes. Hansen et al. (2011, 2015) provide excellent analyses of sea-level changes caused by recurrent changes of the orbit of the Moon and other phenomena.

Mechanism 2 – with the important exception of earthquakes and tsunamis - typically operates over long (geological) time scales and is not significant on human time scales. It may relate to variations in the sea-floor spreading rate, causing volume changes in mid-ocean mountain ridges, and to the slowly changing configuration of land and oceans. Another effect may be the slow rise of basins due to isostatic offloading by deglaciation after an ice age. The floor of the Baltic Sea and the Hudson Bay are presently rising, causing a slow net transfer of water from these basins into the adjoining oceans. Slow changes of very big glaciers (ice sheets) and movements in the mantle will affect the gravity field and thereby the vertical position of the ocean surface. Any increase of the total water mass as well as sediment deposition into oceans increase the load on their bottom, generating sinking by viscoelastic flow in the mantle below. The mantle flow is directed towards the surrounding land areas, which will rise, thereby partly compensating for the initial sea level increase induced by the increased water mass in the ocean.

Mechanism 3 (temperature-driven expansion) only affects the uppermost part of the oceans on human time scales. Usually, temperature-driven changes in density are more important than salinity-driven changes. Seawater is characterised by a relatively small coefficient of expansion, but the effect should however not be overlooked, especially when interpreting satellite altimetry data. Temperature-driven expansion of a column of seawater will not affect the total mass of water within the column considered and will therefore not affect the potential at the top of the water column. Temperature-driven ocean water expansion will therefore not in itself lead to any lateral displacement of water, but only locally lift the ocean surface. Near the coast, where people are living, the depth of water approaches zero, so no temperature-driven expansion will take place here (Mörner 2015). Mechanism 3 is for that reason not important for coastal regions.

Mechanism 4 (changes in glacier mass balance) is an important driver for global sea-level changes along coasts, for human time scales. Volume changes of floating glaciers – ice shelves – has no influence on the global sea-level, just like volume changes of floating sea ice has no influence. Only the mass-balance of grounded or land-based glaciers is important for the global sea-level along coasts.

Summing up: Mechanism 1 and 4 are the most important for understanding sea-level changes along coasts.

34

References:

Carter R.M., de Lange W., Hansen, J.M., Humlum O., Idso C., Kear, D., Legates, D., Mörner, N.A., Ollier C., Singer F. & Soon W. 2014. Commentary and Analysis on the Whitehead& Associates 2014 NSW Sea-Level Report. Policy Brief, NIPCC, 24. September 2014, 44 pp. http://climatechangereconsidered.org/wp-content/uploads/2014/09/NIPCC-Report-on-NSW-Coastal-SL-9z-corrected.pdf
Hansen, J.-M., Aagaard, T. and Binderup, M. 2011. Absolute sea levels and isostatic changes of the eastern North Sea to central Baltic region during the last 900 years. Boreas, 10.1111/j.1502-3885.2011.00229.x. ISSN 0300–9483.
Hansen, J.-M., Aagaard, T. and Huijpers, A. 2015. Sea-Level Forcing by Synchronization of 56- and 74-YearOscillations with the Moon's Nodal Tide on the Northwest European Shelf (Eastern North Sea to Central Baltic Sea). Journ. Coastal Research, 16 pp.
Mörner, Nils-Axel 2015. Sea Level Changes as recorded in nature itself. Journal of Engineering Research and Applications, Vol.5, 1, 124-129.

Global sea level from satellite altimetry, updated to January 2018
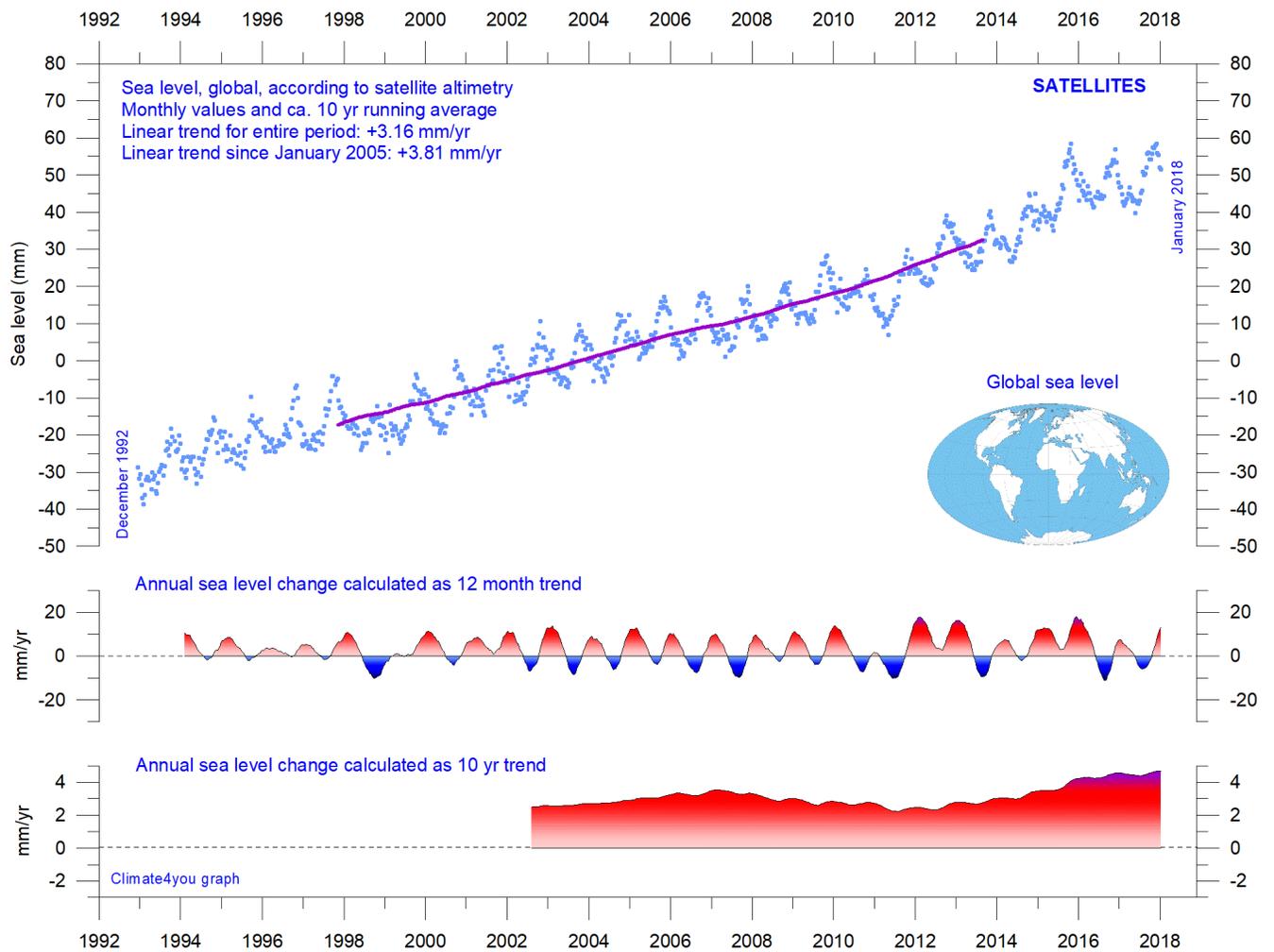
Global sea level since December 1992 according to the Colorado Center for Astrodynamics Research at University of Colorado at Boulder. The blue dots are the individual observations, and the purple line represents the running 121-month (ca. 10 year) average. The two lower panels show the annual sea level change, calculated for 1 and 10-year time windows, respectively. These values are plotted at the end of the interval considered. Data from the TOPEX/Poseidon mission have been used before 2002, and data from the Jason-1 mission (satellite launched December 2001) after 2002.

35

Global sea level from tide-gauges, updated to December 2017
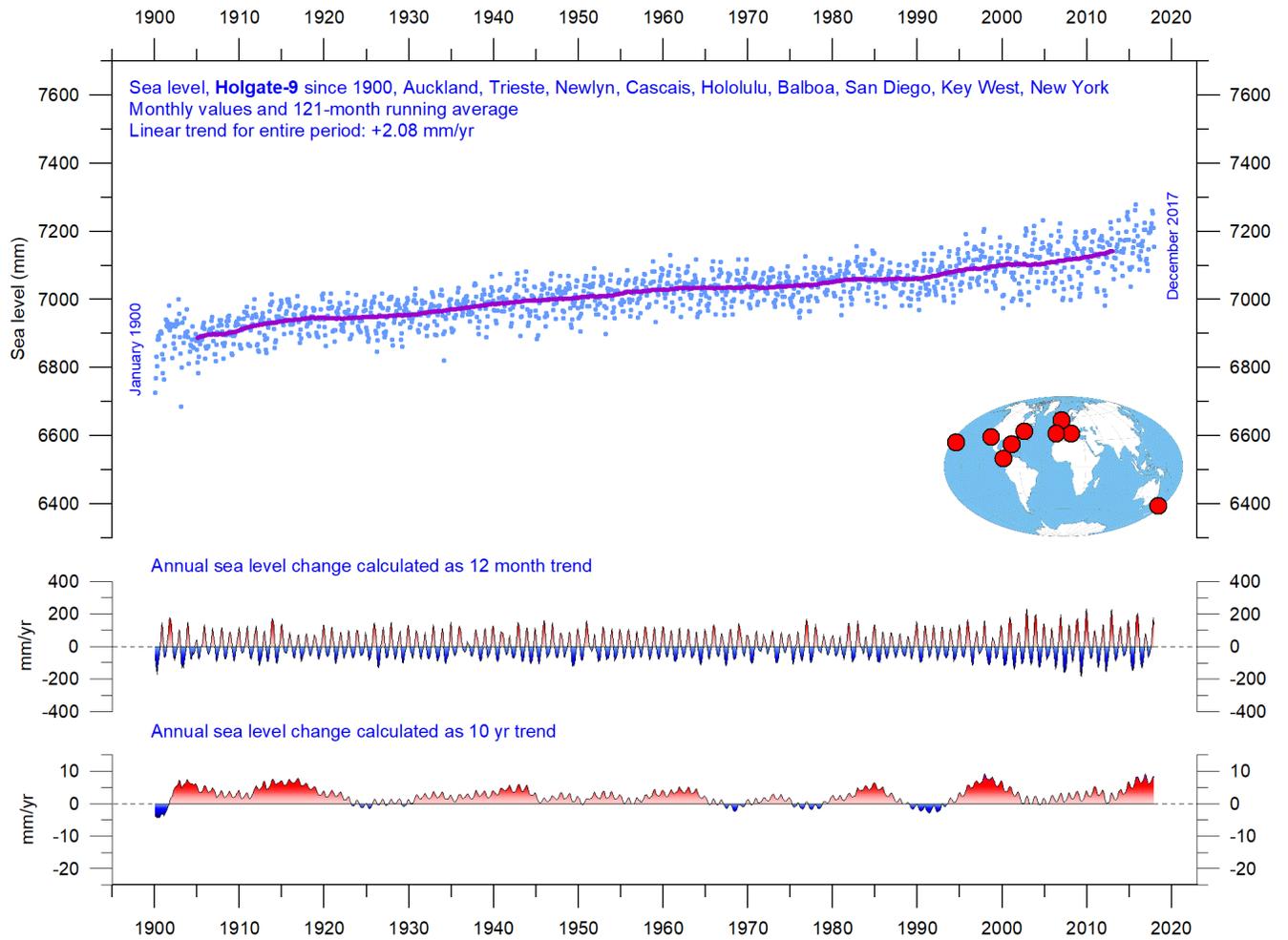
Holgate-9 monthly tide gauge data from PSMSL Data Explorer. Holgate (2007) suggested the nine stations listed in the diagram to capture the variability found in a larger number of stations over the last half century studied previously. For that reason, average values of the Holgate-9 group of tide gauge stations are interesting to follow. The blue dots are the individual average monthly observations, and the purple line represents the running 121-month (ca. 10 year) average. The two lower panels show the annual sea level change, calculated for 1 and 10-year windows, respectively. These values are plotted at the end of the interval considered.

Reference:

Holgate, S.J. 2007. On the decadal rates of sea level change during the twentieth century. Geophys. Res. Letters, 34, L01602, doi:10.1029/2006GL028492

Northern Hemisphere weekly and seasonal snow cover, updated to November 2018
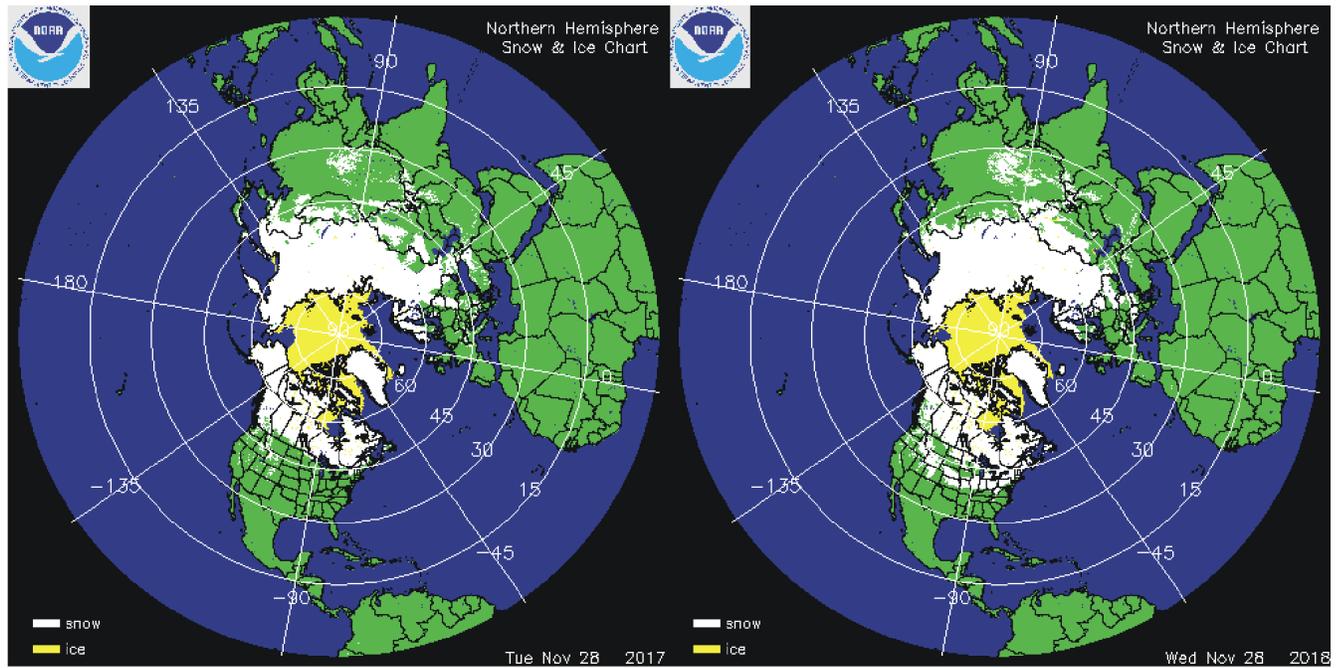
Northern hemisphere snow cover (white) and sea ice (yellow) 28 November 2017 (left) and 2018 (right). Map source: National Ice Center (NIC).
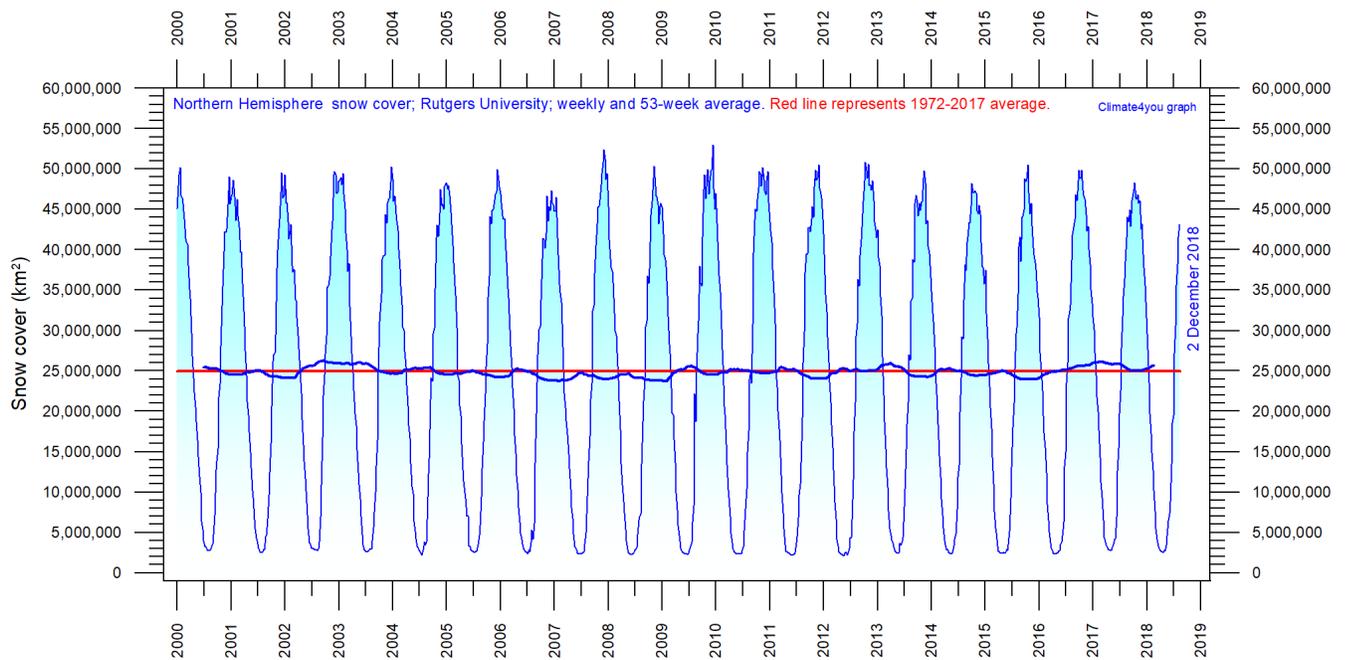
Northern hemisphere weekly snow cover since January 2000 according to Rutgers University Global Snow Laboratory. The thin blue line is the weekly data, and the thick blue line is the running 53-week average (approximately 1 year). The horizontal red line is the 1972-2017 average.
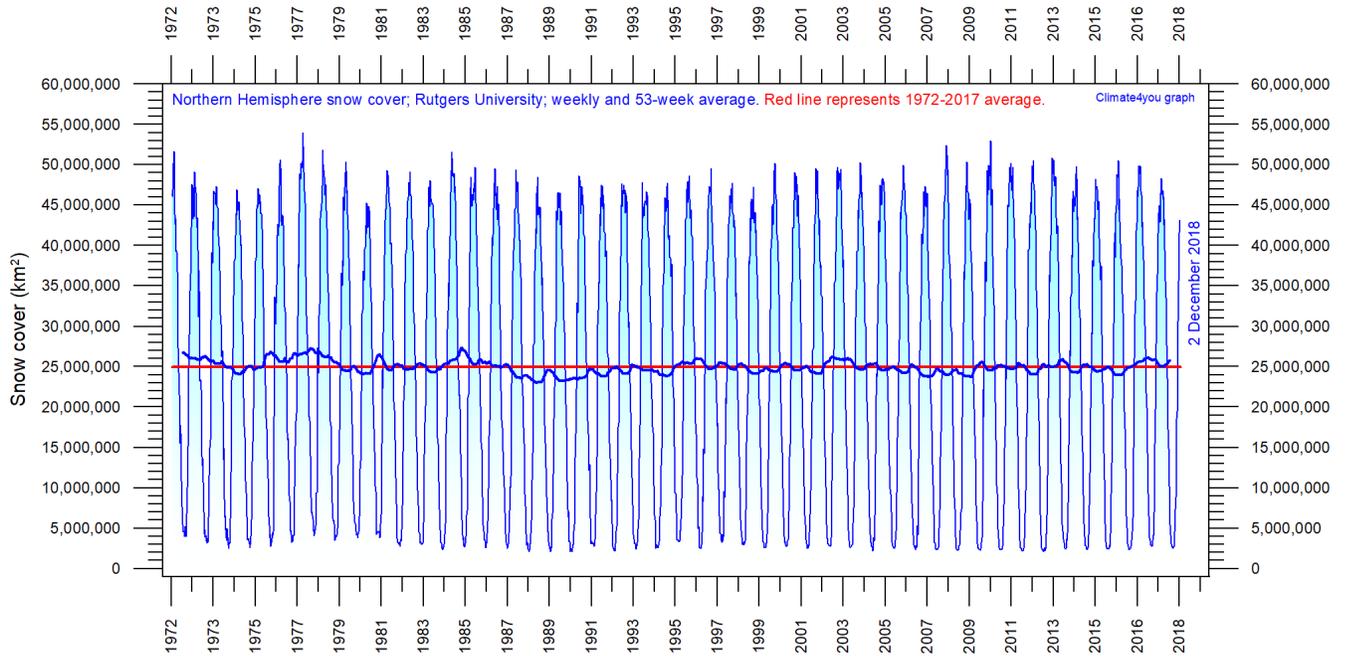
Northern hemisphere weekly snow cover since January 1972 according to Rutgers University Global Snow Laboratory. The thin blue line is the weekly data, and the thick blue line is the running 53-week average (approximately 1 year). The horizontal red line is the 1972-2017 average.
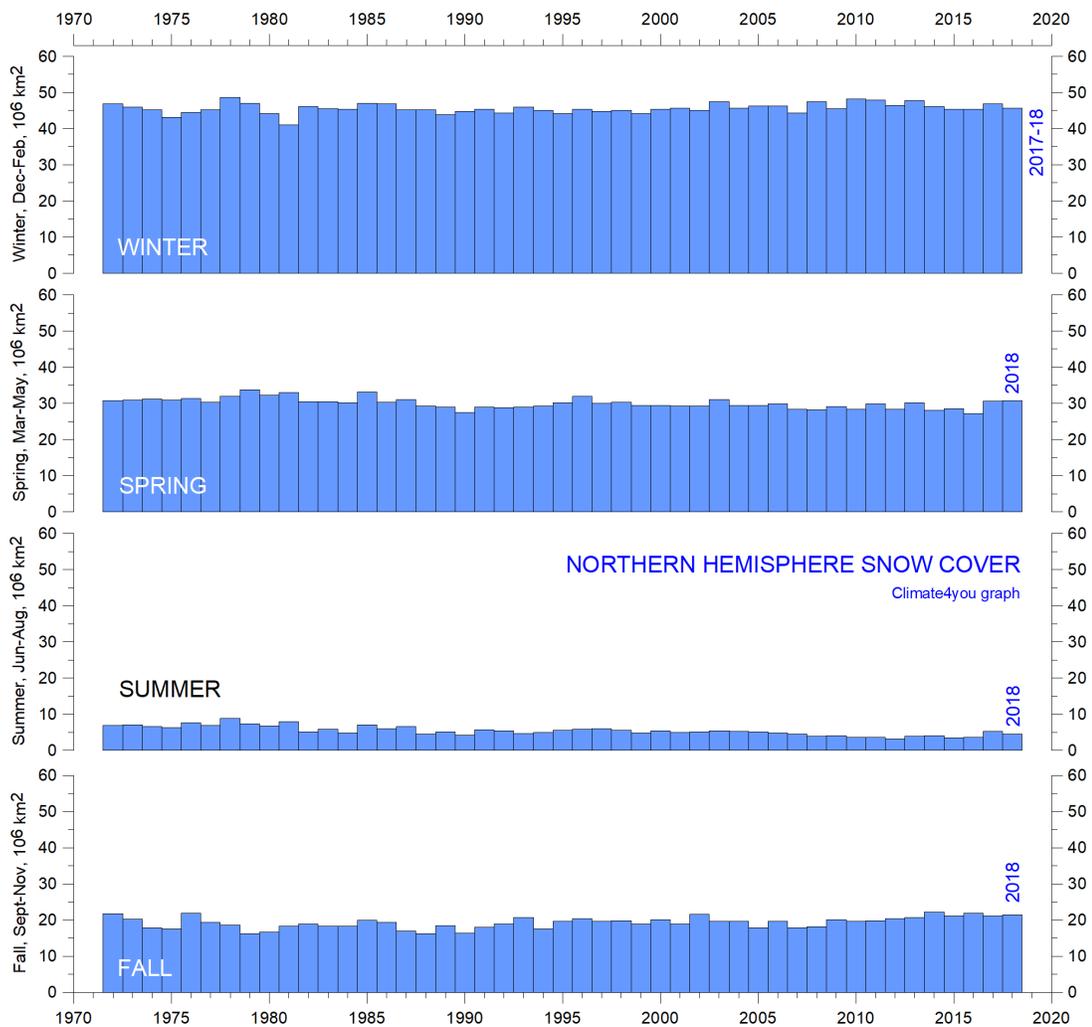
Northern hemisphere seasonal snow cover since January 1972 according to Rutgers University Global Snow Laboratory.

Atmospheric specific humidity, updated to November 2018
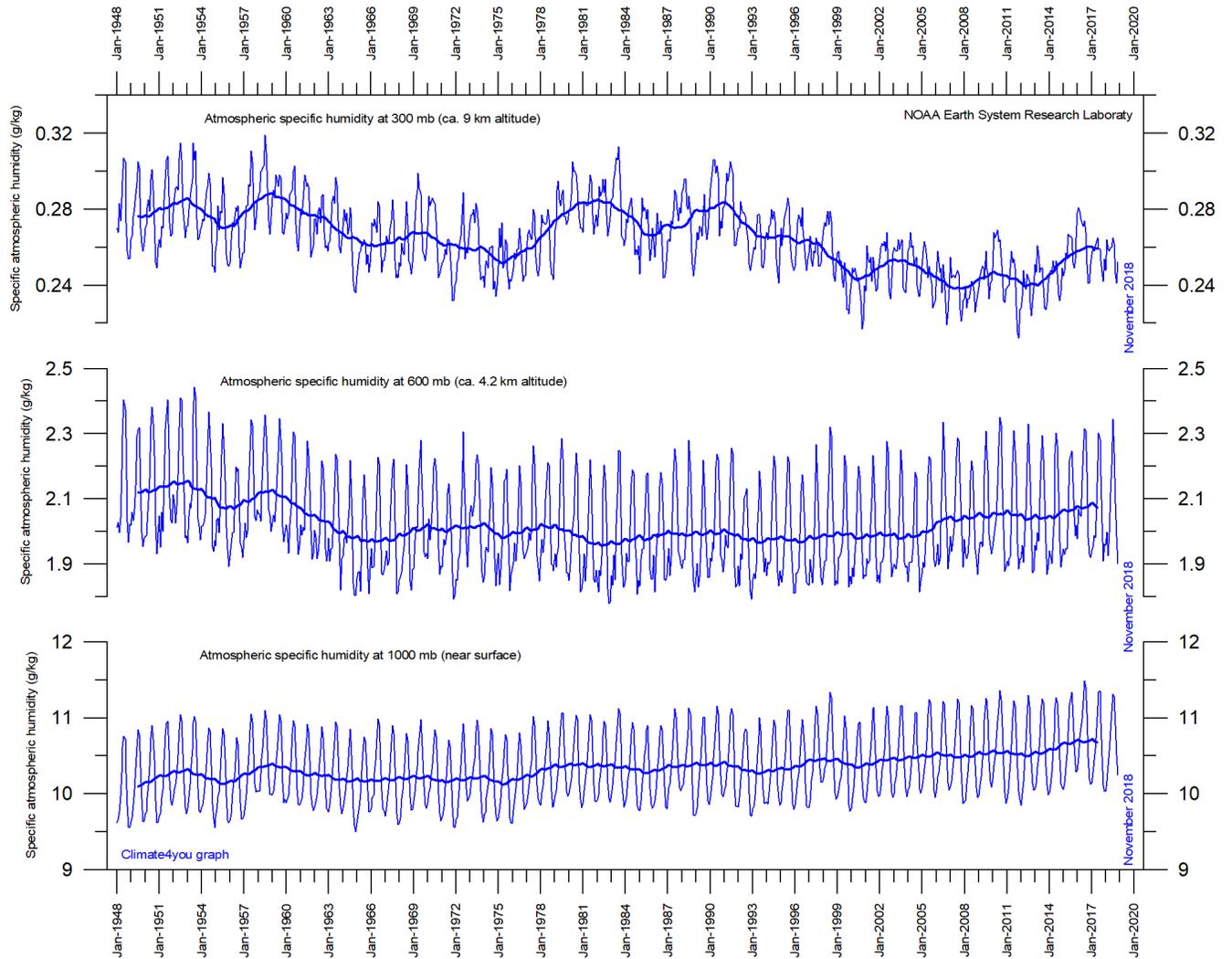
Specific atmospheric humidity (g/kg) at three different altitudes in the lower part of the atmosphere (*the Troposphere*) since January 1948 (*Kalnay et al. 1996*). The thin blue lines show monthly values, while the thick blue lines show the running 37-month average (about 3 years). Data source: *Earth System Research Laboratory (NOAA)*.

<u>Note</u>: Water vapour is the most important greenhouse gas in Earth's atmosphere, much more important than CO_2.

Atmospheric CO₂, updated to November 2018
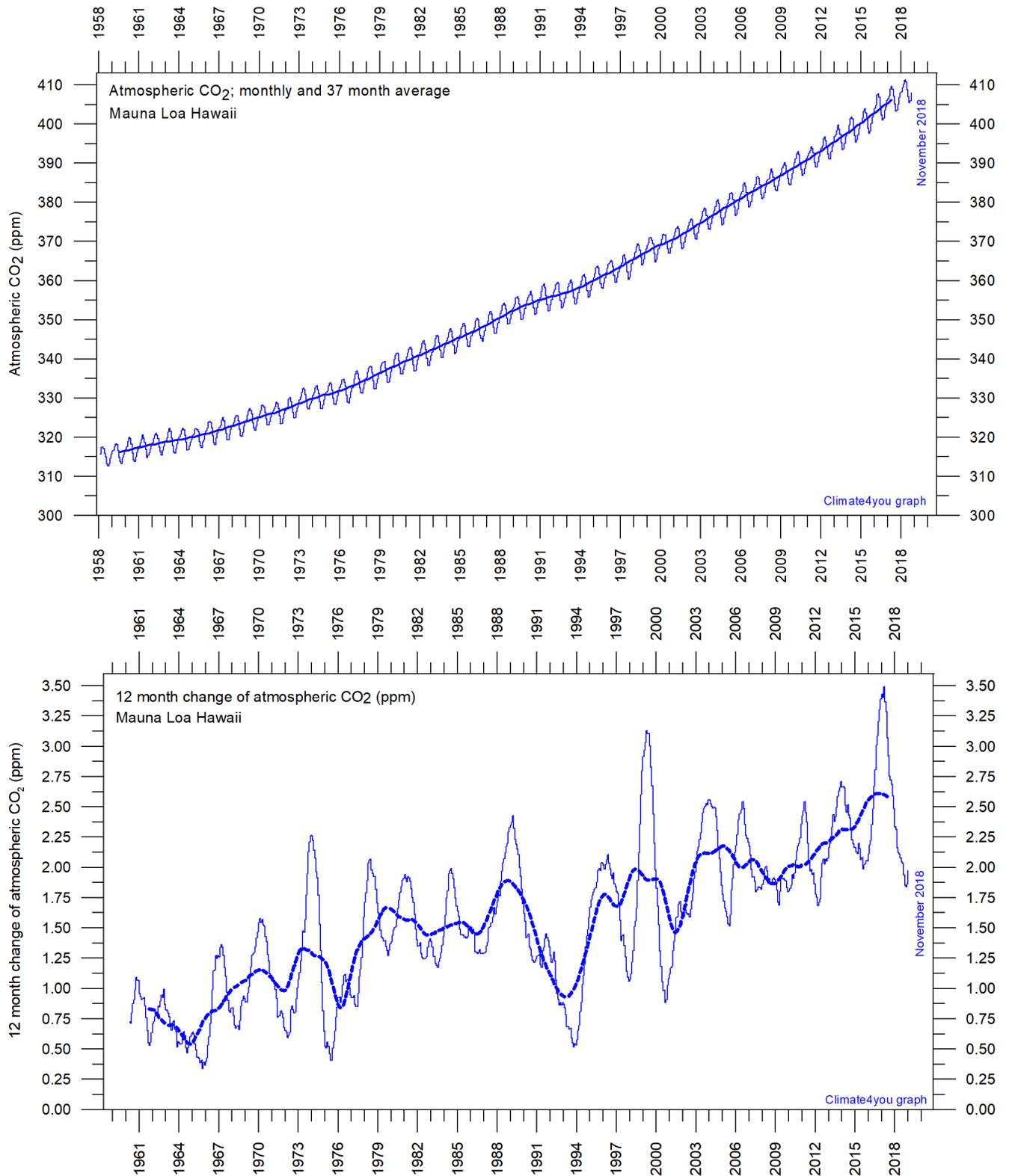
Monthly amount of atmospheric CO_2 (upper diagram) and annual growth rate (lower diagram); average last 12 months minus average preceding 12 months, thin line) of atmospheric CO_2 since 1959, according to data provided by the _Mauna Loa Observatory_, Hawaii, USA. The thick, stippled line is the simple running 37-observation average, nearly corresponding to a running 3-year average.

The relation between annual change of atmospheric CO_2 and La Niña and El Niño episodes, updated to November 2018
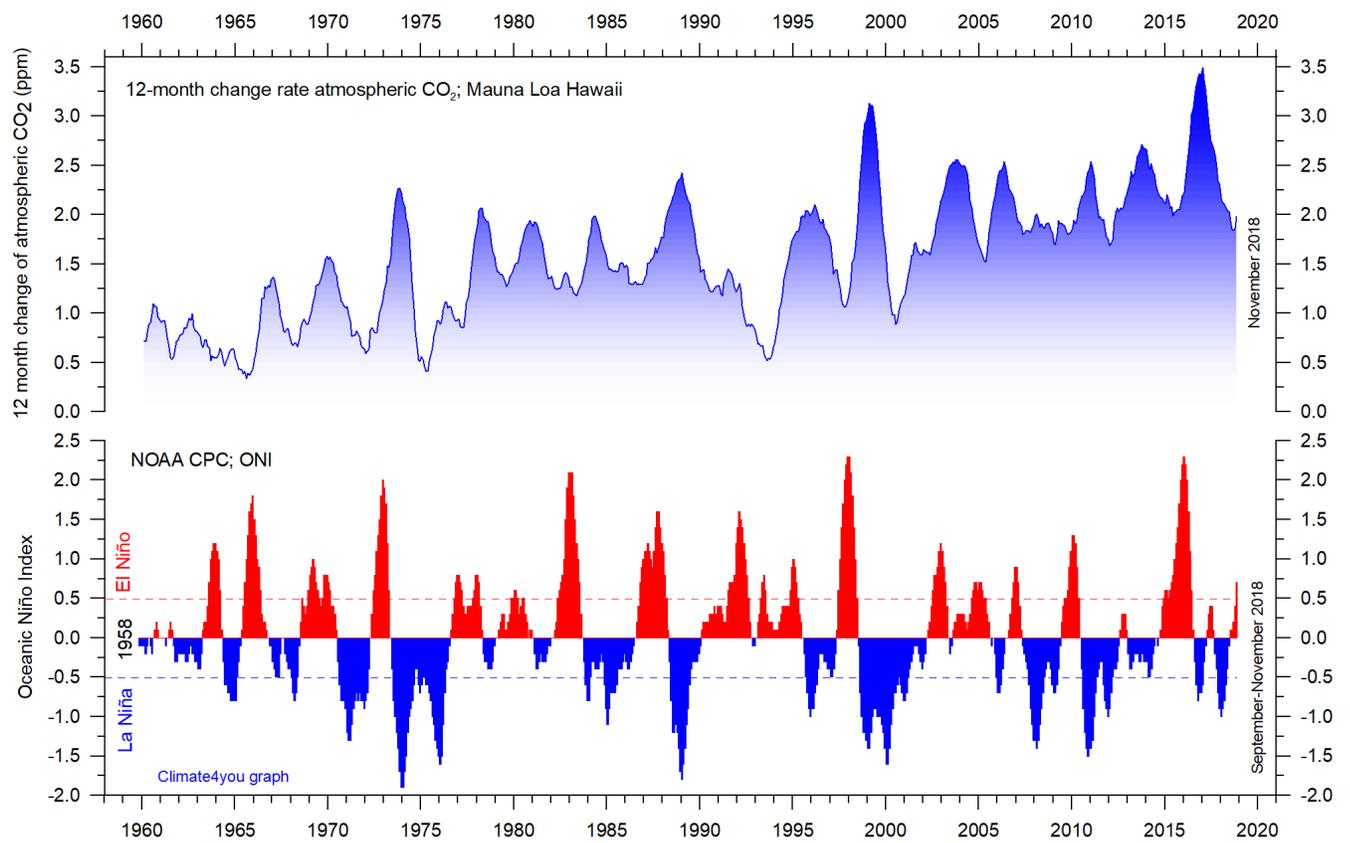
Visual association between annual growth rate of atmospheric CO_2 (upper panel) and Oceanic Niño Index (lower panel). See also diagrams on page 40 and 22, respectively.

The phase relation between atmospheric CO₂ and global temperature, updated to October 2018
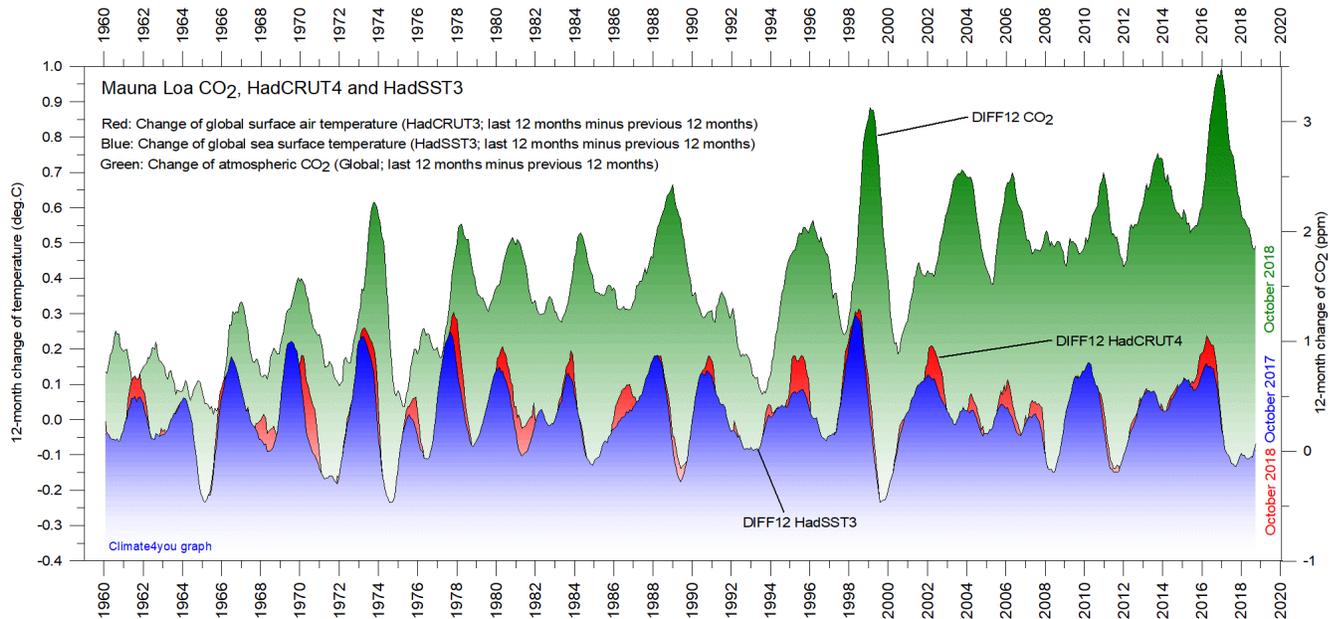
12-month change of global atmospheric CO₂ concentration (Mauna Loa; green), global sea surface temperature (HadSST3; blue) and global surface air temperature (HadCRUT4; red dotted). All graphs are showing monthly values of DIFF12, the difference between the average of the last 12 month and the average for the previous 12 months for each data series.

42

Note: The typical sequence of events is seen to be that changes in the global atmospheric CO₂ follows changes in global surface air temperature, which again follows changes in global ocean surface temperatures. Thus, changes in global atmospheric CO₂ are lagging 9.5–10 months behind changes in global air surface temperature, and no less than 11–12 months behind changes in global sea surface temperature.

References:

Humlum, O., Stordahl, K. and Solheim, J-E. 2012. The phase relation between atmospheric carbon dioxide and global temperature. Global and Planetary Change, August 30, 2012.
http://www.sciencedirect.com/science/article/pii/S0921818112001658?v=s5

Global air temperature and atmospheric CO₂, updated to November 2018

Atmospheric CO₂ (Mauna Loa)
Global temperature anomaly (HadCRUT4)

October 2018

HADCRUT average 1961-1990

Climate4you graph

Negative   Positive   Weak

Atmospheric CO₂ (Mauna Loa)
Global temperature anomaly (GISS)

November 2018

GISS average 1951-1980

Climate4you graph

Negative   Positive   Weak
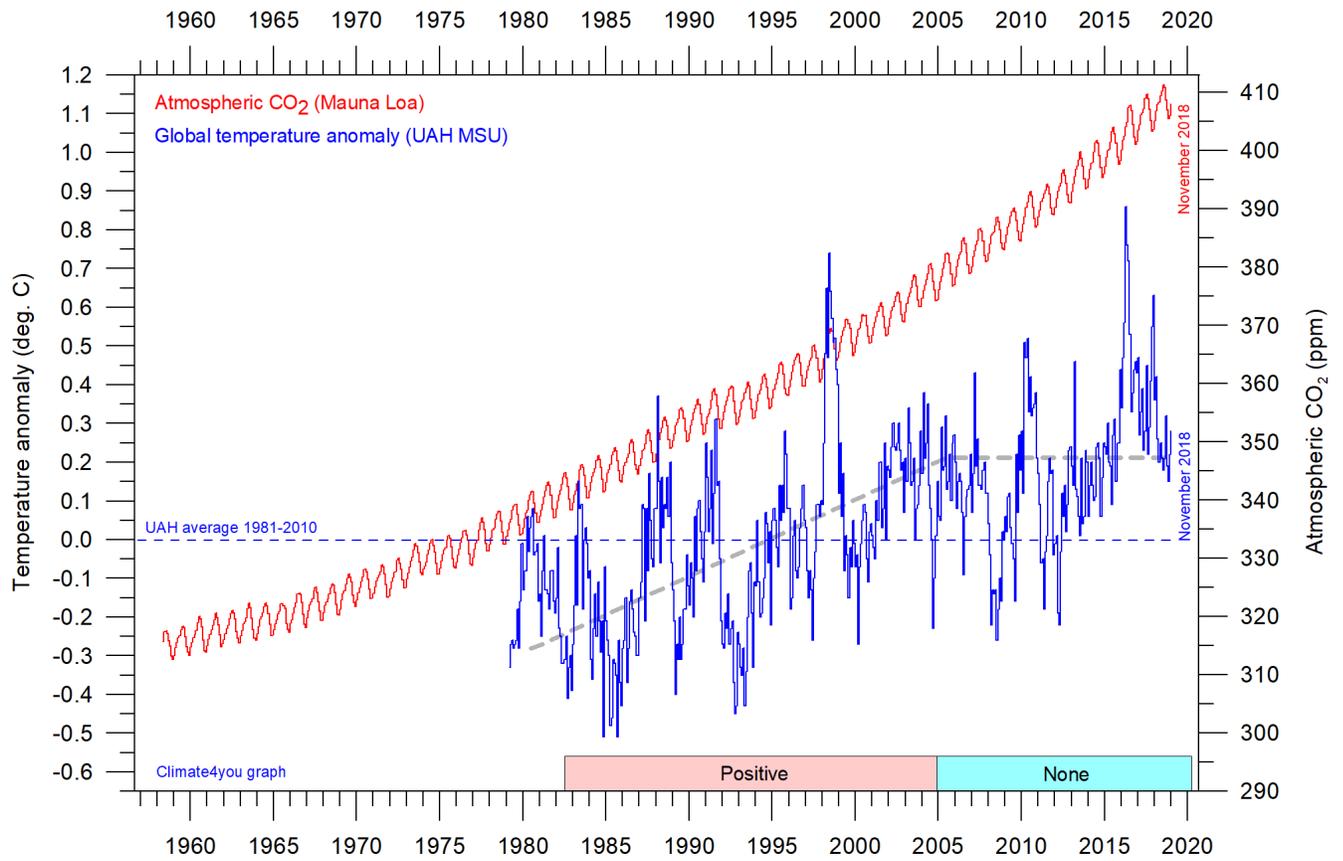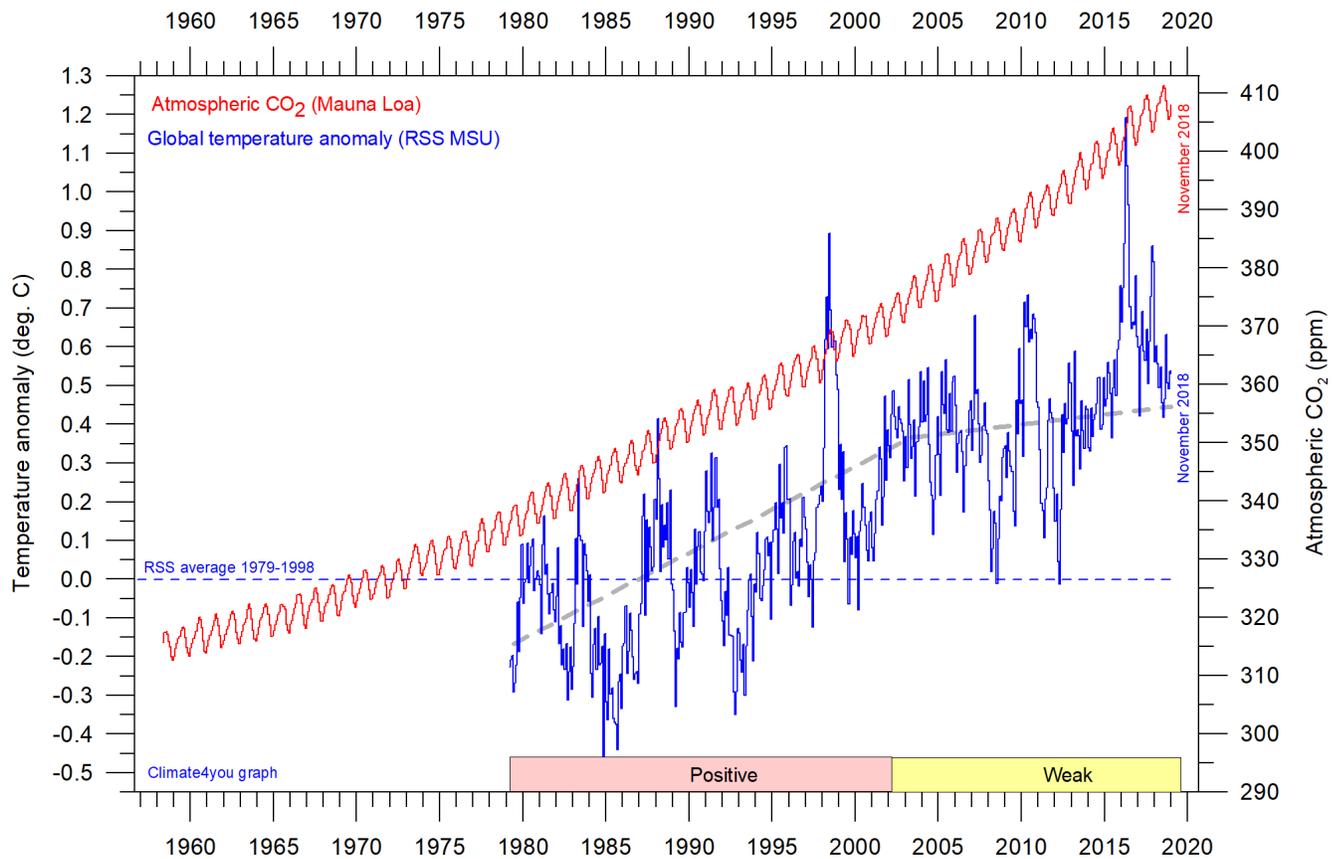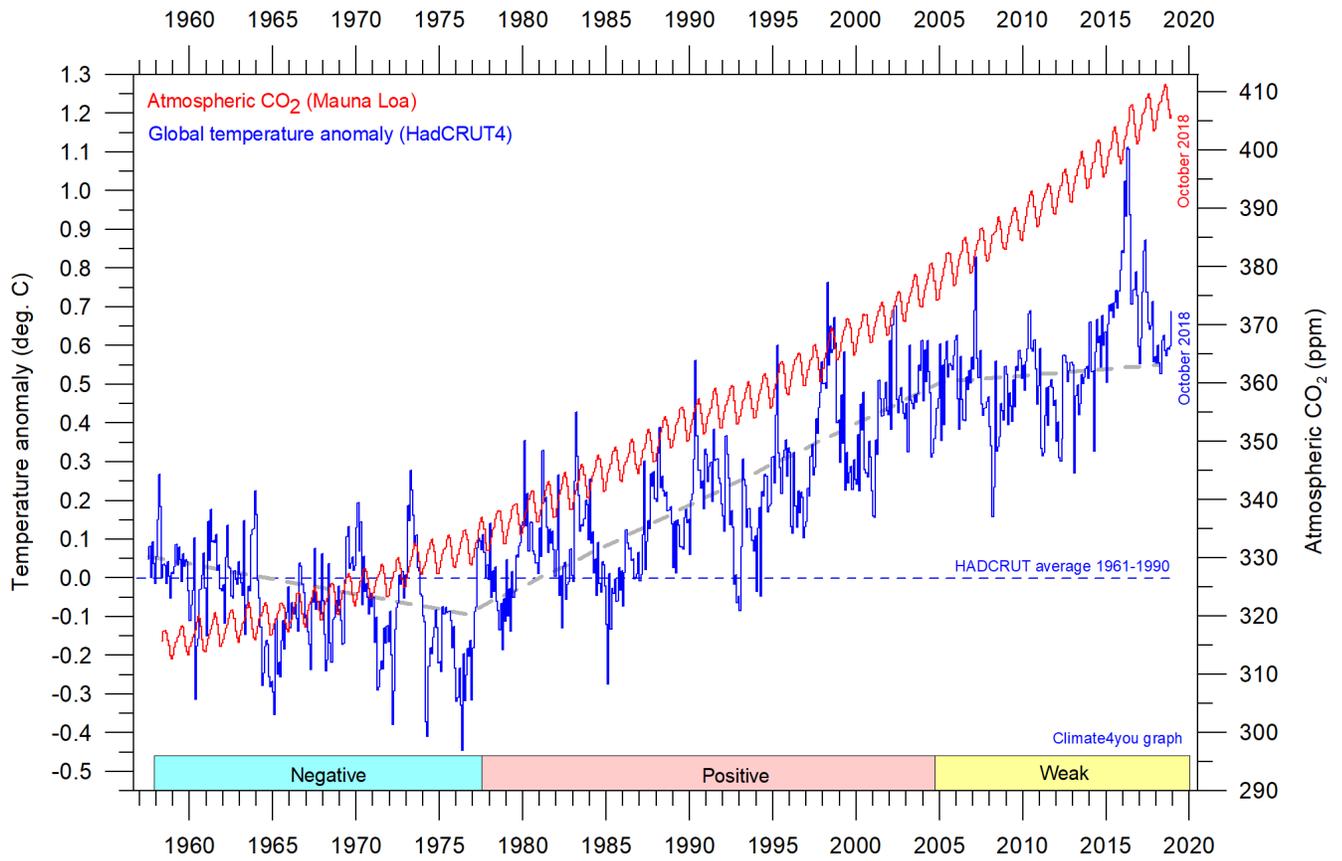
Diagrams showing UAH, RSS, HadCRUT4, GISS, and NCDC monthly global air temperature estimates (blue) and the monthly atmospheric CO_2 content (red) according to the [Mauna Loa Observatory](#), Hawaii. The Mauna Loa data series begins in March 1958, and 1958 was therefore chosen as starting year for the all diagrams above. Reconstructions of past atmospheric CO_2 concentrations (before 1958) are not incorporated in this diagram, as such past CO_2 values are derived by other means (ice cores, stomata, or older measurements using different methodology), and therefore are not directly comparable with direct atmospheric measurements. The dotted grey line indicates the approximate linear temperature trend, and the boxes in the lower part of the diagram indicate the relation between atmospheric CO_2 and global surface air temperature, negative or positive. Please note that the HadCRUT diagram (p.44) is not yet updated beyond October 2018.

Most climate models are programmed to give the greenhouse gas carbon dioxide CO_2 important influence on global temperature. It is therefore relevant to compare different temperature records with measurements of atmospheric CO_2, as shown in the diagrams above.
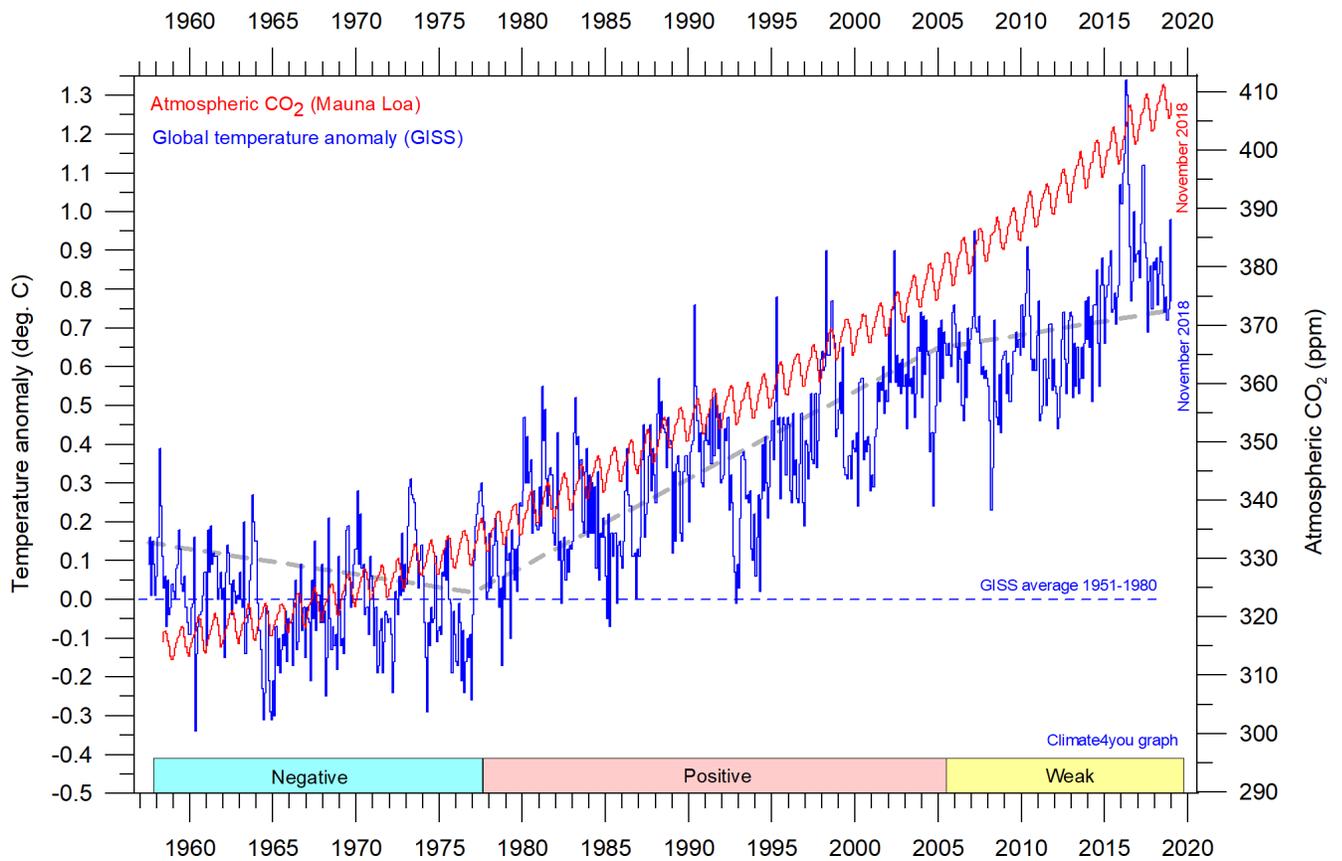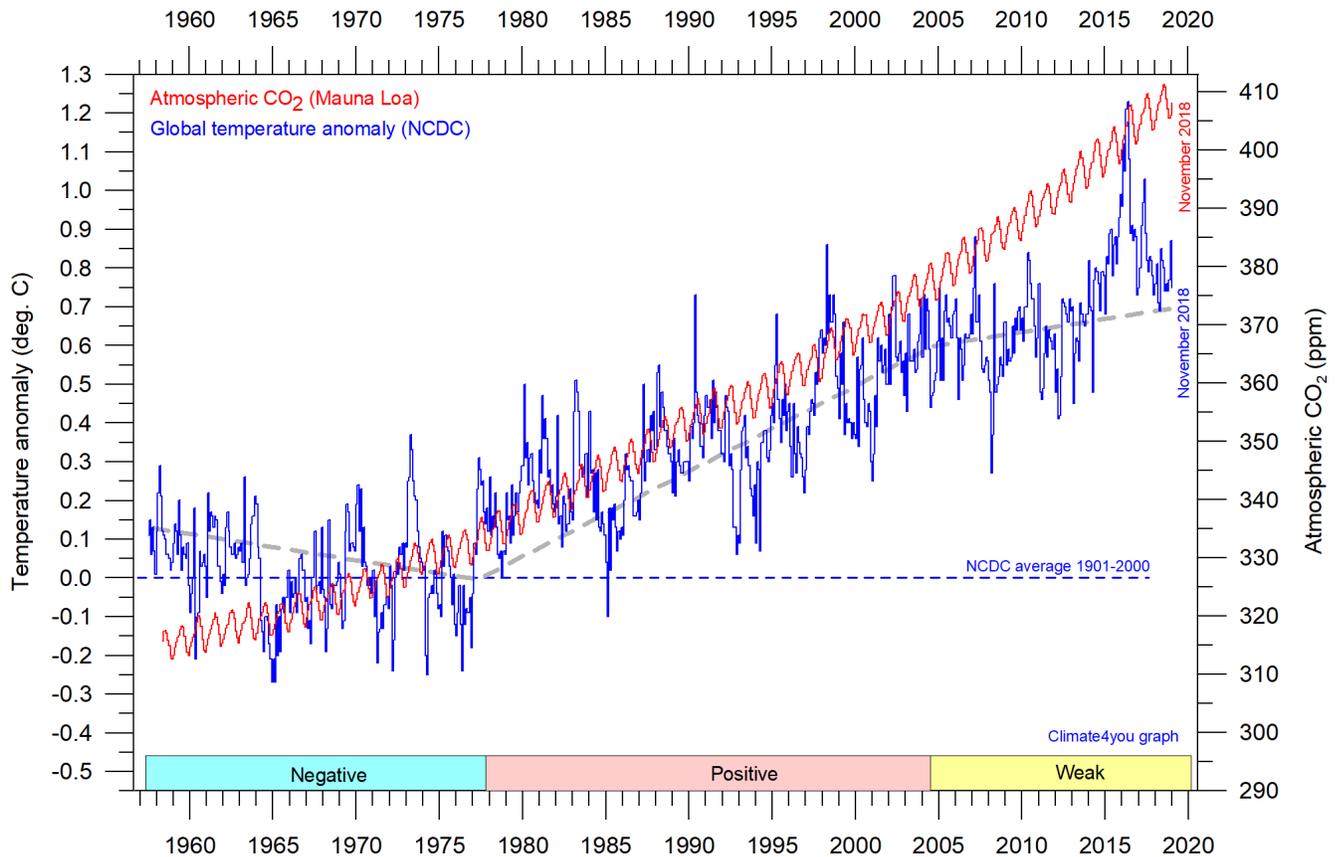
Any comparison, however, should not be made on a monthly or annual basis, but for a longer time, as other effects (oceanographic, cloud cover, etc.) may well override the potential influence of CO_2 on short time scales such as just a few years.

It is of cause equally inappropriate to present new meteorological record values, whether daily, monthly or annual, as support for the hypothesis ascribing high importance of atmospheric CO_2 for global temperatures. Any such meteorological record value may well be the result of other phenomena. Unfortunately, many news media repeatedly fall into this trap.

What exactly defines the critical length of a relevant period length to consider for evaluating the alleged importance of CO_2 remains elusive and represents a theme for discussion. However, the length of the critical period must be inversely proportional to the temperature sensitivity of CO_2, including feedback effects. Thus, if the net temperature effect of atmospheric CO_2 is strong, the critical period will be short, and vice versa.

However, past climate research history provides some clues as to what has traditionally been considered the relevant length of period over which to compare temperature and atmospheric CO_2. After about 10 years of concurrent global temperature- and CO_2-increase, IPCC was established in 1988. For obtaining public and political support for the CO_2-hyphotesis the 10-year warming period leading up to 1988 most likely was considered important. Had the global temperature instead been decreasing, politic support for the hypothesis would have been difficult to obtain in 1988.

Based on the previous 10 years of concurrent temperature- and CO_2-increase, many climate scientists in 1988 presumably felt that their understanding of climate dynamics was enough to conclude about the importance of CO_2 for global temperature changes. From this it may safely be concluded that 10 years was considered a period long enough to demonstrate the effect of increasing atmospheric CO_2 on global temperatures. The 10-year period is also basis for the anomality diagrams shown on page 2.

Adopting this approach as to critical time length (at least 10 years), the varying relation (positive or negative) between global temperature and atmospheric CO_2 has been indicated in the lower panels of the diagrams above.

Latest 20-year QC1 global monthly air temperature changes, updated to November 2018
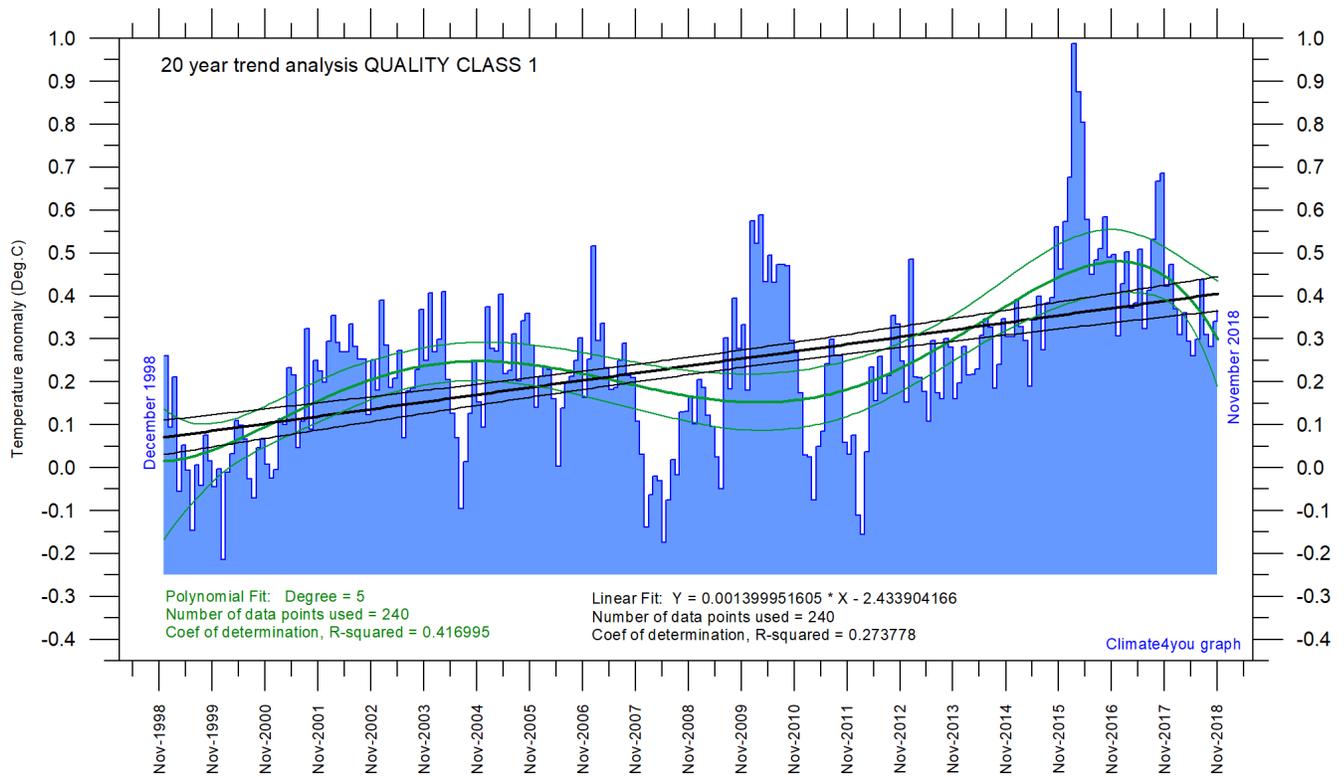
Last 20 years' global monthly average air temperature according to Quality Class 1 (UAH and RSS; see p.10) global monthly temperature estimates. The thin blue line represents the monthly values. The thick black line is the linear fit, with 95% confidence intervals indicated by the two thin black lines. The thick green line represents a 5-degree polynomial fit, with 95% confidence intervals indicated by the two thin green lines. A few key statistics are given in the lower part of the diagram (please note that the linear trend is the monthly trend).

In the still ongoing climate debate the following about the global surface air temperature is often put forward: Is the surface air temperature still increasing or has it basically remained without significant changes during the last about 15 years?

The diagram above may be useful in this context and demonstrates the differences between two often used statistical approaches to determine recent temperature trends. Please also note that such fits only attempt to describe the past, and usually have small, if any, predictive power. In addition, before using any linear trend (or other) analysis of time series a proper statistical model should be chosen, based on statistical justification.

For temperature time series, there is no *a priori* physical reason why the long-term trend should be linear in time. In fact, climatic time series often have trends for which a straight line is not a good approximation, as can clearly be seen from several of the diagrams in the present report.

For an excellent description of problems often encountered by analyses of temperature time series analyses, please see Keenan, D.J. 2014: Statistical Analyses of Surface Temperatures in the IPCC Fifth Assessment Report.

Sunspot activity and QC1 average satellite global air temperature, updated to November 2018
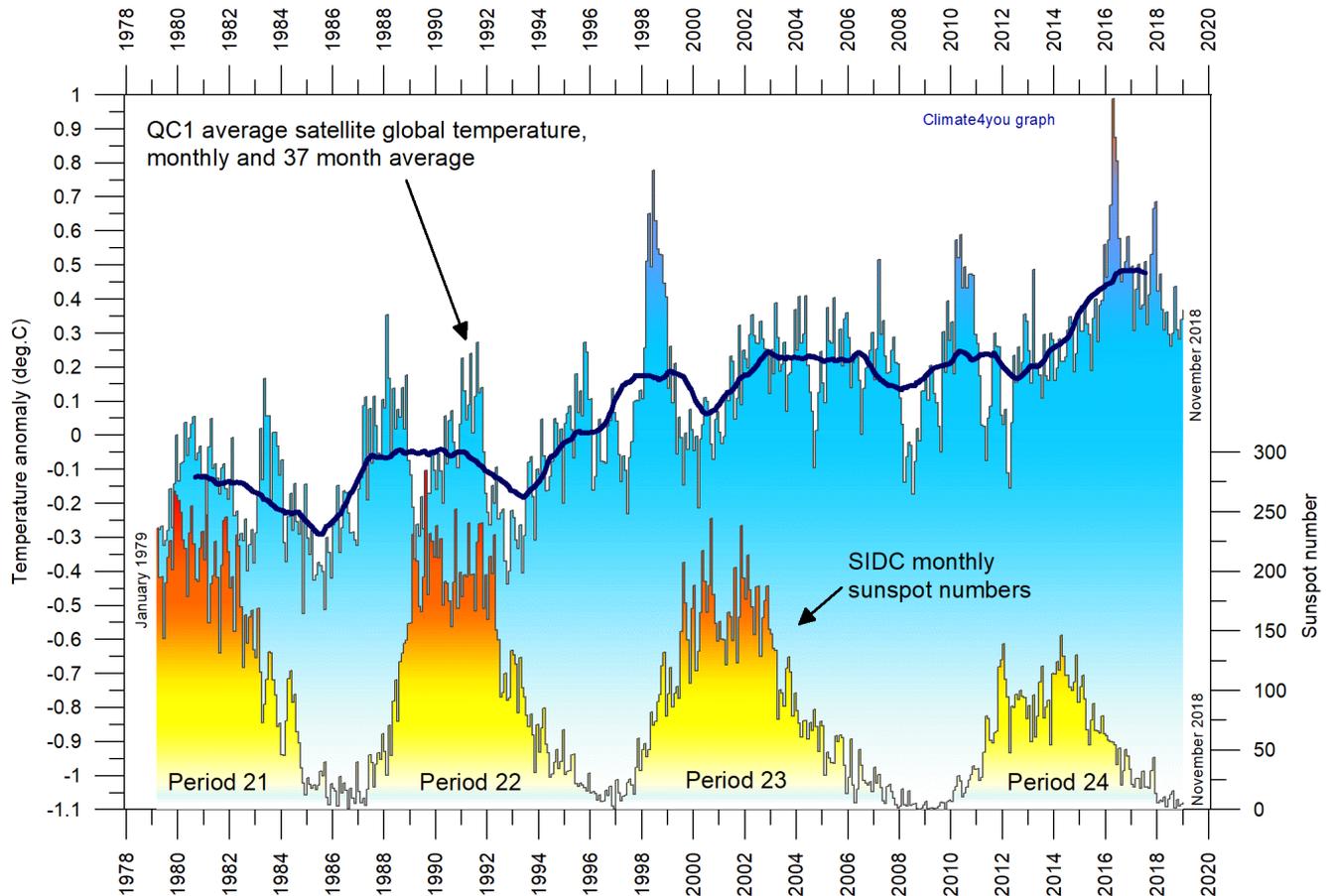
Variation of global monthly air temperature according to Quality Class 1 (UAH and RSS; see p.4) and observed sunspot number as provided by the Solar Influences Data Analysis Center (SIDC), since 1979. The thin lines represent the monthly values, while the thick line is the simple running 37-month average, nearly corresponding to a running 3-year average. The asymmetrical temperature 'bump' around 1998 is influenced by the oceanographic El Niño phenomenon in 1998, as is the case also for 2015-16.

1851: Jakobshavn calving glacier (Jakobshavn Isbræ) in West Greenland reaches Little Ice Age maximum and begins to retreat

Disko Bay and Jakobshavn Isbræ, a calving outlet glacier from the Greenland Ice Sheet, seen from southwest. Jakobshavn Isfjord and Jakobshavn Isbræ is seen near the centre of the picture. Disko Island is seen to the left, and part of the Greenland Ice Sheet is seen in the background. The distance from southernmost Disko Island to the mouth of the ice-filled Jakobshavn Isfjord (Ilulissat Icefjord) is about 100 km. Picture source: Google Earth.

The Disko Bay region in central West Greenland (c. 70°N) is characterised by large outlet glaciers from the Greenland Ice Sheet. The large calving glacier Jakobshavn Isbræ is situated in a major subglacial valley, which can be traced inland for about 100 km (Echelmeyer et al. 1991). The water depth in the fjord reaches 1500 m in its outer parts (Iken et al. 1993).

The first thorough glaciological studies in this area were those by Rink (1853), who introduced the terms Inland Ice (ice sheet) and ice streams. The Disko Bay was deglaciated rapidly around 10.500-

10.000 years ago, in the early part of the present interglacial, the Holocene (Weidick 1968).

When the retreating ice front at that time reached the coastline at the mouth of the Jakobshavn Isfjord (Ilulissat Icefjord), the retreat was interrupted while the glacier front was grounded on a bank 200-300 m below the present sea level, shortly south of the town Ilulissat. Later, the glacier again retreated and reached the modern position c. 7.000 years ago. However, the retreat continued beyond that position, and by 5000 years before now the glacier front was east of the modern position, about 20 km

east of the ice margin position in 1964 (Weidick et al. 1990).

Global cooling after 5.000 year before then resulted in significant growth of the Greenland Ice Sheet, and the resulting advance of Jakobshavn Isbræ culminated around the year 1850, during the Little Ice Age, bring the glacier front to a position about 15-16 km east of Ilulissat (see figure below). From 1851 the calving glacier began retreating, and at the end of the 19th century the glacier front was about 10 km east of the maximum position reached in 1851 (Bauer et al. 1968). The seasonal fluctuations of the glacier terminus were recorded 1879-1880 by Hammer (1883), who also described local inuit legends describing that the embayment Tissarissoq (figure below) formerly was ice-free and used as a hunting locality. If this is correct, open water probably extended east of the early 21st century glacier front position before the onset of the Little Ice Age (Weidick et al. 2004).

Jakobshavn Isbræ today is the main outlet glacier from the Greenland Ice Sheet, draining ice from about 6.5% of the total area of the ice sheet, and producing 30-45 km^3 icebergs per year. This corresponds to more than 10% of the total output of icebergs from the Greenland Ice Sheet, and the Jakobshavn Isbræ is the most productive glacier in the Northern Hemisphere. The glacier flow velocity is also high, typically 20-22 meters per day.

It is likely that the iceberg which sank Titanic in April 1912 originated by calving from Jakobshavn Isbræ.
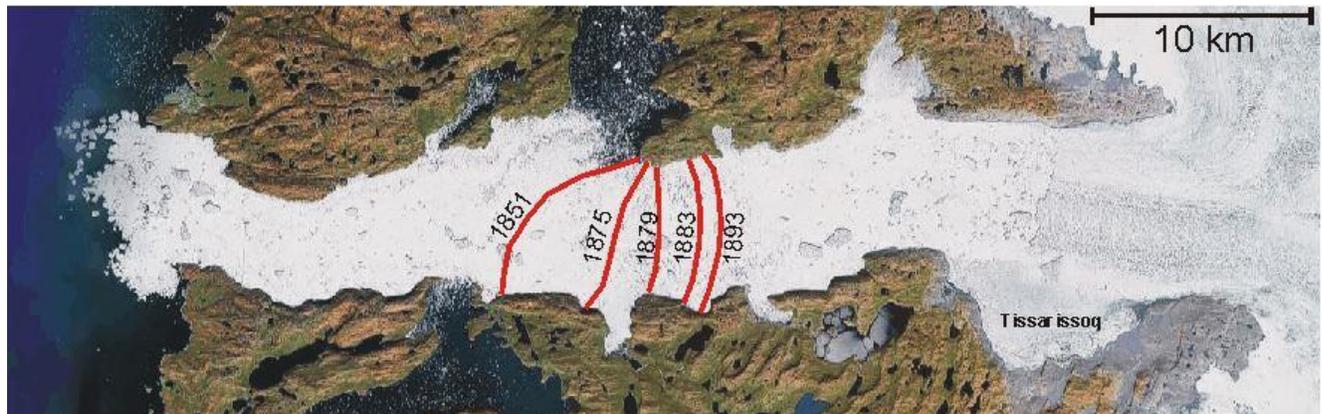
Frontal positions of calving Jakobshavn Isbræ in the latter half of the 19th century, after reaching the maximum Little Ice Age position around 1850 (Bauer et al. 1968). Between 1851 and 1893 the glacier front retreated about 10 km. The early 21st century (2001) glacier front is seen about 14 km east of the 1893 position. According to inuit legends, the embayment Tissarissoq used to be glacier-free and was used as hunting area (Hammer 1883), most likely before before the Little Ice Age glacier advance (Weidick et al. 2004). Picture source: Google Earth.

REFERENCES:

Bauer, A., Baussart, M., Carbonnell, M., Kasser, P., Perroud, P. and Renaud, A. 1968. Missions aériennes de reconnaissance au Groenland 1957-1958. Observations aériennes et terrestres, exploitation des photographies aeriennes, determination des vitesses des glaciers vĕlant dans Disko Bugt et Umanak Fjord. *Meddelser om Grønland* 173(3), 116 pp.

Bauer, A., Baussart, M., Carbonnell, M., Kasser, P., Perroud, P. and Renaud, A. 1968. Missions aériennes de reconnaissance au Groenland 1957-1958. Observations aériennes et terrestres, exploitation des photographies aeriennes, determination des vitesses des glaciers vĕlant dans Disko Bugt et Umanak Fjord. *Meddelser om Grønland* 173(3), 116 pp.

Echelmeyer, K., Clarke, T.S. and Harrison, W.D. 1991. Surficial glaciology of Jakobshavns Isbræ, West Greenland. Part I: Surface morphology. *Journal of Glaciology* 37(127), 368-382.

Hammer, R.R.J. 1883. Undersøgelser ved Jakobshavn Isfjord og nærmeste Omegn i Vinteren 1879-1880. *Meddelelser om Grønland* 4(1), 68 pp.

Iken, A., Echelmeyer, K. and Funk, M. 1993. Mechanism of fast flow in Jakobshavn Isbræ, West Greenland. Part I: Measurements of temperature and water level in deep bore holes. *Journal of Glaciology* 39, 15-25.

Rink, H. 1853. Om den geographiske Beskaffenhed af de danske Handelsdistrikter i Nordgrønland, tilligemed en Udsigt over Nordgrønlands Geognosi. *Det Kongelige Danske Videnskabernes Selskabs Skrifter*, 5. Række, Naturvidenskabelige og Mathematiske Afdeling 3, 37-70.

Weidick, A. 1968. Observations on some Holocene glacier fluctuations in West Greenland. *Meddelelser om Grønland* 165(6), 202 pp.

Weidick, A., Oerter, H., Reeh, N., Thomsen, H.H. and Thorning, L. 1990. The recession of the Inland Ice margin during the Holocene climatic optimum in the Jakobshavn Isfjord area of West Greenland. *Palaeogeography, Palaeoclimatology, Palaeoecology* 82, 289-399.

Weidick, A., Mikkelsen, N., Mayer, C. and Podlech, S. 2004. Jakobshavn Isbræ, West Greenland: the 2002-2003 collapse and nomination for the UNESCO World Heritage List. *Geological Survey of Denmark and Greenland Bulletin* 4, 85-88.

51

*****

All diagrams in this report, along with any supplementary information, including links to data sources and previous issues of this newsletter, are freely available for download on www.climate4you.com

Yours sincerely, and Season's Greetings,

Ole Humlum (Ole.Humlum@gmail.com)

Arctic Historical Evaluation and Research Organisation, Longyearbyen, Svalbard

December 19, 2018.